METHODS

The Bottom-Up Solution to the Triacylglycerol Lipidome Using Atmospheric Pressure Chemical Ionization Mass Spectrometry

William Craig Byrdwell*

Department of Chemistry & Biochemistry, Florida Atlantic University, Boca Raton, Florida 33431

ABSTRACT: Presented here is an approach to representing the data from atmospheric pressure chemical ionization (APCI) mass spectrometry (MS) of triacylglycerols (TAG) using a set of one, two, or three Critical Ratios. These Critical Ratios may be used directly to provide structural information concerning the regioisomeric composition of the triacylglycerols (TAG), and about the degree of unsaturation in the TAG. An AAA-type, or Type I, TAG has only one Critical Ratio, the ratio of the protonated molecule, $[M + H]^+$, to the DAG fragment ion, $[AA]^+$. The Critical Ratio for a Type I TAG is $[MH]^+/\Sigma[DAG]^+$, and the mass spectrum of a Type I TAG can be reproduced from only this one ratio. An ABA/AAB/BAA, or Type II, TAG has two Critical Ratios, the $[MH]^+/\Sigma[DAG]^+$ ratio and the $[AA]^+/[AB]^+$ ratio. The $[AA]^+/[AB]^+$ ratio for a single TAG or TAG mixture can be compared with the $[AA]^+/[AB]^+$ ratios of pure regioisomeric standards, and the percentage of each regioisomer can be estimated. The abundance of the protonated molecule and the abundances of the two $[DAG]^+$ fragment ions can be calculated from the two Critical Ratios for a Type II TAG. To calculate the abundances, the Critical Ratios are processed through the Bottom-Up Solution to the TAG lipidome. First, Critical Limits are calculated from the Critical Ratios, and then the Critical Ratios are classified into Cases by comparison with the Critical Limits. Once the Case classification is known, the equation for the abundance of each ion in the mass spectrum is given by the Bottom-Up Solution. A Type III TAG has three different FA and three Critical Ratios. The $[MH]^+/\Sigma[DAG]^+$ ratio is the first Critical Ratio, the $[AC]^+/([AB]^+ + [BC]^+)$ ratio is the second Critical Ratio, and the $[BC]^+/[AB]^+$ ratio is the third Critical Ratio. The second critical ratio for a Type III TAG can be compared with regioisomeric standards to provide an estimate of the percentage composition of the regioisomers. The three Critical Ratios for a Type III TAG can be processed through the Bottom-Up Solution to calculate the four ion abundances that make up the APCI-MS mass spectrum. The Critical Ratios constitute a reduced data set that provides more information in fewer values than the raw abundances.

Paper no. L9524 in *Lipids 40*, 383–417 (April 2005).

Work over the last decade has proved that HPLC combined with atmospheric pressure chemical ionization (APCI) MS is

an instrumental technique capable of accomplishing qualitative and quantitative analyses of complex mixtures of many classes of lipids. HPLC/APCI-MS is useful for qualitative and/or quantitative analysis of FA (1–4), TAG (5–11), phospholipids (12–16), ceramides (17), carotenoids (18–22), steroids (23–25), and others. Reviews of the applications of APCI-MS for lipid analysis have been published in recent years (26–29).

An important aspect of TAG analysis is the determination of the positional placement of the FA on the glycerol backbone (30). Plants synthesize lipids with structural specificity, namely, saturated FA are most often preferentially located on the *sn*-1 and *sn*-3 positions of the glycerol backbone, and PUFA are preferentially found in the *sn*-2 position. TAG are metabolized by enzymes in the human digestive system with structural specificity, with FA in the *sn*-1 and *sn*-3 positions being removed from the glycerol backbone first. Furthermore, enzymatic synthesis of TAG can be used to produce structured TAG with particular FA located in regiospecific locations (31). Therefore, knowledge of the composition of molecular species in a mixture of TAG, and of the regioisomeric configurations of selected TAG for which standards are available, could provide valuable information to be considered in the planning of dietary, nutritional, metabolic, and related studies. It has been demonstrated by a growing literature precedent that APCI-MS, preceded by a variety of HPLC or supercritical fluid chromatography (SFC) techniques, or simply by direct infusion, provides much of the information sought by those engaged in dietary studies of natural and/or synthetic TAG.

We have been interested in the qualitative and quantitative analysis of TAG. In 1995, we reported the first applications of reversed-phase (RP)-HPLC/APCI-MS to a mixture of synthetic TAG (6). In that initial work, we described basic characteristics of APCI-MS mass spectra of TAG and showed that APCI-MS mass spectra of TAG molecules exhibited primarily two types of ions. One is the protonated molecule and the other is DAG-like ions. We noted that the amount of the protonated molecule depends on the number of sites of unsaturation in the molecule. TAG with more sites of unsaturation form larger protonated molecule abundances (and small $[DAG]^+$ abundances), whereas those TAG with few sites of unsaturation form only small abundances of the protonated molecule (and large abundances of $[DAG]^+$). In summary, the abundance of the protonated molecule in a mass spectrum obtained by APCI-MS is proportional to (increases with) the amount of unsaturation in a TAG molecule and is inversely proportional to the abundances

*Address correspondence at Department of Chemistry & Biochemistry, Florida Atlantic University, 777 Glades Rd., P.O. Box 3091, Boca Raton, FL 33431. E-mail: byrdwell@fau.edu

Abbreviations: APCI, atmospheric pressure chemical ionization; BUS, Bottom-Up Solution; CID, collision-induced dissociation; EIC, extracted ion chromatogram; ESI, electrospray ionization; ITMS, ion-trap MS; L, linoleic acid; Ln, linolenic acid; O, oleic acid; P, palmitic acid; RP, reversed-phase; S, stearic acid; SFC, supercritical fluid chromatography; TIC, total ion current chromatogram; TSQ, triple-stage quadrupole.

of the [DAG]+ fragment ions. Although proportional in some way, the relationship between the degree of unsaturation and the abundance of the protonated molecule is not simply linear. The nature of the relationship remains to be characterized.

APCI-MS of TAG

Early reports. Shortly after the first report (6), we studied several qualitative applications of RP-HPLC/APCI-MS to TAG in normal and genetically modified seed oils (32) and in industrial seed oils containing epoxide and alkyne functional groups (33). We went on to study the quantitative analysis of TAG using response factors and have presented these results in several reports (7,34,35).

Meanwhile, other researchers used APCI-MS for qualitative analysis of TAG, with an emphasis on the identification of regioisomers. Laakso and Voutilainen (8) used silver-ion (argentation) chromatography with APCI-MS for analysis of 10 structurally specific regioisomers of TAG. The authors combined the partial separation of isomers of polyunsaturated TAG by the silver-loaded column with the detection ability of APCI-MS. The authors presented data for several di-acid TAG, which contain two different FA, A and B, to form three possible TAG regioisomers: ABA, AAB, or BAA. The authors showed that the DAG-like fragment ions, [DAG]+, seen in the APCI-MS mass spectrum of a di-acid TAG were formed in proportions that were other than statistically expected, which led to the understanding that the ratio of the abundances of the fragment ions, [AA]+/[AB]+, can be correlated with the identities of specific regioisomers. They showed that the [DAG]+ fragment ion formed by the loss of the FA chain in the *sn*-2 position was less abundant than the [DAG]+ formed by loss of the *sn*-1 or *sn*-3 FA. This demonstrated that the relative amounts of the fragment ions could potentially be used to identify the positional isomers present in a mixture of TAG. Also in 1996, Laakso (36) applied RP-HPLC/APCI-MS to the analysis of berry oils. Although the chromatographic behavior of the isomeric TAG was reversed on the RP column compared with the silver-loaded column, the APCI-MS mass spectra exhibited the same trends as described above. Manninen and Laakso (37) later applied SFC coupled with APCI-MS for analysis of regioisomers in berry oils.

In 1996, Mottram and Evershed (10) also demonstrated that the loss of the acyl chain from the *sn*-1 or *sn*-3 position was energetically favored over loss from the *sn*-2 position. These authors, in collaboration with other colleagues, went on to report the identities of regioisomers in a variety of vegetable oils (11) and in animal fats (38). Both Mottram and Evershed and colleagues (10,11,38), and Laakso and coworkers (8,36,37) reported several important qualitative trends. First, they agreed that the DAG-like ion, [DAG]+, formed by loss of the FA chain in the *sn*-2 position was less abundant than the [DAG]+ formed by loss of the *sn*-1 or *sn*-3 FA for di-acid TAG. Mottram and Evershed (10) were the first to mention that the APCI-MS mass spectrum of a TAG having three different FA, a tri-acid TAG, showed three [DAG]+ fragments, and that the [DAG]+ ion that had the lowest abundance was the *sn*-1,3 [DAG]+ fragment formed by loss of the *sn*-2 FA chain. A TAG having three different FA is referred to as an ABC TAG; alternatively, it is termed a Type III TAG. Unless further specified, an ABC-type TAG can have six possible structures: ABC, BAC, BCA, CBA, CAB, and ACB. However, the *sn*-1 and *sn*-3 regioisomers cannot be distinguished by on-line APCI-MS without derivatization. To simplify reference to ABC-type TAG, they can be considered as ABC, BAC and BCA, with the understanding that the *sn*-1 and *sn*-3 positions can be reversed. So simply referring to a TAG as ABC cannot be assumed to represent one specific regioisomer having A at *sn*-1, B at *sn*-2, and C at *sn*-3. Because of the inherent ambiguity in the label ABC, we refer to this type of TAG as a Type III TAG herein, because no regiospecificity is inherently implied, and thus there is no inherent ambiguity.

The results of Laakso (36), Laakso and Voutilainen (8), Mottram, Evershed, and colleagues (10,11,38), and Laakso and Manninen (9) revealed that the [DAG]+ fragment ions formed by the loss of the *sn*-2 FA had the lowest abundance of the [DAG]+ fragment ions. Thus, the specific *sn*-1,3 [DAG]+ fragment could be identified. They also indicated that no preference for the *sn*-1 vs. *sn*-3 positions on the glycerol backbone of the TAG was observed. A preference was reported by Laakso and Voutilainen (8), Manninen and Laakso (37), and Laakso (36) that indicated that, for PUFA, a closer proximity of the double bonds to the glycerol backbone led to a larger abundance of the fragment formed by loss of the PUFA than when the double bonds were further away. Specifically, when γ-linolenic (n-6) acid (Ln) was compared with α-Ln (n-3), the former showed a more abundant [*sn*-1,3-DAG]+ fragment ion than the latter when the PUFA was in the *sn*-2 position.

Herein, when the APCI-MS data are used to specify the regiospecific structure of a TAG, the name of the TAG is placed in bold, as in **OPS**, compared with OPS, POS, or PSO (where S = stearic acid, P = palmitic acid, and O = oleic acid). This indicates that the *sn*-1,3 [DAG]+ (e.g., [**OS**]+) has been identified by its minimal abundance in an APCI-MS mass spectrum. Of course, these are also equal to **SPO**, compared with SPO, SOP, or OSP, all else being equal. This will be discussed further below.

Statistical and nonstatistical considerations for Type II TAG. A TAG having two different FA chains is referred to herein as a Type II TAG. It is also referred to as an ABA/AAB TAG. Of course, this is equal to ABA/BAA. These possibilities can also be referred to as ABA/(AAB/BAA). Since Type II TAG have two of one FA, A, and one of the other FA, B, there is a likelihood of 2/3 (= 66.67% statistical probability) that any [DAG]+ fragment would contain one A FA combined with a B FA, which would give either an [AB]+ or [BA]+ fragment ion, which are two possibilities with equivalent mass, in contrast to [AA]+. Since the [AB]+ and [BA]+ ions have the same mass, they are indistinguishable by APCI-MS, so these two ions may be considered as a single group and should represent 66.67% of the abundances of all [DAG]+ fragment ions, all else being equal. On the other hand, there is a 1/3 chance (= 33.33% statistical probability) that any [DAG]+ that is observed would contain two A FA, which would give the [AA]+ fragment, out of the three possible [DAG]+ fragment structures.

Statistical considerations can be used for determining what relative abundances of the [DAG]$^+$ fragment ions could be expected in an APCI-MS mass spectrum of a TAG. Based solely on statistical considerations, all Type II TAG contain two A FA and one B FA and so should give a ratio of abundances [AA]$^+$/([AB]$^+$ + [BA]$^+$) equal to (1/3)/(2/3) = 1/2, or 0.5. Regardless of their absolute abundances, from 100% to less than 1.00%, the ratio of the abundances of the [AA]$^+$ and [AB]$^+$ fragment ion *m/z* values should be 0.5. Observed conditions can lead to nonstatistical abundances of [AA]$^+$ and [AB]$^+$ [DAG]$^+$ fragment ions in APCI-MS mass spectra.

The [AA]$^+$ ion that is observed at a given *m/z* value will represent [*sn*-1,3-AA]$^+$, [*sn*-1,2-AA]$^+$, and [*sn*-2,3-AA]$^+$. Similarly, the [AB]$^+$ ion at a particular *m/z* value will represent [*sn*-1,3-AB]$^+$, [*sn*-1,2-AB]$^+$, and [*sn*-2,3-AB]$^+$, and also [*sn*-1,3-BA]$^+$, [*sn*-1,2-BA]$^+$, and [*sn*-2,3-BA]$^+$.

By using APCI-MS mass spectra of the pure regioisomers of *sn*-1,3 ABA TAG vs. *sn*-1,2 AAB TAG, it has been shown that the abundance of the [DAG]$^+$ fragment ion formed as [*sn*-1,3-AA]$^+$ from [**ABA** + H]$^+$ is smaller than that formed as [*sn*-1,2-AA]$^+$ from [**AAB** + H]$^+$, even though these ions are expected with equal statistical probability. Mottram and Evershed (10) and Hsu and Turk (39) mentioned that this indicated that the formation of the [*sn*-1,3-AA]$^+$ ion was energetically disfavored, because it involves loss of the *sn*-2 FA instead of one of the more labile *sn*-1 or *sn*-3 chains. Hsu and Turk (39), who used electrospray ionization (ESI) MS of TAG as their lithiated adducts, proposed that the *sn*-1 and *sn*-3 chains are promoted to leave by participation of the labile α-hydrogens of the neighboring FA. They suggest that the α-hydrogens of the middle FA are more labile than the α-hydrogens of the *sn*-1 or *sn*-3 chains and so help the *sn*-1 or *sn*-3 chains to leave more readily. Regardless of the specific mechanism that is assumed to operate, the observed ratios of [AA]$^+$/[AB]$^+$ are different for the different pure isomers of regiospecific TAG.

Table 1 shows the [AA]$^+$/[AB]$^+$ ratios for a variety of pure isomers, most of them commercially available. It is notable that the [AA]$^+$/[AB]$^+$ ratios of the two isomers are not equal for any

TABLE 1
Fragment Ratios Reported by Various Authors for Regiospecific Analysis by APCI-MS[a]

Authors[b]	Ionization method	AAB	[AA]$^+$/[AB]$^+$	ABA	[*sn*-1,3-AA]$^+$/ [*sn*-1,2- or *sn*-2,3-AB]$^+$
LV	APCI	PPO	0.89	POP	0.34
ME	APCI	PPO	0.95 ± 0.30	POP	0.20 ± 0.08
BN	APCI	PPO	0.87	POP	0.29
BN	ESI	PPO	0.68	POP	0.23
ML	APCI	PPO	0.79	POP	0.41
FHAFD	APCI	PPO	2.07[c]	POP	0.22
LV	APCI	OOP	0.70	OPO	0.09
BN	APCI	OOP	0.51	OPO	0.17
BN	ESI	OOP	0.67	OPO	0.24
ML	APCI	OOP	0.48	OPO	0.16
FHAFD	APCI	OOP	0.43	OPO	0.07
LV	APCI	OOLn (n-6)	1.97[c]	OLnO (n-6)	0.90[c]
ML	APCI	OOLn (n-6)	1.29[c]	OLnO (n-6)	0.63
L	APCI			OLnO (n-3)	0.17
L	APCI			OLnO (n-6)	0.64
LV	APCI	PPL	0.76		
ML	APCI	PPL	0.70		
FHAFD	APCI	PPL	2.99[c]	PLP	0.40
LV	APCI			SLS	0.38
ML	APCI			SLS	0.41
LV	APCI	SSP	0.56		
FHAFD	APCI	PPS	0.94	PSP	0.15
FHAFD	APCI	PPA	10.64[c]	PAP	1.56[c]
FHAFD	APCI	AAP	0.09	APA	0.02
BN	APCI	OOS	0.54		
BN	ESI	OOS	0.64		
FHAFD	APCI	OOS	0.44	OSO	0.11
ME	APCI	SSO	1.07 ± 0.16	SOS	0.29 ± 0.12
L	APCI	SSO	1.33[c]		
FHAFD	APCI	SSO	1.81[c]	SOS	0.26
L	APCI	LLO	1.24[c]		
JJF	APCI	LLO	0.7028	LOL	0.2289
FHAFD	APCI	LLS	1.52[c]	LSL	0.37

[a]Ratio of the abundances of [AA]$^+$ to [AB]$^+$ in AAB and ABA TAG.
[b]LV: Laakso and Voutilainen (8); ME: Mottram and Evershed (10); BN: Byrdwell and Neff (43); ML: Manninen and Laakso (SFC/APCI-MS) (37); L: Laakso (36); JJF: Jakab, Jablonkai, and Forgacs (42); FHAFD: Fauconnot, Hau, Aeschlimann, Fay, and Dionisi (40).
[c]Much higher than expected statistically. APCI, atmospheric pressure chemical ionization; SFC, supercritical fluid chromatography; P, palmitic acid; S, stearic acid; O, oleic acid; Ln, linolenic acid; A, arachidonic acid.

TAG. The two pure isomers each give different characteristic ion abundance ratios [AA]$^+$/[AB]$^+$, and these are almost all at nonstatistically expected ratios. The variation of the [AA]$^+$/[AB]$^+$ ratio with different regioisomers demonstrates that the positional placement of the FA on the glycerol backbone exerts a nonstatistical effect on the abundances of the ions formed by APCI-MS.

When comparing APCI-MS spectra of TAG, one must differentiate between (i) the APCI-MS mass spectrum of an individual TAG with unknown regiospecificity; (ii) the APCI-MS mass spectrum of a pure positional isomer of a TAG; (iii) a mass spectrum of a mixture of pure positional isomers; (iv) a mass spectrum of mixtures of several isomers in synthetic mixtures; and (v) mass spectra of combinations of TAG in natural mixtures. Knowing the type of sample being examined is essential to proper use of the [AA]$^+$/[AB]$^+$ ratio obtained from the sample. The actual [AA]$^+$/[AB]$^+$ ratio observed for any TAG or mixture of TAG is due to nonstatistical effects acting in combination with the expected ratio of 0.5. When considering the variety of pure TAG and TAG mixtures, the nonstatistical effects on the [AA]$^+$/[AB]$^+$ ratio can include: (i) differences in composition from 100% isomers to combinations of TAG regioisomers in TAG mixtures; (ii) formation of the *sn*-1,3 isomer, which is energetically disfavored under APCI-MS conditions, leading to a lower [AA]$^+$/[AB]$^+$ ratio when [AA]$^+$ is the *sn*-1,3 isomer; and (iii) a disparity in the amount of unsaturation in FA A vs. B, and (iv) differences in the positions of the sites of unsaturation in the FA chains.

Characterization of the relationship between the identities of TAG structures and the [DAG]$^+$ fragment ions in the APCI-MS mass spectra of TAG has been the subject of primarily qualitative investigations of regioisomers of TAG. Such studies have shown that each of the foregoing categories of TAG and TAG mixtures gives different [AA]$^+$/[AB]$^+$ ratios, based on the structure(s) of the TAG. Pure regioisomers give [AA]$^+$/[AB]$^+$ ratios that represent the upper and lower boundaries of the [AA]$^+$/[AB]$^+$ ratio that should be obtained by any mixture of regioisomers of a particular TAG.

Using APCI-MS mass spectra for qualitative analysis of TAG regioisomers. As mentioned, Laakso and Voutilainen (8), Mottram and Evershed and colleagues (10,11), and Laakso (36) showed that the [DAG]$^+$ fragment ions formed by the loss of the *sn*-2 FA chain have the lowest abundance of the [DAG]$^+$ fragment ions. The APCI-MS mass spectra of pure TAG isomers reported by the above authors demonstrated that the ion abundances and, more conveniently, the ratio of the ion abundances, [AA]$^+$/[AB]$^+$, are expected to change with the regioisomeric composition of a mixture of TAG regioisomers. These authors reported that if the FA A chains in an ABA/AAB/BAA TAG are located in the *sn*-1,3 positions, i.e., [*sn*-1,3-AA]$^+$, the [DAG]$^+$ fragment ion has a lower abundance than the 0.5 ratio statistically expected.

This tendency was used by Laakso (36) and Manninen and Laakso (37) to describe, in a semiquantitative way, the compositions of regioisomers in natural berry and other oils. This represented an early attempt at quantitative analysis of the relative amounts of regioisomers. These articles described another interesting observation that must be taken into consideration. They showed that the positions of the double bonds in polyunsaturated TAG had a substantial impact on the relative abundances of [AA]$^+$ and [AB]$^+$ fragment ions. This trend can clearly be seen in Table 1 by comparing the [AA]$^+$/[AB]$^+$ ratios of the O(n-6)LnO and O(n-3)LnO regioisomers [where O = oleic acid, (n-6)Ln = γ-linolenic acid, and (n-3)Ln = α-linolenic acid]. The O(n-3)LnO isomer has a low [AA]$^+$/[AB]$^+$ ratio (= 0.17) typical of most pure *sn*-1,3 isomers. On the other hand, the O(n-6)LnO isomer has [AA]$^+$/[AB]$^+$ ratios (= 0.63 to 0.90) that are higher than the 0.5 that is statistically expected, and the OO(n-6)Ln isomer gives an even higher [AA]$^+$/[AB]$^+$ ratio. Observations such as these constitute the trends that can be correlated with certain ratios.

In addition to the observations previously mentioned, Table 1 shows several other trends. First, every ABA TAG gave an [AA]$^+$/[AB]$^+$ ratio that was smaller than the ratio from the corresponding AAB TAG. This, of course, reflects the fact that the loss of *sn*-2 chain is energetically disfavored. When the [AA]$^+$ corresponds to the *sn*-1,3 isomer, its abundance is diminished. Another trend is that the [AA]$^+$/[AB]$^+$ ratio for almost all *sn*-1,3 isomers, ABA, is substantially below the statistically expected value of 0.5. The isomer that contained the (n-6)Ln was the exception to this trend. It can also be seen in Table 1 that most, but not all, AAB isomers gave [AA]$^+$/[AB]$^+$ ratios larger than the statistically expected value of 0.5. Hence, the [AA]$^+$/[AB]$^+$ ratio may by more useful for identifying some AAB TAG (e.g., PPO, where P = palmitic acid) than others (e.g., OOP).

Recent articles allow us to move toward a more numeric and quantitative method for analysis of TAG regioisomers. Articles cited below describe approaches that have been demonstrated to be useful to obtain a quantitative estimation of the percentage compositions of any regioisomers for which calibration standards are available. However, three other qualitative considerations should be mentioned. First, the [DAG]$^+$ fragment ions that are produced by APCI-MS are isobaric with a normal intact DAG minus a water group. In the process of leaving, the R_xCOO that is lost from a TAG in the APCI source takes the glycerol oxygen with it to form an [M + H − RCOOH]$^+$ ion. These same [DAG]$^+$ fragment ions are formed during ESI-MS/MS of TAG. According to Hsu and Turk (39), who performed deuterium-labeled experiments on lithiated TAG by ESI-MS, the carbonyl oxygen of the FA neighboring the one that is lost carries out nucleophilic attack on the glycerol carbon atom that contains the leaving group, forming a five- or six-membered ring, with the participation of the α-hydrogen of the ring-attached FA chain.

Second, plants produce TAG with regiospecificity as well as single enantiomers of asymmetric TAG having the L configuration. TAG that are produced by the chemical interesterification of glycerol and FA, such as the 35-TAG mixture used as an example herein, are a mixture of enantiomers.

Third, the integrated areas under the ion chromatograms of the [M + H]$^+$ ion and of [DAG]$^+$ fragment ions over a specific time range can be used to produce a mass spectrum that appears

the same as an averaged mass spectrum across the same time range. Since all [DAG]$^+$ fragments originate in the APCI source, all fragments that occur from a particular TAG must occur at the retention time associated with that TAG. So integrated areas under ion chromatograms corresponding to the fragments will be in the same proportions as the ion abundances in an averaged mass spectrum across the same time range. Therefore, quantitative estimation of the regioisomeric composition based on the [AA]$^+$/[AB]$^+$ ratio can use either integrated areas under ion chromatograms or abundances in an average mass spectrum across the chromatographic peak. The method for the quantitative analysis of TAG molecular species that we developed and have reported extensively before (7,34,35) uses the areas under ion chromatograms for quantitative analysis of TAG molecular species. These same data will also be used to construct the [AA]$^+$/[AB]$^+$ ratio and other ratios presented herein. Fauconnot *et al*. (40) also used areas under ion chromatograms for quantitative analysis of TAG regioisomers. The areas under the peaks of the [M + H]$^+$ and [DAG]$^+$ fragment ions determined by APCI-MS were used to calculate the Critical Ratios given in Table 2.

Using APCI-MS mass spectra for quantitative analysis of TAG regioisomers. In 2003, Byrdwell (29) cited the need for improved methods for quantitative analysis of regioisomers. In discussing the quantification of TAG positional isomers, he said:

> A comprehensive study using the greatest possible number of positional isomers with disparate amounts of unsaturation needs to be undertaken for both APCI-MS and ESI-MS/MS. In our initial work, we did not address this issue because we felt that it would require lengthy quantification of the abundances of DAG fragment ions from a large series of standards to address the issue adequately. We believed that the proper approach would be to perform APCI-MS of a wide range of structured lipids, determine the ratios of DAG fragment ions that are produced, and then interpolate between the ratios for the 1,2- versus the 1,3- isomers to get a quantitative estimation of the relative amounts of each of these isomers in real samples. Unfortunately, only a limited number of structured lipids are commercially available, so full treatment of this subject will require synthesis of an array of structured lipids, followed by their analysis. Until then, great care must be exercised in using APCI-MS for positional isomer identification, especially for polyunsaturated TAG (41).

A recent article by Jakab, Jablonkai, and Forgacs (42) constitutes the first example of the process described above. Jakab *et al*. (42) described the use of APCI-MS for analysis of mixtures of pure positional isomers of LOL/LLO (where L = linoleic acid). They demonstrated that a calibration curve could be constructed that plotted the ratio of abundances of [DAG]$^+$ fragment ions vs. the percentage of the LLO isomer (the LOL isomer percentage could just as easily be plotted). This calibration curve, reproduced in Figure 1, accomplished quantification of the relationship between the abundances of ions in APCI-MS mass spectra and, more specifically, the ratio of abundances, [AA]$^+$/[AB]$^+$ (i.e., [LL]$^+$/[LO]$^+$), to the relative amount of the **ABA** isomer, i.e., the LOL isomer.

The equation shown by Jakab *et al*. (42) and seen in Figure 1 is the least-squares best-fit line equation, based on 11 mixtures representing the concentration range from 0% LOL/(LLO + OLL) to 100% LOL/(LLO + OLL). Of course, 0% LOL represents 100% (LLO + OLL), and, conversely, 100% LOL represents 0% (LLO + OLL). Any mixture of TAG should contain an amount of the ABA isomer somewhere between 0 and 100%, so this calibration line should apply to any mixture of these TAG, to correlate the amount of the [*sn*-1,3-AA]$^+$ isomer with the [AA]$^+$/[AB]$^+$ ratio.

These authors (42) simplified the complex situation mentioned by Byrdwell (41) by examining only the two isomers of one TAG. Nevertheless, they clearly demonstrated that the approach—of determining the DAG fragment ratios for a series of standard solutions and then interpolating the ratio of positional isomers from the DAG fragment ratios of actual samples—is effective for determining the relative amounts of two isomers. Of course, every TAG for which positional isomers are to be determined requires isomeric standards and multiple solutions of each standard pair of isomers to be quantified. As Figure 1 shows, Jakab *et al*. (42) used 11 solutions to cover the range from 0 to 100%, inclusive, by 10% increments. Five replicate measurements of each of these standard solutions represent at least 55 experiments that were performed to produce the calibration line shown in Figure 1. These experiments would need to include a larger number of pure regiospecific standards to be more widely applicable. Nevertheless, the approach taken by Jakab *et al*. (42) appears to be the most appropriate approach for accurate quantitative estimation of the relative amounts of regioisomers.

The full set of standard solutions serves to demonstrate that there is an approximately linear relationship (r^2 = 0.9884) between the [AA]$^+$/[AB]$^+$ ratio and the percent composition of regioisomers. One could say that the [AA]$^+$/[AB]$^+$ ratio can be used as a Critical Ratio for the determination of the percentage composition of mixtures of regioisomeric standards. Therefore, the question arises: Can this accurate quantitative analysis of TAG regioisomers be accomplished with fewer experimental data? Can one derive the same or similar results from a less extensive set of experiments? If so, then this would be an advantage. The first simplification would be to construct a line directly between the two end points of the line. This is experimentally equal to determining only the mass spectra and therefore the [AA]$^+$/[AB]$^+$ ratios for 100% pure **LLO** (0% **LOL**) and for 100% pure **LOL** (0% **LLO**). The equation for the line formed between the two average (n = 5) end point values in Figure 1 can be compared with the line formed by the least-squares best-fit line end points.

For instance, in the data presented by Jakab *et al*. (42), the observed extremes had average [AA]$^+$/[AB]$^+$ ratios of 0.7028 and 0.2289, for 100% **LLO** (= 0% **LOL**) and 100% **LOL** (= 0%

TABLE 2
TAG Composition and Critical Ratios from the Synthetic 35-TAG Mixture[a], Determined by APCI-MS (three replicates)

ECN	TAG	Statistical % comp.	Adjusted APCI-MS	$[M + H]^+$/ $\Sigma[DAG]^+$	±SD	$[AA]^+/[AB]^+$	±SD	±SD2	$[BC]^+/[AB]^+$	±SD
48	PPP	0.84	0.75	0.00	0.00					
54	SSS	0.94	0.82	0.00	0.00					
48	OOO	0.85	0.88	3.24	0.39					
42	LLL	0.77	0.78	120.07	12.40					
36	LnLnLn	0.62	0.78	222.80	22.45					
50	PSP/PPS	2.62	2.40	0.00	0.00	49.26	0.84	0.84		
48	POP/PPO	2.54	2.49	0.55	0.12	65.28	2.35	2.35		
46	PLP/PPL	2.45	2.87	0.40	0.28	84.11	2.45	2.45		
44	PLnP/PPLn	2.28	2.53	12.81	2.34	69.94	3.11	3.11		
52	SPS/SSP	2.72	2.44	0.00	0.00	40.91	3.31	3.31		
52	SOS/SSO	2.73	2.48	0.45	0.04	75.14	2.78	2.78		
50	SLS/SSL	2.64	2.96	0.42	0.12	82.89	2.08	2.08		
48	SLnS/SSLn	2.45	2.75	9.59	1.12	60.98	3.16	3.16		
48	OPO/OOP	2.55	2.72	1.89	0.19	36.12	1.42	1.42		
50	OSO/OOS	2.65	2.76	1.12	0.32	39.82	1.73	1.73		
46	OLO/OOL	2.47	2.54	11.93	1.12	50.10	2.20	2.20		
44	OLnO/OOLn	2.30	2.27	36.94	3.35	41.62	2.52	2.52		
44	LPL/LLP	2.38	2.00	27.64	8.83	88.84	9.62	9.62		
46	LSL/LLS	2.47	2.29	43.47	8.73	76.07	8.61	8.61		
44	LOL/LLO	2.39	2.33	44.44	9.15	74.62	7.01	7.01		
40	LLnL/LLLn	2.15	2.21	101.35	36.30	51.97	17.86	3.70		
40	LnPLn/LnLnP	2.06	1.94	101.33	24.18	74.69	17.68	13.63		
42	LnSLn/LnLnS	2.13	1.96	61.31	12.99	95.10	20.10	10.10		
40	LnOLn/LnLnO	2.07	2.26	101.34	43.98	83.80	34.13	9.97		
38	LnLLn/LnLnL	2.00	2.15	128.01	26.00	64.08	12.94	5.77		
50	OPS	5.27	5.11	0.47	0.09	37.64	2.06		69.79	2.12
48	SPL	5.09	5.89	0.46	0.11	35.39	2.50		59.43	2.95
46	SPLn	4.73	5.42	9.28	1.57	39.78	2.36		76.70	3.46
46	LOP	4.93	4.57	6.44	1.33	40.39	2.10		98.27	2.51
44	LnOP	4.59	4.60	27.18	7.84	42.00	4.41		91.76	5.68
42	LnLP	4.43	3.78	48.86	18.13	36.71	13.38		73.38	23.84
48	LOS	5.11	5.72	7.45	0.87	43.86	2.99		85.70	4.63
46	OLnS	4.75	4.38	19.95	5.10	42.47	1.97		89.53	2.14
44	LnLS	4.59	4.00	45.35	14.32	38.65	11.15		78.57	20.52
42	LLnO	4.45	4.20	56.61	24.69	40.18	16.88		77.66	26.09
	Sum	100.01	100.03			$= [AC]^+/([AB]^+ + [BC]^+)$				

[a]ECN, equivalent carbon number = # carbon atoms in FA chains – (2 × # sites of unsaturation); Ln, 18:3, linolenic acid; L, 18:2, linoleic acid; O, 18:1, oleic acid; S, 18:0, stearic acid; P, 16:0, palmitic acid. The statistical composition is the composition calculated based on the FA composition. The adjusted APCI-MS composition is the composition determined by three replicate chromatographic runs, adjusted using response factors calculated from the FA composition (35). SD2, simple standard deviation of the three numberic $[AA]^+/[AB]$ ratio values. For other abbreviations see Table 1.

LLO), respectively. These values are shown in Table 1. Similarly, each set of $[AA]^+/[AB]^+$ ratios of TAG positional isomers in Table 1 defines the range of DAG fragment ion ratios that should be encountered in APCI-MS (as well as some ESI-MS) mass spectra of TAG. An equation of the line that approximately describes the $[AA]^+/[AB]^+$ ratio for any combination of TAG positional isomers can be constructed from these two end points. If one puts the line in Figure 1 in the form of $y = mx + b$, then $y = ([AA]^+/[AB]^+) = m \cdot (\% \textbf{LOL}) + b$. In this equation, b would equal the $([AA]^+/[AB]^+)$ ratio at 0% **LOL**. In terms of x and y, the coordinates of the two end points would be (0% **LOL**, $([AA]^+/[AB]^+)_{AAB}$) and (100% **LOL**, $([AA]^+/[AB]^+)_{ABA}$), where the subscripts represent the $([AA]^+/[AB]^+)$ ratios of pure standards of AAB and ABA, i.e., **LLO** (= 0% **LOL**) and **LOL**, which would be explicitly: (0%, 0.7028), (100%, 0.2289). The equation of the line constructed from these end points would be: $m = (\Delta y)/(\Delta x) = (y_2 - y_1)/(x_2 - x_1) = (((([AA]^+/[AB]^+)_{ABA}) -$

$([AA]^+/[AB]^+)_{AAB}))/(100 - 0)$ and $b = ([AA]^+/[AB]^+)_{AAB}$. In terms of the data reported by Jakab *et al.* (42), this gives: $m = (\Delta y)/(\Delta x) = (y_2 - y_1)/(x_2 - x_1) = ((([LL]^+/[OL]^+)_{LOL}) - ([LL]^+/[OL]^+)_{LLO}))/(100 - 0) = (0.2289 - 0.7028)/(100 - 0) = (-0.4739)/(100) = -0.004739$; and $b = ([LL]^+/[OL]^+)_{LLO} = 0.7028$. From this line comes the relationship:

$$\left(\frac{[LL]^+}{[OL]^+}\right) = (-0.004739) \cdot (\% \textbf{LOL}) + 0.7028$$

This equation can be seen to be in the general form:

$$\left(\frac{[AA]^+}{[AB]^+}\right)_{Obs} = \left(\left(\left(\frac{[AA]^+}{[AB]^+}\right)_{ABA} - \left(\frac{[AA]^+}{[AB]^+}\right)_{AAB}\right) \cdot \left(\frac{\% \textbf{ABA}}{100}\right) + \left(\frac{[AA]^+}{[AB]^+}\right)_{AAB} \quad [1]$$

To get a line with a positive slope, the y values, $([AA]^+/[AB]^+)$, can be arranged from lowest to highest, which means that the x values should be put in terms of % LLO to make x also go from low to high as $([AA]^+/[AB]^+)$ goes from low to high. The
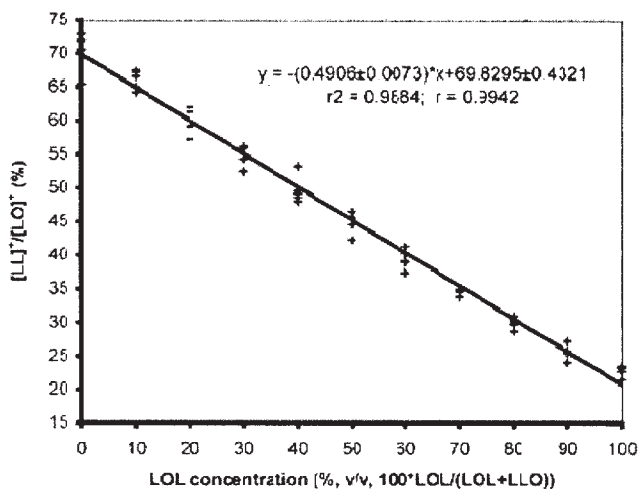
FIG. 1. Ratio of the [LL]⁺ and [LO]⁺ fragment ions (%) in mixtures of LOL and LLO at various percentages (calibration curve). L, linoleic acid; O, oleic acid. From A. Jakab, I. Jablonkai, and E. Forgacs, *Rapid Commun. Mass Spectrom. 17*, 2295–2302 (2003). Copyright John Wiley & Sons Ltd. Reprinted with permission.

equivalent points that would give a positive slope would be: (x_1, y_1), $(x_2, y_2) = (0\% \text{ LLO}, ([AA]^+/[AB]^+)_{ABA})$, $(100\% \text{ LLO}, ([AA]^+/[AB]^+)_{AAB})$, or $(0, 0.2289)$, $(100, 0.7028)$. In terms of the average end point data by Jakab *et al.* (42), this would be a line having the equation:

$$\left(\frac{[LL]^+}{[LO]^+}\right) = (0.004739) \cdot (\% \textbf{ LLO}) + 0.2289$$

This equation can be written in a general form as:

$$\left(\frac{[AA]^+}{[AB]^+}\right)_{Obs} = \left(\left(\frac{[AA]^+}{[AB]^+}\right)_{AAB} - \left(\frac{[AA]^+}{[AB]^+}\right)_{ABA}\right) \cdot \left(\frac{\% \textbf{AAB}}{100}\right) + \left(\frac{[AA]^+}{[AB]^+}\right)_{ABA} \qquad [2]$$

One can solve Equations 1 and 2 for the following relationships.

One may rearrange Equation 1 (and multiply by $(-1)/(-1)$) to solve for the % **ABA** as follows:

$$(\% \textbf{ ABA}) = \left(\frac{\left(\frac{[AA]^+}{[AB]^+}\right)_{AAB} - \left(\frac{[AA]^+}{[AB]^+}\right)_{Obs}}{\left(\frac{[AA]^+}{[AB]^+}\right)_{AAB} - \left(\frac{[AA]^+}{[AB]^+}\right)_{ABA}}\right) x100 \qquad [3]$$

Similarly, one may rearrange Equation 2 to solve for the % **AAB** as follows:

$$(\% \textbf{ AAB}) = \left(\frac{\left(\frac{[AA]^+}{[AB]^+}\right)_{Obs} - \left(\frac{[AA]^+}{[AB]^+}\right)_{ABA}}{\left(\frac{[AA]^+}{[AB]^+}\right)_{AAB} - \left(\frac{[AA]^+}{[AB]^+}\right)_{ABA}}\right) x100 \qquad [4]$$

And these two percentages share the relationship that % **LOL** + % LLO (= **LLO + OLL**) = 100%.

Therefore, whenever one percentage is known, % ABA or % AAB, the other may be known as % AAB (= % **AAB** + % **BAA**) = 100 − % **ABA** or % **ABA** = 100 − % AAB, respectively.

Equations 3 and 4 allow the direct calculation of the percentage composition of either one regiospecific isomer, % **ABA**, or the sum of two isomers, % AAB (= % **AAB** + % **BAA**). Of course, the ([AA]⁺/[AB]⁺) ratios of pure known standards of each individual TAG must be determined for each TAG for which quantification is sought. These ([AA]⁺/[AB]⁺) ratios of pure known standards potentially can be tabulated. We have compiled the ([AA]⁺/[AB]⁺) ratios of pure known standards before and have noted the references that allow the instrument type and conditions under which these values were obtained to be determined. If a researcher has a similar instrument and obtains ([AA]⁺/[AB]⁺) ratios of pure known standards on his or her instrument that are similar to those of the tabulated values, then these results lend credibility to the possibility that tabulated values might be helpful in assessing the percentages of regioisomers in a TAG mixture of unknown composition. The minimal approach to linear interpolation would require the analysis of two pure regioisomeric standards, and then the ([AA]⁺/[AB]⁺)_{Obs} ratio of a mixture of unknown regioisomeric content might be interpolated between the ([AA]⁺/[AB]⁺) ratios obtained for pure isomers, and a quantitative estimate of the % **ABA** or % AAB could be obtained with relative ease.

For example, Table 1 shows the ratio of [PP]⁺/([PO]⁺,[OP]⁺), which is more simply referred to as the [PP]⁺/[PO]⁺ ratios for two commercially available regiospecific isomers, POP and PPO. Four out of five authors using APCI-MS have reported low values for the [PP]⁺/[PO]⁺ = [AA]⁺/[AB]⁺ ratio, in the range of 0.20 to 0.34 (8,10,40,43). Three of four of those authors reported [AA]⁺/[AB]⁺ ratios between 0.87 and 0.95 for pure PPO, by APCI-MS. The fourth example of POP/PPO data in Table 1 had a higher [AA]⁺/[AB]⁺ ratio for POP (= 0.41) and a lower value for PPO (= 0.79) (37). Our reports and those of many others have been obtained on TSQ 700 and 7000 tandem triple-stage quadrupole instruments. The data by Fauconnot *et al.* (40) included in Table 1 were obtained on a tandem sector quadrupole instrument with a Z-spray interface. Unlike collision-induced dissociation (CID), which exhibits differences between TSQ and ion-trap MS (ITMS) instruments in fragment ions formed, full-scan APCI-MS mass spectra on a TSQ instrument can appear nearly identical to an APCI-MS mass spectrum obtained on an ITMS instrument. The reason for this is that fragmentation occurs in the ionization source, so the [DAG]⁺ fragment ions are formed before they reach the first or subsequent mass analyzers, whether quadrupole or ion trap. In fact, the APCI ionization heads on the TSQ 700 and LCQ Deca instruments in our laboratory are nearly identical and have interchangeable parts but are not themselves interchangeable between instruments. This is in contrast to CID, which exhibits different ratios of fragment ions in TSQ vs. ITMS instruments. Hsu and Turk (44) reviewed the mechanisms of fragmentation of phospholipids and TAG by ESI-MS/MS in their recent book chapter.

The equations above, which are based on only two pure regioisomers, must be compared with the more accurate line described by the full set of standards analyzed by Jakab *et al.* (42). The equation for the best-fit line given in Figure 1 is $y = 0.4906 \cdot x + 69.83$, but the y axis gives [AA]⁺/[AB]⁺ as a percentage. The

equation of the line for the $[AA]^+/[AB]^+$ as a pure ratio (not a percentage) would therefore be:

$$\left(\frac{[LL]^+}{[LO]^+}\right) = (-0.004906)\cdot(\%\,\mathbf{LOL}) + 0.6983$$

The best-fit line gives an ($[AA]^+/[AB]^+$) ratio of 0.6983 for 0% LOL and 0.2077 for 100% LOL.

These best-fit values for the pure positional isomers can be inserted into Equation 3 to give the following equation:

$$(\%\,\mathbf{LOL}) = \left(\frac{0.6983 - \left(\dfrac{[AA]^+}{[AB]^+}\right)_{Obs}}{0.6983 - 0.2077}\right) x100$$

This can be used to calculate the % LOL from the $([AA]^+/[AB]^+)_{Obs}$ ratio for a mixture. For instance, a hypothetical $[AA]^+/[AB]^+$ ratio of 0.5348 would give a calculated % LOL of 33.33%. This is the $[AA]^+/[AB]^+$ ratio that would be expected from a statistically randomly distributed combination of two FA, L and O, onto the three possible positions of the glycerol backbone of a TAG, on the instrument and under the conditions reported by Jakab *et al.* (42). Thus, nonstatistical influences on the abundances of the $[DAG]^+$ fragments formed shift the $[AA]^+/[AB]^+$ ratio from the statistically expected value of 0.5 to a hypothetical $[AA]^+/[AB]^+$ ratio of 0.5348, calculated from the best-fit line using 11 standard solutions.

For comparison, the equation based only on the average values of the two pure standards, given in the form of Equation 3 above, is:

$$(\%\,\mathbf{LOL}) = \left(\frac{0.7028 - \left(\dfrac{[AA]^+}{[AB]^+}\right)_{Obs}}{0.7028 - 0.2289}\right) x100$$

This equation gives a calculated % LOL of 35.45% from the same ($[AA]^+/[AB]^+)_{Obs}$ ratio of 0.5438. Although this is not identical to the 33.33% obtained from the best-fit line made from 11 standards, it is a good approximation of the more accurate value and can be obtained with only two authentic standards, instead of a large number of mixtures containing various compositions. Certainly in the range 0 to 100%, narrowing the composition down to 35.45% LOL would represent a good approximation of 33.33%, but with much less data required. Of course, if greater accuracy is required for a particular application, more standards can be analyzed, and the same equations can be used with the slope and intercept calculated from the best-fit line.

The above equations allow one to quantify the relative amounts of positional isomers in a mixture. It is expected that the $[AA]^+/[AB]^+$ ratios of a greater variety of regiospecific isomers will be reported and compared, and this method will be applied to a greater variety of TAG mixtures. These equations also demonstrate the utility of the $[AA]^+/[AB]^+$ ratio for determination of the regiospecific composition of a TAG mixture. This ratio allows one to move from qualitative analysis of TAG to a more quantitative approximation of the composition of TAG regioisomers.

Even more recently, another article appeared that describes the linear relationship between the abundances of $[AA]^+$ and $[AB]^+$ fragments and the compositions of known standard mixtures of TAG regioisomers. Fauconnot *et al.* (40) reported calibration curves for regioisomers of seven pairs of Type II TAG standards. The authors showed the growing importance of the $[AA]^+/[AB]^+$ ratio in their statement: "Identification of the major regioisomers of an AAB/ABA pair of TGs was shown to be enabled by comparing the ratios of abundances of $c(AA^+)/c(AB^+)$ with the statistically expected value of 0.5."

In their calibration curves, though, they plotted what they called the *regioisomeric purity*, r_{AA}, which they defined as:

$$r_{AA} = \frac{100\%c(AA^+)}{c(AA^+) + c(AB^+)}$$

This equation can be shown to be equivalent to

$$r_{AA} = \frac{1}{1 + \dfrac{1}{\dfrac{(AA^+)}{(AB^+)}}} x100$$

It is much more convenient and useful to use the ratio $[AA]^+/[AB]^+$ directly. This is a simpler ratio, which can be used directly with Equations 3 and 4 to calculate the relative percentages of the regioisomers. This is also the approach used by Jakab *et al.* (42). Nevertheless, the data by Fauconnot *et al.* (40) also demonstrated the linear relationship between the $[AA]^+/[AB]^+$ ratio and the percent composition of the regioisomers.

CONSTRUCTION OF THE CRITICAL RATIOS

Construction and use of the $[AA]^+/[AB]^+$ ratio for a Type II TAG. If the APCI-MS or ESI-MS mass spectrum of a Type II TAG exhibits a ratio of ion abundances other than 0.50, then it is due to nonstatistical influences. Several of the nonstatistical influences already have been mentioned, but another nonstatistical influence that has been observed deserves further discussion. Laakso and Voutilainen (8), Manninen and Laakso (37), and Laakso (36) reported results for the effect of unsaturation on the abundances of $[DAG]^+$ fragment ions and showed that O(n-3)LnO behaved much like a normal, less unsaturated TAG, by exhibiting a low $[AA]^+/[AB]^+$ ratio of 0.17 (Table 1), owing primarily to the well-reported effect of being the $[DAG]^+$ fragment formed by loss of the *sn*-2 chain. Conversely, they showed that when the double bonds were closer to the carbonyl end of the chain, i.e., n-6 vs. n-3, a much greater amount of the [*sn*-1,3-AA]$^+$ fragment was formed, which led to a larger $[AA]^+/[AB]^+$ ratio, which had a larger value than the 0.5 that was statistically expected. The authors attributed the difference in the n-6 polyunsaturated TAG to the fact that the proximity of the double bonds to the carbonyl end of the chain helped make the PUFA a better leaving group. This made the polyunsaturated group, even in the *sn*-2 position, easily lost. This was reflected in the higher $[AA]^+/[AB]^+$ ratio for all of the n-6 FA, which, for the ABA isomer, was higher than statistically expected, and which, for the

AAB/BAA isomers, was higher than 1. Thus, more information could potentially be derived from the [AA]$^+$/[AB]$^+$ ratio.

The only reported [AA]$^+$/[AB]$^+$ ratio greater than 1 for a pure synthetic [*sn*-1,3-AA]$^+$ isomer was for *sn*-1,3-PAP (dipalmitoyl, arachidonyl TAG, 16:0, 20:4, 16:0) by Fauconnot *et al.* (40), seen in Table 1. The authors used an instrument with a Z-spray interface, whereas most other reports were based on data from ThermoFinnigan TSQ or LCQ instruments. Several values obtained on this instrument and shown in Table 1 were higher than the values obtained by other instruments, and many were much higher than the statistically expected value of 0.5. A notable exception was the TAG regioisomer pair APA/AAP. These both gave a virtually nonexistent [AA]$^+$ ion, the diarachidonyl [DAG]$^+$ fragment, apparently because the arachidonic chain is lost so easily that two of them cannot both remain attached. Arachidonic acid is an n-6 FA, like the (n-6)Ln in the OLnO/OOLn pair that Laakso and Voutilainen (8) and Manninen and Laakso (37) reported. The proposition that n-6 arachidonic acid is more easily lost would also explain why the [AA]$^+$/[AB]$^+$ ratios of the PAP/PPA isomer standards were much higher than statistically expected. If the arachidonic chain is lost easily from the TAG PAP because it is an n-6 FA, this would explain why a higher than expected abundance of the [PP]$^+$, dipalmitoyl DAG fragment ion, was observed. This again demonstrates that the [AA]$^+$/[AB]$^+$ Critical Ratio can be used to correlate observations in mass spectra with structural characteristics.

Another benefit to constructing the [AA]$^+$/[AB]$^+$ ratio is that two abundances, [AA]$^+$ and [AB]$^+$, which are two separate numbers, can now be represented by only one number, the numeric ratio [AA]$^+$/[AB]$^+$. It will be demonstrated that, using the [AA]$^+$/[AB]$^+$ Critical Ratio, both abundances can be accurately reconstructed from this one number when classified correctly. This means that the same amount of information can be conveyed in less space, one number instead of two. When this number and one other number are processed through the Bottom-Up Solution (BUS), the complete mass spectrum of a Type II TAG can be reproduced and would exhibit two [DAG]$^+$ fragment ion abundances, [AA]$^+$ and [AB]$^+$, and a protonated molecule abundance, for three abundances. These three ions constitute all of the primary peaks that provide the M.W. and DAG fragment structural information. The [AA]$^+$/[AB]$^+$ ratio can be used to store two of the three numbers for that mass spectrum as one ratio. Then a second ratio is used to provide the third value, and the relationship between the third value and the first two. The second ratio is the [MH]$^+$/Σ[DAG]$^+$ ratio, which provides information for the value of [M + H]$^+$ and its relationship to [AA]$^+$ and [AB]$^+$. This ratio will be discussed shortly. Masses for each of these ions are specified by the *m/z* value from which came each peak area integrated over time. The known masses are compared with tabulated values, and all possible identities for each mass are known, including isobaric species. Chromatographic information is used with the mass information to identify and differentiate isobaric species (7,34,35).

The [AA]$^+$/[AB]$^+$ ratio as provided at face value can be used

in Equations 3 and 4 to provide direct information regarding the percent compositions of regioisomers, compared with standard solutions. This Critical Ratio, along with one other number (the [MH]$^+$/Σ[DAG]$^+$ ratio), can be used with the BUS to accurately reproduce the exact three abundances that represent the mass spectrum. These characteristics of the BUS—of saving space and providing more information in fewer values—will be seen with the other Critical Ratios as well. All Critical Ratios provide more information than the raw abundances, but the raw abundances can be reconstructed at will by processing them through the BUS.

Construction of the [MH]$^+$/Σ[DAG]$^+$ ratio for all TAG. Durin*g* the preparation of a recent review (45), Byrdwell sought quantifiable numerical values that could be related to observed mass spectrometric fragmentation characteristics. Some empirically determined Critical Ratios were sought that could be used to describe, in a more quantitative way, the characteristics that were ascribed to APCI-MS mass spectra in that chapter. Among the fragmentation characteristics was the dependence of the abundance of the protonated molecule, [M + H]$^+$ or [MH]$^+$, on the amount of unsaturation in the TAG FA. TAG containing numerous sites of unsaturation have a protonated molecule, [M + H]$^+$ as the base peak, whereas TAG with fewer sites of unsaturation give a [DAG]$^+$ fragment as the base peak. Saturated TAG give a [DAG]$^+$ fragment as the base peak, with no or practically no [M + H]$^+$ abundance. This dependence of [M + H]$^+$ abundance on the amount of unsaturation often has been noted and was observed in our first report on the HPLC/APCI-MS analysis of TAG (6). Since that first report, we have sought ways to describe this undefined relationship in a qualitative or quantitative way. In 1997 (34), the relationship between the ratio of the abundance of the [M + H]$^+$ ion of a TAG to the sum of all ions, [M + H]$^+$ plus [DAG]$^+$, was modeled as using:

$$\frac{[\text{TAG}]^+}{[\text{TAG}]^+ + \Sigma[\text{DAG}]^+}$$

An equation was shown, referred to as *the TAG quotient 1/3 power fit*, that was an approximate representation of the curve described when this ratio was plotted vs. the number of sites of unsaturation in the TAG. This ratio has now been calculated to equal the following:

$$\frac{[\text{TAG}]^+}{[\text{TAG}]^+ + \Sigma[\text{DAG}]^+} = \frac{1}{1 + \dfrac{1}{\dfrac{[\text{TAG}]^+}{\Sigma[\text{DAG}]^+}}}$$

It is simpler, and is preferred, to use the [MH]$^+$/Σ[DAG]$^+$ ratio instead of the inverse of its inverse.

The ratio of the TAG protonated molecule, [TAG + H]$^+$, [M + H]$^+$, or [MH]$^+$, to Σ[DAG]$^+$ is referred to in the BUS as the [MH]$^+$/Σ[DAG]$^+$ ratio.

One important aspect of the relationship between the [M + H]$^+$ ion and the sum of the [DAG]$^+$ fragment ions is that they are inverses: When one goes up, the other goes down. This dependence is not linear, but it is inverse in some way. Since

one value goes up and one goes down, the ratio of these two values highlights, or accentuates, the dependence of $[M + H]^+$ on the degree of unsaturation. This ratio will show more movement in its numeric value than the abundance alone as the number of sites of unsaturation changes, since the ratio contains two abundances that have an inverse relationship. Therefore, the dependence of the abundance of the proton-ated molecule, $[M + H]^+$, on the degree of unsaturation is best reflected in the ratio of the protonated molecule, $[MH]^+$, to the sum of the DAG fragment ion abundances, $\Sigma[DAG]^+$, to give $[MH]^+/\Sigma[DAG]^+$. This ratio can be used as a Critical Ratio to provide information regarding the number of sites of unsaturation in the molecule, which determines whether the $[M + H]^+$ or a $[DAG]^+$ is the base peak. TAG containing numerous sites of unsaturation have an $[MH]^+/\Sigma[DAG]^+$ larger than 1, and thus have a $[M + H]^+$ base peak. TAG with few sites of unsaturation have a low $[MH]^+/\Sigma[DAG]^+$ ratio, and a $[DAG]^+$ base peak. Saturated TAG are expected to have an $[MH]^+/\Sigma[DAG]^+$ ratio of zero, because they often give no $[M + H]^+$ ion.

An important aspect of the BUS construct is that the Critical Ratios are chosen, or constructed, based on observations in APCI-MS mass spectra, and keep them from going to catastrophic values. It has been observed that the $[M + H]^+$ ion can be zero for saturated TAG, so if this number were alone in the denominator of a ratio, then the ratio would take a value of 1/0 for saturated TAG and would become unsolvable. Since it is known that the $[M + H]^+$ ion goes to zero for some TAG, but that $\Sigma[DAG]^+$ never goes to zero, one can choose to calculate the $[MH]^+/\Sigma[DAG]^+$ ratio instead of the $\Sigma[DAG]^+/[MH]^+$ ratio, so that the number that can go to zero is in the numerator. Thus, judicious selection of the ratio that is constructed can keep the system completely bounded in all observed circumstances. The $[MH]^+/\Sigma[DAG]^+$ ratio can be classified into one of two cases: $[MH]^+/\Sigma[DAG]^+ \leq 1$, or $[MH]^+/\Sigma[DAG]^+ > 1$. The case when $[MH]^+/\Sigma[DAG]^+ = 0$ is a subset of the case when $[MH]^+/\Sigma[DAG]^+ \leq 1$, so a special case for $[M + H]^+ = 0$ is not required. Therefore, selecting the $[MH]^+/\Sigma[DAG]^+$ ratio as the Critical Ratio to represent the abundance of the $[M + H]^+$ ion and its relationship to the $[DAG]^+$ fragment ions is the better choice, because it leads to a simpler construct, which requires only two cases and remains bounded in all observed circumstances. In all instances, the Critical Ratios, which are the primary elements in the BUS construct, have been chosen to be as simple as possible and yet still convey more information in fewer variables than the raw mass spectrum.

There is another consideration and guiding principle that is inherent in the BUS. Since the BUS is a construct based on data from MS, it inherently incorporates and reflects the two important rules for data from MS: (i) All relative abundances are limited to a maximum individual value of 100%, and (ii) one ion abundance must be 100%. Since the tallest peak in a mass spectrum is normalized to 100%, one peak always represents 100%. The BUS ensures that all calculated values are less than or equal to 100%, since this is the limit imposed by MS. And the BUS determines which peak is the tallest and establishes it as

100%. Of course, 100 per*cent* (one hundred per hundred) as a pure ratio is 1.00. The Critical Limits within the BUS are what keep all values limited to being within the two rules imposed by MS. The value of 1.00 for several of the ratios also has other inherent meanings that provide structural information regarding the TAG (for instance, if $[AA]^+/[AB]^+ > 1$ for a Type II TAG, this provides structural information regarding the identity of the regioisomers).

For a Type II TAG, only the first two Critical Ratios mentioned earlier are necessary to specify the appearance of the mass spectrum. The $[AA]^+/[AB]^+$ ratio is used at face value in Equations 3 and 4 to provide information on the composition of the regioisomers of the TAG. The other Critical Ratio, $[MH]^+/\Sigma[DAG]^+$, may be used to provide insight into the degree of unsaturation in the TAG. These two numbers, the two Critical Ratios for a Type II TAG, provide more information in fewer values than the three raw abundances that constitute the raw mass spectrum. The mass spectrum of a Type III TAG contains four primary peaks and so requires three critical ratios. However, the $[MH]^+/\Sigma[DAG]^+$ ratio provides the same kind of information about a Type III TAG as it does for a Type II TAG. The $[MH]^+/\Sigma[DAG]^+$ ratio provides information to correlate the total amount of unsaturation in the three FA to the abundance of the protonated molecule. For a Type I TAG, the mass spectrum contains only two peaks, which are the $[M + H]^+$ peak and one single $[DAG]^+$ fragment ion. For a Type I TAG, the BUS requires only the $[MH]^+/\Sigma[DAG]^+$ ratio to reproduce the mass spectrum, and it also provides information regarding the number of sites of unsaturation in the TAG molecular species. This critical ratio provides information regarding the abundance of the $[M + H]^+$ ion, when properly classified, and also provides information to relate the abundance of this ion to the $[DAG]^+$. So with the $[MH]^+/\Sigma[DAG]^+$ ratio, as with the $[AA]^+/[AB]^+$ ratio already discussed, more information is provided in this Critical Ratio than in the raw abundances. The proper selection of the complete set of Critical Ratios for Types I, II, and III TAG, of which the first Critical Ratio is the $[MH]^+/\Sigma[DAG]^+$ ratio, allows the BUS to be completely self-contained and to operate within the rules imposed by MS in all observed circumstances.

Construction of the $[AC]^+/([AB]^+ + [BC]^+)$ ratio for a Type III TAG. A Type III TAG has three different FA, ABC, and these produce three possible $[DAG]^+$ fragment ions, $[AB]^+$, $[BC]^+$, and $[AC]^+$. These fragment ions may contain A, B, and C in any combination of *sn*-1, *sn*-2, and *sn*-3 positions, and in a randomized mixture, these are observed to be statistically distributed throughout all positions (7). Statistically speaking, the abundances of all three ions, $[AB]^+$, $[BC]^+$, and $[AC]^+$, should be identical in the absence of nonstatistical influences. However, fragment ions are not observed with equal abundance in APCI-MS or ESI-MS/MS mass spectra. It has been observed (10,11) that the abundance of the ion formed from loss of the FA in the *sn*-2 position, which gives the $[sn-1,3-AC]^+$ fragment, is the lowest of the three possible $[DAG]^+$ fragment ions. With this rule, all Type III TAG could be categorized, and the identities of the FA in the *sn*-2 position known. All four possibilities for the

A and C FA with B still remain: $[sn\text{-}1,2\text{-}AB]^+$ and $[sn\text{-}2,3\text{-}BC]^+$ or $[sn\text{-}1,2\text{-}CB]^+$ and $[sn\text{-}2,3\text{-}BA]^+$. But the $[sn\text{-}1,3\text{-}AC]^+$ isomer can be identified as the ion with the lowest abundance, so a piece of structural information may be known from the ion having the lowest abundance.

For simplicity, the isobaric $[sn\text{-}1,3\text{-}AC]^+$ or $[sn\text{-}1,3\text{-}CA]^+$ regioisomers are usually referred to more briefly as $[sn\text{-}1,3\text{-}AC]^+$, with the understanding that APCI-MS cannot distinguish between the $[sn\text{-}1,3\text{-}AC]^+$ and $[sn\text{-}1,3\text{-}CA]^+$ isomers, and so both possibilities are always implied herein. By putting the $[sn\text{-}1,3\text{-}AC]^+$ abundance alone in the numerator of the second Critical Ratio of the Type III TAG (the $[MH]^+/\Sigma[DAG]^+$ ratio is the first Critical Ratio for all TAG), the second Critical Ratio can be used to reflect the trend in the $[sn\text{-}1,3\text{-}AC]^+$ abundance with regioisomeric structure. This is analogous to the way the $[AA]^+/[AB]^+$ ratio is used to provide structural information for a Type II TAG, except the means for quantitative analysis of the regioisomers of Type III TAG have not yet been developed as thoroughly as the quantification of Type II TAG has (see Jakab *et al.* (42) and Eqs. 3 and 4).

Thus, the Critical Ratio $[AC]^+/([AB]^+ + [BC]^+)$ for a Type III TAG first provides a piece of information, which is the identity of the $[sn\text{-}1,3\text{-}AC]^+$ isomer, and then allows the abundance of the $[sn\text{-}1,3\text{-}AC]^+$ isomer to be calculated, when properly classified by the Critical Limits. This Critical Ratio also contains information to relate the $[AC]^+$ ion abundance to the two other ions that make up the mass spectrum.

In a complex mixture of TAG, the complete identification of all TAG molecular species requires the chromatographic information provided by the on-line separation, in addition to the masses provided by APCI-MS, to differentiate the many isobaric molecular species having overlapping masses, such as $[OO]^+$ and $[SL]^+$, $[OL]^+$ and $[SLn]^+$, etc. $[OO]^+$ and $[SL]^+$ are separated by a good chromatographic method (35), and so these can be differentiated and the characteristic Critical Ratios for each TAG molecular species can be constructed.

For a Type III TAG, if all FA in a TAG were distributed statistically and there was no influence by different levels of unsaturation or preferential loss, then the $[AC]^+$, $[AB]^+$, and $[BC]^+$ fragment abundances should all be equal, and the $[AC]^+/([AB]^+ + [BC]^+)$ ratio would be 0.5. An $[AC]^+/([AB]^+ + [BC]^+)$ ratio other than 0.5 indicates that nonstatistical influences are affecting the abundances. An $[AC]^+/([AB]^+ + [BC]^+)$ ratio greater than 1 would certainly indicate a preference for $[AC]^+$. According to literature precedent, one should be able to identify the $[sn\text{-}1,3\text{-}AC]^+$ fragment as the fragment with the lowest $[AC]^+/([AB]^+ + [BC]^+)$ ratio, and thus have a substantial piece of information regarding the TAG, which came from just this one Critical Ratio. Thus, one should choose to construct the $[AC]^+/([AB]^+ + [BC]^+)$ ratio using the smallest abundance in the numerator, since this has been correlated (10,11) with being the $[sn\text{-}1,3\text{-}AC]^+$ isomer.

Throughout this work, the identities of A, B, and C are irrespective of mass but reflect only the regioisomeric position of the FA on the backbone. This is analogous to the Type II TAG, in which, for OPO, the FA represented by A, out of ABA, has

a larger mass than the FA in the B position. On the other hand, in POP, the A FA has a mass that is lower than the FA in the B position. ABC refers to the regioisomeric positions of FA, when properly assigned, whereas the identities of the $[DAG]^+$ are characterized first by mass, then by their chromatographic elution at that mass, and then by comparison with tabulated masses (11). With this approach, the A and C can be identified and labeled specifically, and the FA in the *sn*-2 position can be identified.

With the FA in the *sn*-2 position known, the identities of the FA in the *sn*-1 and *sn*-3 positions are known to constitute the isobaric $[DAG]^+$ fragment possibilities, $[sn\text{-}1,2\text{-}AB]^+$ and $[sn\text{-}2,3\text{-}BC]^+$, or $[sn\text{-}1,2\text{-}BA]^+$ and $[sn\text{-}2,3\text{-}CB]^+$. No definitive trend has yet been reported to distinguish between $[sn\text{-}1,2\text{-}AB]^+$ and $[sn\text{-}2,3\text{-}BA]^+$ or between $[sn\text{-}2,3\text{-}BC]^+$ and $[sn\text{-}1,2\text{-}CB]^+$. It is reasonable to expect that, after the $[AC]^+/([AB]^+ + [BC]^+)$ ratios of a sufficient number of Type III TAG have been tabulated, trends in this ratio will be observable and will be correlated with the regioisomeric structures of the TAG.

The literature precedent for APCI-MS analysis of Type III TAG is currently based on a limited number of observations (10,11). Because of this, the ability to use the $[AC]^+/([AB]^+ + [BC]^+)$ ratio for identification of regioisomers in complex mixtures of TAG has not yet been developed. Also, not all nonstatistical influences have been characterized. The influence of the number of double bonds and their positions in the fatty chain (n-6 vs. n-3) has already been discussed herein in detail for a Type II TAG, and so it is reasonable to expect that similar trends, relating increased levels of polyunsaturation to increased abundances of ions containing the FA with more double bonds, will be observed for Type III TAG. Furthermore, the positions of the double bonds were shown to have an influence on Type II TAG, as discussed herein, so the positions of the double bonds in the FA of Type III TAG could also be expected to exert an influence on the abundances of ions observed in APCI-MS mass spectra. If the $[AC]^+/([AB]^+ + [BC]^+)$ ratios of numerous Type III TAG from different mixtures of TAG having known compositions of regioisomers are accumulated and tabulated (as is done with Type II TAG), it may be possible to move toward a more quantitative interpretation of this Critical Ratio. For now, some expected and probably some unexpected nonstatistical influences remain to be characterized. Regardless of how specifically information from this Critical Ratio can be derived at this time, it is clear that the $[AC]^+/([AB]^+ + [BC]^+)$ ratio as a single number already provides more information than the raw abundance alone. The $[AC]^+$ abundance must be compared with the other abundances to know whether it is the smallest and whether it is therefore the $[sn\text{-}1\text{-}AC]^+$. The abundance does not provide the desired information if used by itself. It provides the desired information regarding the regiospecific identity of the ion exhibiting that abundance only if it is taken as a ratio to the other ions. As with the other Critical Ratios, the numerator provides the abundance of one ion directly, when classified correctly in the BUS, and the ratio provides information to relate this ion to the other ions.

So while it remains to be further characterized, this Critical

Ratio as a single numeric value for a Type III TAG provides not only the same, but more information, when used with the BUS, than the original raw abundance of [AC]$^+$ as a single number.

Construction of the [BC]$^+$/[AB]$^+$ ratio. No distinctive preference for the [*sn*-1,2-AB]$^+$ position compared with the [*sn*-2,3-BC]$^+$ position has been reported using APCI-MS data. There appears to be minimal difference energetically, in an APCI source, between loss of the FA in the *sn*-1 position and loss of the FA in the *sn*-3 position. Nevertheless, if there is any *sn*-1,2 vs. *sn*-2,3 preference, this would be reflected in the ratio [BC]$^+$/[AB]$^+$, if [BC]$^+$ is the abundance of the *sn*-2,3 isomer and [AB]$^+$ is the abundance of the *sn*-1,2 isomer, regardless of mass. The ratio [BC]$^+$/[AB]$^+$ would constitute the Critical Ratio necessary to specify any [*sn*-1,2-AB]$^+$ vs. [*sn*-2,3-BC]$^+$ preference (or vice versa). Based on previous reports, at this time no observed trends that correlate regioisomeric structures of Type III TAG with different amounts of unsaturation in the [*sn*-1,2-AB]$^+$ vs. [*sn*-2,3-BC]$^+$ FA can be cited. However, several expected trends can be discussed.

Just as was observed with Types I and II TAG, the amount of unsaturation in the FA should have an influence on the abundances of the [DAG]$^+$ fragment ions that contain the FA. Since there appears to be minimal influence due to the regioisomeric position of the FA in the TAG at the *sn*-1,2 vs. *sn*-2,3 positions, the degree of unsaturation in the fragment [AB]$^+$, compared with the unsaturation in [BC]$^+$, may exhibit a greater influence on the [BC]$^+$/[AB]$^+$ ratio than the unreported influence due to the regioisomeric identity. Of course, the locations and number of the double bonds were of primary importance in determining the effect of the double bonds on the ion abundances for Type II TAG and therefore should be expected to exert a similar influence on Type III TAG that contain PUFA.

Although the amount of information that can be derived from the [BC]$^+$/[AB]$^+$ ratio is currently limited, it does provide one piece of information at face value. This information is found by comparing the [BC]$^+$/[AB]$^+$ ratio to its inherent Critical Value of 1. If the [BC]$^+$/[AB]$^+$ ratio is greater than 1, the [BC]$^+$ ion is larger than [AB]$^+$ ion, but if this third Critical Ratio for a Type III TAG is less than 1, [AB]$^+$ is larger than [BC]$^+$. It can be seen that this third Critical Ratio for a Type III TAG can be used with the BUS, which incorporates the rules of MS, to provide the two numerical values that are the raw abundances of the [BC]$^+$ and [AB]$^+$ fragment ions from the one numerical value. Thus, this Critical Ratio provides the same information (two abundances) in less space (one number instead of two) than the raw abundances. Whether more information can be derived from this ratio will be determined by future reports.

Summary of the construction of the Critical Ratios. The Critical Ratios just described can be constructed and directly interpreted at face value to provide information regarding structural trends. These ratios provide a method for visualizing trends that is more direct than using the raw abundances alone. The trends are not as apparent in the raw data as they are in the Critical Ratios. Therefore, is it useful to construct these Critical Ratios as an aid to qualitative analysis of TAG.

Not only do these Critical Ratios highlight structural trends, but also they constitute a reduced data set from which the mass spectrum of any TAG can be reconstructed in its entirety. The Critical Ratios can be used with inherent Critical Values and calculated Critical Limits to classify all TAG into Cases. The Case into which a TAG is classified provides all of the equations necessary to calculate the abundances of every ion in the mass spectrum as well as the sum of all ions. This report will present the basic equations that encompass every structural possibility within the TAG Lipidome. The solution to the *Triacylglycerol Lipidome* comes in the form of the Critical Ratios operated into the BUS, to accomplish the classification of the TAG into the proper Cases, based on the Critical Values and Critical Limits. The ratios are applied with an interpretation matrix that provides structural information from the Critical Ratios as they operate through the Critical Values and Critical Limits. Once a TAG is properly classified by its Critical Ratios, the Case indicates the correct equations to use for the solution of all ion abundances. This combination of Critical Ratios with Critical Values and Critical Limits used to define the Cases, along with the interpretation matrix and the equations for each Case constitutes the BUS to the TAG Lipidome. This solution allows the primary ions in the mass spectrum of any TAG to be reproduced, and the Critical Ratios can be used for a quantitative description for the set of structural possibilities exhibited by the TAG.

Method for quantitative analysis based on ion abundances determined by APCI-MS. During the routine processing of data from LC/APCI-MS using the quantitative method of Byrdwell *et al.* (7,34,35), the area under every peak is integrated in every extracted ion chromatogram (EIC) of each *m/z* value for every [DAG]$^+$ fragment ion and protonated molecule, [M + H]$^+$. The peaks that gave the areas of [DAG]$^+$ fragment ions and protonated molecules, [M + H]$^+$, that come from a particular TAG must elute at the same specific retention time, since they come from the same TAG. Therefore, the areas under the fragment ion and protonated molecule chromatographic peaks constitute an average mass spectrum across the retention time window used for integration. The average mass spectrum is calculated as the normalized percent composition of the areas of the fragment ions and the protonated molecule across the integrated chromatographic retention time window for a particular TAG. Small differences in retention times at the beginning and end of the fragment peaks have no substantial impact on the integrated area of each peak. The integrated areas provide a good representation of the mass spectrum averaged across a chromatographic peak. Typical ion chromatograms that are integrated to give peak areas are shown and discussed in the subsequent section entitled Implementation of the BUS. All solutions provided herein work equally well on an average mass spectrum that is produced from integrated peak areas or from manual qualitative analysis, or from a single mass spectrum manually acquired. Of course, there is some variability in abundances between single replicate mass spectra, and this variability is greater for TAG present at low levels. Whichever abundances

are used to produce the Critical Ratios, the mass spectrum from which they come is exactly reproduced by the BUS.

As mentioned, the first Critical Ratio is the ratio of the percent abundance of the protonated molecule as a ratio to the sum of all $[DAG]^+$ fragment ions:

$$\text{Critical Ratio 1} = \left(\frac{[MH]^+}{\sum [DAG]^+} \right) \qquad [5]$$

Table 2 lists the Critical Ratios for a 35-TAG mixture of synthetic TAG. The critical ratios are listed as a percentage simply for the most convenient display of four (or five) significant figures, with up to two decimal places. This is the same method of representation that Jakab *et al.* (42) used in their analysis of the $[AA]^+/[AB]^+$ ratio for characterization of mixtures of LOL/LLO. It is important to realize that the Critical Ratios as percentages must be converted to pure ratios (fractions), by dividing by 100, before they are used in the equations below. Throughout the following discussion, all ratios are expressed in pure fraction form, not percentage form. As a fraction, 100% equals 1.00, so 1.00 is the upper limit in the equations below. In the spreadsheet formulas used for the automated implementation of the BUS, the division of the ratio by 100 is incorporated into the formulas.

As already discussed, the first Critical Ratio can be used to define the overall unsaturation of a molecule. It is well known that saturated TAG have a $[MH]^+/\Sigma[DAG]^+$ ratio that is either very low or zero. The polyunsaturated TAG have large values of the $[MH]^+/\Sigma[DAG]^+$ ratio. The $[MH]^+/\Sigma[DAG]^+$ ratio for OOO is a very low value of 0.0324, and so for this Type I TAG (a mono-acid TAG), a $[DAG]^+$ is the base peak, and the protonated molecule abundance is simply the $[MH]^+/\Sigma[DAG]^+$ ratio, expressed as a percentage, 3.24%. For LLL and LnLnLn, the large $[MH]^+/\Sigma[DAG]^+$ ratio indicates that $[M + H]^+$ is the base peak, and the $[DAG]^+$ abundance is easily calculated from the inverse of the $[MH]^+/\Sigma[DAG]^+$ ratio.

The second Critical Ratio depends on whether the molecule is a Type II or Type III TAG. For a Type II TAG, the second Critical Ratio is $[AA]^+/[AB]^+$. For a Type III TAG, the second Critical Ratio is $([AC]^+/([AB]^+ + [BC]^+))$:

$$\text{Type II}:$$
$$\text{Critical Ratio 2} = \left(\frac{[AA]^+}{[AB]^+} \right) \qquad [6a]$$

$$\text{Type III}:$$
$$\text{Critical Ratio 2} = \left(\frac{[AC]^+}{([AB]^+ + [BC]^+)} \right) \qquad [6b]$$

This second Critical Ratio has an obvious relationship to the positional preference of a TAG. It is expected that the $([AA]^+/[AB]^+)$ ratio should always be less than 1, unless there is a strong $[AA]^+$ positional preference. Likewise, the ratio $([AC]^+/([AB]^+ + [BC]^+))$ should be less than 1 unless there is a strong $[AC]^+$ positional preference. But the degree of unsaturation in the $[AB]^+$ or $[AC]^+$ fragment also has an effect on this ratio. Deconstruction of the second Critical Ratio of an ABC TAG into the two components of positional preference and de-

gree of unsaturation remains to be accomplished. For now, this ratio can simply be compared to positional isomer standards.

The third Critical Ratio is only observed from Type III TAG. It is the ratio of $[BC]^+/[AB]^+$, or the ratio of the *sn*-2,3 $[DAG]^+$ to the *sn*-1,2 $[DAG]^+$. For now, it is assumed that there is no particular preference between these two, but evidence at a future date may allow quantification of a preference for the *sn*-1,2 $[DAG]^+$ peak over the *sn*-2,3 $[DAG]^+$ peak or vice versa. All else being equal, a $[BC]^+/[AB]^+$ of ≤1 is used herein as the default assumption (assume $[AB]^+ \geq [BC]^+$). The reason for this is discussed shortly. In the absence of any preference or assumption, the $[BC]^+/[AB]^+$ ratio may be less than one or greater than 1 with equal statistical probability, thereby giving an equal probability of Case 5 or Case 6.

THE BUS

The BUS for a Type I TAG. Now that the critical ratios have been defined, it is useful to examine the visualization approach that led to the definition of the Cases. Figure 2 shows the appearance of idealized APCI-MS mass spectra of TAG. The axes in these figures have a maximum value of 1, representing 100% as a pure ratio. AAA TAG are shown first in this figure.

Since an AAA TAG has only one $[DAG]^+$ and the $[M + H]^+$, it is obvious that the Critical Value that determines which peak is the base peak occurs when both $[AA]^+$ and $[MH]^+$ have their maximal values, and $[MH]^+/\Sigma[DAG]^+$ is equal to 1. The Critical Value for an AAA TAG is depicted in the upper right panel of Figure 2, Part I. From this Critical Value of $[MH]^+/\Sigma[DAG]^+$ = 1, if the $[MH]^+$ were to diminish by the least amount, the $[MH]^+/\Sigma[DAG]^+$ ratio would be less than 1 and $[AA]^+$ would be the base peak. This is referred to as Case 1, and the solution would use the equation shown in Scheme 1, Part I, for Case 1.

On the other hand, if the $[DAG]^+$ were to diminish by the least amount, then the $[MH]^+/\Sigma[DAG]^+$ ratio would be larger than 1 and $[M + H]^+$ would be the base peak. This is referred to as Case 2, and the solution would use the equation listed in Scheme 1, Part I, for Case 2. No other Critical Limit is necessary to specify the Case for a Type I TAG. Once the case has been specified, the actual percentages of $[M + H]^+$ and the $[AA]^+$ abundances are given by the equations in Scheme 1, Part I, for either the Case 1 solution $[AA]^+$ base peak) or the Case 2 solution $[M + H]^+$ base peak). The value of 1 serves as a Critical Value for all Types I, II, and III TAG. If the $[MH]^+/\Sigma[DAG]^+$ ratio is greater than 1 for any TAG, this automatically means that $[M + H]^+$ is the base peak and specifies a Case 2 solution. More generally, if any Critical Ratio has a value greater than 1, the numerator is automatically the largest peak of the peaks used to construct the ratio.

Using a Type I TAG as an example, the pattern in the equations in the BUS can now be described. The sum of all ions can be referred to as the $\Sigma(I^+)$ for any TAG. For a Type I TAG, the sum of all ions, $\Sigma(I^+)$, is simply equal to the sum of the protonated molecule ion and the single $[DAG]^+$ fragment ion, $\Sigma([MH]^+ + [DAG]^+)$. Thus, $\Sigma(I^+) = \Sigma([MH]^+ + [DAG]^+)$. Similarly, the sum of all ions for any TAG is equal to the sum
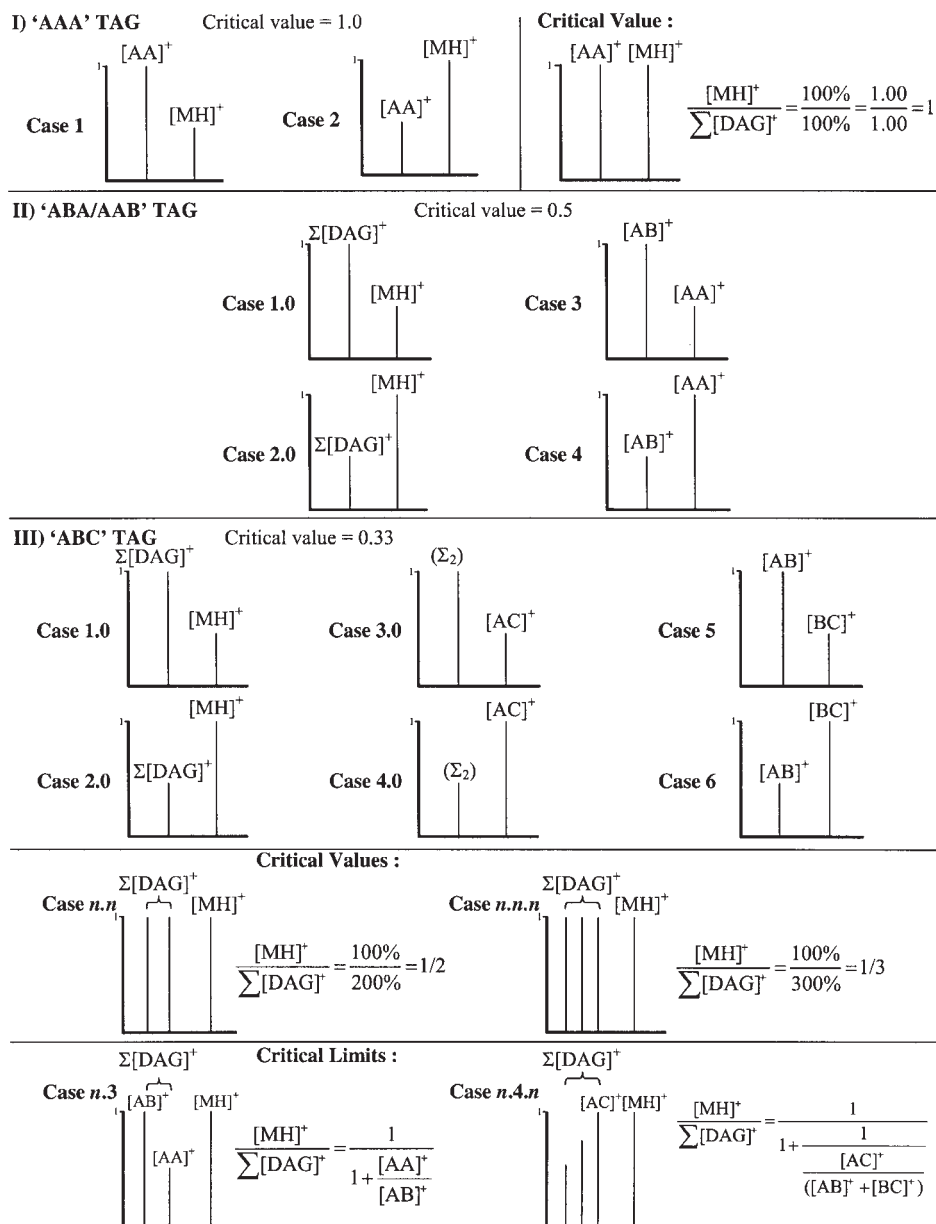
FIG. 2. Generalized representations of mass spectra used to calculate Critical Ratios. Also, generalized mass spectra that demonstrate Critical Values and Critical Limits are shown.

of the protonated molecule plus the sum of the [DAG]$^+$ fragment ions: $\Sigma(I^+) = \Sigma([MH]^+ + \Sigma[DAG]^+)$. The BUS for a Type I TAG shows that if the [MH]$^+$/Σ[DAG]$^+$ ratio is less than the Critical Value of 1, then the solution obeys Case 1. According to Case 1, the [DAG]$^+$ fragment is the base peak and has an abundance of 100% (= 1.00 as a pure ratio). In such a case, the sum of the ions $\Sigma(I^+)$ is (1 + ([MH]$^+$/Σ[DAG]$^+$)). For instance, OOO has an [MH]$^+$/Σ[DAG]$^+$ ratio of 0.0324. This ratio is less than 1, so OOO is solved using Case 1.

Classifying this TAG as a Case 1 TAG first provides a piece of information, which is that the [DAG]$^+$ fragment is the base peak, and then it provides the equation to use to calculate the abundance of the [M + H]$^+$ ion. The percent abundance of the

[M + H]$^+$ ion is given by ([MH]$^+$/Σ[DAG]$^+$) $\times$ 100, as shown in Scheme 1 Part I, or (0.0324 $\times$ 100) = 3.24%. Then the sum of all ions is $\Sigma(I^+) = \Sigma([DAG]^+ + [MH]^+) = 100\% + 3.24\% = 103.24\%$, which is 1.0324 as a pure ratio. Thus, for this Case 1 TAG, the following equivalences are true:

$$\sum(I^+) = \sum\left([MH]^+ + [DAG]^+\right) = \left(1 + \left(\frac{[MH]^+}{\sum[DAG]^+}\right)\right) = (1 + .0324) = 1.0324, \text{ or } = 103.24\%$$

On the other hand, a TAG such as LLL has an [MH]$^+$/Σ[DAG]$^+$ ratio of 1.2007. This is greater than 1, and so Scheme 1, Part I, shows that this would be classified as a Case 2 solution. This classification immediately provides a piece of information, which is that the protonated molecule, [M + H]$^+$, is the base

peak, and then it provides the equation used to calculate the abundance of the [DAG]$^+$ fragment ion. The [DAG]$^+$ ion abundance (%) is given by $(1/([MH]^+/\Sigma[DAG]^+)) \times 100$, or $(1/1.2007) \times 100$, which equals 0.8328×100, or 83.28%. Thus, the base peak is known by the classification process, and the other abundance is given by the equation dictated by the classified BUS. The sum of the ions in the mass spectrum is $100 + 83.28\% = 183.28\%$, or 1.8328 as a pure ratio. The second solution can be seen to give the following equivalences:

$$\sum(I^+) = \sum([MH]^+ + [DAG]^+) = \left(1 + \frac{1}{\frac{[MH]^+}{\sum[DAG]^+}}\right) = \left(1 + \frac{1}{1.2007}\right) = 1.8328, \text{ or } = 183.28\%$$

There are only two possible solutions for a Type I TAG, and these may be summarized by the equivalence:

$$\sum(I^+) = \sum([MH]^+ + [DAG]^+) = \left\{ \overset{\text{Case 1}}{\left(1 + \left(\frac{[MH]^+}{[DAG]^+}\right)\right)} \text{ or } \overset{\text{Case 2}}{\left(1 + \frac{1}{\left(\frac{[MH]^+}{[DAG]^+}\right)}\right)} \right\}$$

This equation shows that the sum of all ions is equal to the sum of the protonated molecule plus the one [DAG]$^+$ fragment ion, and this is equal to one of two possibilities, depending on whether it is a Case 1 or a Case 2 solution, as determined by whether the $[MH]^+/\Sigma[DAG]^+$ ratio is less than the Critical Value of 1 or larger than 1. Scheme 1, Part I, shows the equivalence just given. The foregoing two examples, for OOO and LLL, demonstrate that this equivalence is true for Type I TAG having an $[MH]^+/\Sigma[DAG]^+$ ratio less than 1 (OOO), or a ratio greater than 1 (LLL).

The BUS for a Type II TAG. For Types II and III TAG, a $[MH]^+/\Sigma[DAG]^+$ ratio greater than 1 certainly indicates that [M + H]$^+$ is the base peak, but an $[MH]^+/\Sigma[DAG]^+$ ratio less than 1 does not, by itself, indicate that [M + H]$^+$ is not the base peak. Thus, for Types II and III TAG, an $[MH]^+/\Sigma[DAG]^+$ ratio greater than 1 is sufficient, but not necessary, to define [M + H]$^+$ as the base peak for any TAG. Types II and III TAG have other Critical Values inherent in the construction of the ratios. The same logic demonstrated for AAA TAG of setting all peaks equal to 1 at the Critical Value and comparing the observed Critical Ratio to this Critical Value to determine the identity of the base peak is also applicable to Types II and III TAG.

The Critical Value for a Type II TAG is depicted in the fourth panel down in Figure 2. At the Critical Value for a Type II TAG, the [M + H]$^+$ and both [DAG]$^+$ have their maximum values of 1.00, or 100%. This circumstance is rarely, if ever, actually observed, but it serves as an inherent arithmetic equivalence point for TAG that fragment to produce two different [DAG]$^+$ ions. For any Type I, II, or III TAG, the Critical Value, at which all ions, $\Sigma(I^+)$, are at their maximum values, produces the limit that represents the minimum $[MH]^+/\Sigma[DAG]^+$ ratio that the TAG could have and still give a protonated molecule, [MH]$^+$. At the Critical Value for the $[MH]^+/\Sigma[DAG]^+$ ratio, if any [DAG]$^+$ fragment were to decrease by the least amount, the $\Sigma[DAG]^+$ would decrease, and the $[MH]^+/\Sigma[DAG]^+$ ratio would increase, and so this value represents the minimum of the ratio. If the [M + H]$^+$ abundance were to decrease by the least amount, it would not be the base peak, and so a piece of information would be known.

I) 'AAA' TAG   Critical Value = 1

Case 1   **Case 2**

$$\sum_1(I^+) = \sum_1([MH]^+ + [DAG]^+) = \quad \left(1 + \left(\frac{[MH]^+}{\sum[DAG]^+}\right)_*\right) \quad or \quad \left(1 + \frac{1}{\left(\frac{[MH]^+}{\sum[DAG]^+}\right)_*}\right)$$

$$\left(\frac{[MH]^+}{\sum[DAG]^+}\right) \overset{?}{<} 1 \quad \xrightarrow{\ \ Y\ \ } \quad \text{Case 1} \quad \text{the } [DAG]^+ = 100\ \% \ \ \text{(base peak)}$$

$$\downarrow N \qquad\qquad\qquad\qquad\qquad \%\ [M+H]^+ = \left(\frac{[MH]^+}{\sum[DAG]^+}\right) x100$$

Case 2
$$\%\ [M+H]^+ = 100\ \% \ \ \text{(base peak)}$$

$$\%\ [DAG]^+ = \frac{1}{\left(\frac{[MH]^+}{\sum[DAG]^+}\right)} x100$$
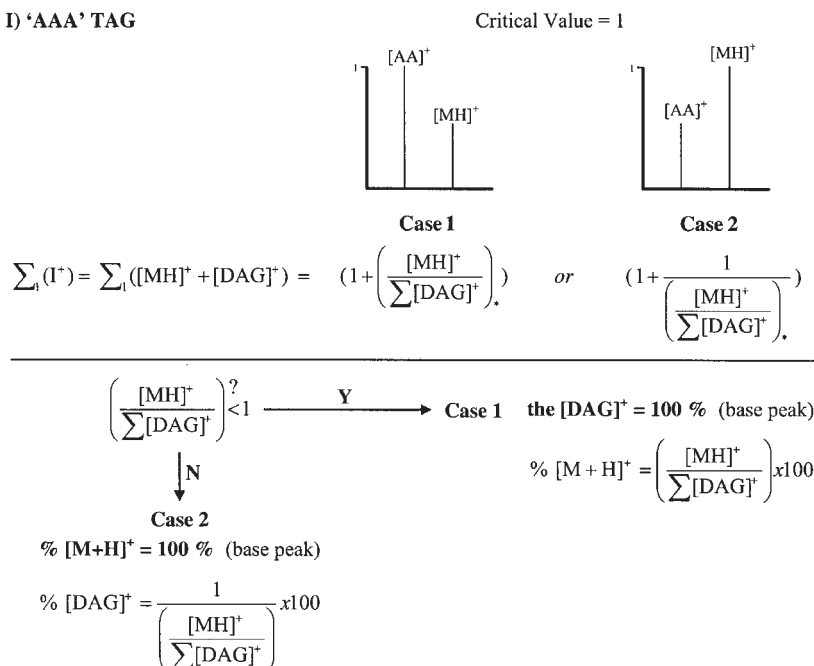
SCHEME 1, PART I. Equations to calculate the relative abundances of the [M + H]$^+$ and the [DAG]$^+$ fragment ion for an AAA TAG using the $[MH]^+/\Sigma[DAG]^+$ Critical Ratio from atmospheric pressure chemical ionization (APCI)-MS data (Table 2).

The Critical Value of the $[MH]^+/\Sigma[DAG]^+$ ratio for a Type II TAG, or ABA/AAB TAG, is 1/2, or 0.5, as shown in the fourth panel down in Figure 2. A mass spectrum with a $[MH]^+/\Sigma[DAG]^+$ ratio less than the Critical Value cannot have a protonated molecule base peak. But a $[MH]^+/\Sigma[DAG]^+$ ratio greater than the Critical Value does not immediately indicate that the protonated molecule is the base peak. The Critical Ratio must be further tested with another limit to determine whether the $[M + H]^+$ is the base peak. The Critical Value serves as the lower limit for the possibility of having a protonated molecule base peak. If the $[MH]^+/\Sigma[DAG]^+$ ratio is greater than the Critical Value, then the next limit to which it is compared is the Critical Limit, discussed next, which is the limit of the $[MH]^+/\Sigma[DAG]^+$ ratio, based on actual $[DAG]^+$ abundances, that defines whether the $[M + H]^+$ is the base peak or a $[DAG]^+$.

The Critical Limit for a Type II TAG. The Critical Limit for a Type II TAG makes use of the inherent limitations imposed by the MS construct, within which all abundances must operate. If it is known by classification that a TAG is Case 1, then a $[DAG]^+$ is known to be the base peak, and, for a Type II TAG, the possibilities for the base peak are narrowed down to two: (i) $[AB]^+$ is larger than $[AA]^+$, and so $[AB]^+$ is the base peak and has an abundance of 100%; or (ii) $[AA]^+$ is larger than $[AB]^+$, and so $[AA]^+$ is the base peak and has an abundance of 100%. In the first case, $[AB]^+$ is larger than $[AA]^+$, and so $[AB]^+$ is 100%, or is 1.00 as a pure ratio; thus, since $[AB]^+ = 1$, $[AA]^+/[AB]^+$ becomes equal to $[AA]^+/(1)$, and so $[AA]^+ = [AA]^+/[AB]^+$. In this case, the sum of the $[DAG]^+$ fragment ions is $[AB]^+ + [AA]^+ = (1.0000 + [AA]^+/[AB]^+)$. This may be summarized as:

$$\Sigma[DAG]^+(\text{ratio}) = \left(1.0000 + \frac{[AA]^+}{[AB]^+}\right) \quad or \quad \Sigma[DAG]^+(\%) = \left(1.0000 + \frac{[AA]^+}{[AB]^+}\right)x100$$

For instance, in the case of OOP, Table 2 gives an $[AA]^+/[AB]^+$ ratio of 0.3612, and since this value is less than 1, it is classified as Case 3. Along with the knowledge of the fact that there is a $[DAG]^+$ base peak, from classifying the $[MH]^+/\Sigma[DAG]^+$ ratio as Case 1, a Case 1.3 solution is dictated. In this case, $[AB]^+ = 100\%$, and so $[AA]^+ = ([AA]^+/[AB]^+) \times 100 = 0.3612 \times 100 = 36.12\%$. Then the sum of the $[DAG]^+$ ions is $1.0000 + 0.3612 = 1.3612$ as a ratio, or 136.12% as percent abundance.

On the other hand, if the ratio $[AA]^+/[AB]^+$ is greater than 1, and so is a Case 1.4 solution, then $[AA]^+$ is the base peak and has an abundance of 100% (= 1.0000). Then, since $[AA]^+ = 1$, $[AB]^+ = (1/[AA]^+/[AB]^+)) = (1/(1)/[AB]^+))$. This may be summarized as follows:

$$\Sigma[DAG]^+(\text{ratio}) = \left(1.0000 + \frac{1}{\frac{[AA]^+}{[AB]^+}}\right) \quad or \quad \Sigma[DAG]^+(\%) = \left(1.0000 + \frac{1}{\frac{[AA]^+}{[AB]^+}}\right)x100$$

Of course, since loss of the B chain in an **ABA** TAG is energetically disfavored, the $[sn\text{-}1\text{-}AA]^+$ fragment is expected and is normally observed to have a low abundance. It is most often observed as a ratio that is not only less than 1, but is often less than the 0.5 that is statistically expected. And so an $[AA]^+/[AB]^+$ ratio greater than 1 normally provides a piece of information, which is that there is a strong nonstatistical influence. This influence may be due to a structural characteristic of the FA (amount and location of unsaturation), which renders the sn-2 FA easily lost and gives an $[AA]^+/[AB]^+$ ratio that is larger than expected. Other nonstatistical influences may be involved that have not yet been elucidated.

To summarize the two preceding pairs of equations, if the Type II TAG is Case 1, then one of the $[DAG]^+$, $[AA]^+$ or $[AB]^+$, would be 1.00, and the sum of the $[DAG]^+$ fragment ions could be calculated as one of either of two possibilities:

$$\Sigma[DAG]^+ = \Sigma([AA]^+ + [AB]^+) = \left\{ 1 + \frac{[AA]^+}{[AB]^+} \quad or \quad 1 + \frac{1}{\frac{[AA]^+}{[AB]^+}} \right\}$$
$$\qquad\qquad\qquad\qquad\qquad\qquad \text{Case 3} \qquad\quad \text{Case 4}$$

On the other hand, if the $[MH]^+/\Sigma[DAG]^+$ ratio is greater than the Critical Limit, then it would be a Case 2 solution, and the $[M + H]^+$ is the base peak. The equations for the $[AA]^+$ and $[AB]^+$ percent relative abundances would then be calculated using the inverses of the preceding two equations. These equations appear in the denominator of the Case 2 solutions. Likewise, these equations for the $\Sigma[DAG]^+$ appear as the denominator of the Critical Limit for a Type II TAG. At this Critical Limit, one of the $[DAG]^+$ fragment ions is 100%, or 1.00, and the other is less than 100%, based on its proper proportion, as given by either the $[AA]^+/[AB]^+$ ratio (Case 3), or $1/([AA]^+/[AB]^+)$ (Case 4). At this Critical Limit, $[MH]^+$ is also 100%, because it is the numerator of the ratio, $[MH]^+/\Sigma[DAG]^+$, for which this is the Critical Limit. The Critical Limit for a Type II TAG is pictured in the fifth (bottom) panel of Figure 2. In the hypothetical spectrum shown, one $[DAG]^+$ fragment is 1 and $[MH]^+$ is 1. From this point, if the $[MH]^+$ were to decrease by the least amount, the $[DAG]^+$ would be the base peak, whereas if the $[DAG]^+$ were to decrease by the least amount, the $[MH]^+$ would be the base peak. Hence, based on a particular $[AA]^+/[AB]^+$ ratio, the Critical Limit is the point that determines whether $[MH]^+$ or a $[DAG]^+$ is the base peak. The Critical Limit, with $[MH]^+ = 1$ and a $[DAG]^+ = 1$, is shown in Figure 2 and can be summarized in this equation:

$$\left(\frac{[MH]^+}{\Sigma[DAG]^+}\right)_{\substack{Critical \\ Limit}} = \frac{1}{1 + \frac{[AA]^+}{[AB]^+}} \quad or \quad \frac{1}{1 + \frac{1}{\frac{[AA]^+}{[AB]^+}}}$$
$$\qquad\qquad\qquad\qquad\qquad \text{Case } n.3 \qquad\quad \text{Case } n.4$$

The area bounded by the equation set in the BUS for a Type II TAG can be envisioned as the structure shown in Figure 3, where the primary vertical axis is the $[MH]^+/\Sigma[DAG]^+$ ratio. The axis needs only to go to 1 in the figure, since anything above 1 automatically means an $[MH]^+$ base peak, and then the $\Sigma[DAG]^+$ is given by $1/[MH]^+/\Sigma[DAG]^+$, the inverse of the $[MH]^+/\Sigma[DAG]^+$ ratio. The $[MH]^+/\Sigma[DAG]^+$ ratio for a Type

$$\left(\frac{[MH]^+}{\Sigma[DAG]^+}\right)_{\substack{Critical \\ Limit}} = \underbrace{\frac{1}{\left(1+\frac{[AA]^+}{[AB]^+}\right)}}_{Case\ 3} \; or \; \underbrace{\frac{1}{\left(1+\frac{1}{\frac{[AA]^+}{[AB]^+}}\right)}}_{Case\ 4}$$

$$\Sigma\left([I]^+\right) = \Sigma([MH]^+ + \Sigma[DAG]^+) = \left\{ \underbrace{\left(1+\frac{[MH]^+}{\Sigma[DAG]^+}\right) \times \Sigma[DAG]^+}_{Case\ 1} \; or \; \underbrace{\left(1+\frac{1}{\frac{[MH]^+}{\Sigma[DAG]^+}}\right)}_{Case\ 2} \right\}$$

$$\frac{1}{\left(\frac{[MH]^+}{\Sigma[DAG]^+} \geq 1\right)}$$

Diagram labels:

$[M+H]^+$ base peak

$\left(\frac{[MH]^+}{\Sigma[DAG]^+}\right)_{\substack{Critical \\ Limt}}$; $\frac{[MH]^+}{\Sigma[DAG]^+}=1$

$\left(\frac{[MH]^+}{\Sigma[DAG]^+}\right)_{Obs}$

$\left(\frac{[MH]^+}{\Sigma[DAG]^+}\right)_{\substack{Critical \\ Value}} = 0.5$

$\frac{1}{\left(\left(\frac{[AA]^+}{[AB]^+}\right)>1\right)}$

Case 2.4

$\left(\frac{[AA]^+}{[AB]^+}\right)=1$; $\left(\frac{[AA]^+}{[AB]^+}\right)_{AAB}$

$\left(\frac{[AA]^+}{[AB]^+}\right)_{Obs.}$; Case 2.3

$\left(\frac{[AA]^+}{[AB]^+}\right)_{ABA}$

$\left(\frac{[AA]^+}{[AB]^+}\right)=0$

Case 1.4

Case 1.3

$\left(\frac{[AA]^+}{[AB]^+}\right)=1$

$\left(\frac{[AA]^+}{[AB]^+}\right)_{AAB}$

$\left(\frac{[AA]^+}{[AB]^+}\right)_{Obs.}$

$\left(\frac{[AA]^+}{[AB]^+}\right)_{ABA}$

$\frac{[MH]^+}{\Sigma[DAG]^+}=0$
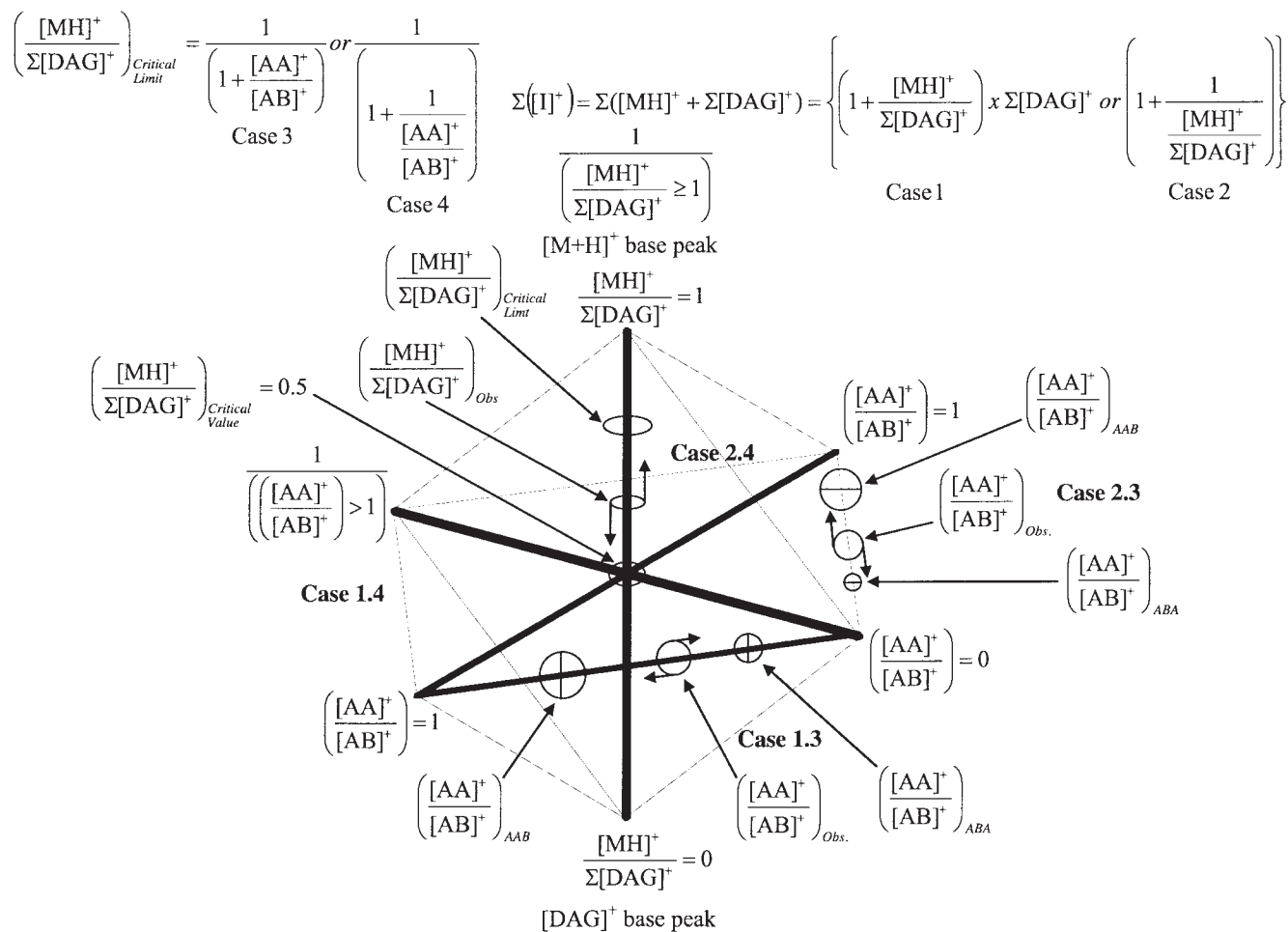
$[DAG]^+$ base peak

FIG. 3. The shape of the Triacylglycerol Lipidome for a Type II TAG. The Critical Value and the Critical Limit determine whether the $[M + H]^+$ or a $[DAG]^+$ fragment is the base peak. The $[AA]^+/[AB]^+$ ratio can be compared with regioisomeric standards for quantitative analysis of the amounts of regioisomers of calibrated TAG. The statistically expected value for the $[AA]^+/[AB]^+$ Critical Ratio = 1/2 = 0.5, Case 1.3 and Case 2.3, is not shown on the equatorial axis.

II TAG has an inherent Critical Value = 0.5, which is the minimum $[MH]^+/\Sigma[DAG]^+$ ratio that a TAG could have and still give an $[MH]^+$ base peak. This Critical Value of 0.5 is inherent in the MS construct pertaining to TAG. The Critical Value can be seen at the intersection of the vertical and equatorial axes in Figure 3. At the Critical Value, both of the $[DAG]^+$ were set to 100% to calculate the minimum possible $[MH]^+/\Sigma[DAG]^+$ ratio that could possibly give an $[MH]^+$ base peak. In real circumstances, $[AA]^+$ and $[AB]^+$ are rarely both equal to 100%, as they are at the theoretical Critical Value. In the rare case where $[AA]^+$ exactly equals $[AB]^+$ (whether 100% or not), either Case 3 or Case 4 could be used for the solution. The "less than" sign is used for Cases 1, 3, and 5, to produce a decision, but at the Critical Values and Critical Limits both Cases are equal.

The Critical Limit for a Type II TAG occurs when the larger of the two $[DAG]^+$ fragment ions is set to 100%, and the $[MH]^+$ is set to 100%, such that a decrease in either value will determine the base peak. The Critical Limit is based on the maximum hypothetical $\Sigma[DAG]^+$ that could be obtained by an observed $[AA]^+/[AB]^+$ ratio. In real circumstances, the $[AA]^+/[AB]^+$ ratio that is observed is often less than the statistically expected value of 0.5, because of the trends already discussed regarding formation of the $[sn\text{-}1,3\text{-}AA]^+$ fragment in the APCI-MS source. For instance, the Critical Limit for the Type II TAG OPO/OOP can be calculated using the $[AA]^+/[AB]^+$ ratio of 0.3612 from Table 2, as follows: *Critical Limit* = 1/(1 + 0.3612) = 1/1.3612 = 0.7346. Of course, in the case of OPO/OOP, the $[MH]^+/\Sigma[DAG]^+$ could be seen to be less than the Critical Value of 0.5, so construction of the Critical Limit would not be necessary to classify it as Case 1, if classifying it manually. In contrast, if the observed $[MH]^+/\Sigma[DAG]^+$ ratio is greater than or equal to the Critical Limit, then it is Case 2, so the $[MH]^+$ is equal to 100%. For instance, the Critical Limit for the Type II TAG LnSLn/LnLnS can be calculated using the $[AA]^+/[AB]^+$ ratio of 0.9510 from Table 2 as follows: *Critical Limit* = 1/(1 + 0.9510) = 0.5126. This Critical Limit for LnSLn/LnLnS is seen in Table 3. The observed $[MH]^+/\Sigma[DAG]^+$ ratio from this TAG, given in

TABLE 3
Calculated Critical Values and Critical Limits[a] Used with the Bottom-Up Solution
to Calculate Ion Abundances from Critical Ratios Determined by APCI-MS

TAG	Critical Value	Critical Limit 1	Critical Limit 2	Case		
PPP	1.00			1		
SSS	1.00			1		
OOO	1.00			1		
LLL	1.00			2		
LnLnLn	1.00			2		
PSP/PPS	0.50	67.00		1	3	
POP/PPO	0.50	60.50		1	3	
PLP/PPL	0.50	54.32		1	3	
PLnP/PPLn	0.50	58.84		1	3	
SPS/SSP	0.50	70.97		1	3	
SOS/SSO	0.50	57.10		1	3	
SLS/SSL	0.50	54.68		1	3	
SLnS/SSLn	0.50	62.12		1	3	
OPO/OOP	0.50	73.46		1	3	
OSO/OOS	0.50	71.52		1	3	
OLO/OOL	0.50	66.62		1	3	
OLnO/OOLn	0.50	70.61		1	3	
LPL/LLP	0.50	52.95		1	3	
LSL/LLS	0.50	56.80		1	3	
LOL/LLO	0.50	57.27		1	3	
LLnL/LLLn	0.50	65.80		2	3	
LnPLn/LnLnP	0.50	57.24		2	3	
LnSLn/LnLnS	0.50	51.26		2	3	
LnOLn/LnLnO	0.50	54.41		2	3	
LnLLn/LnLnL	0.50	60.95		2	3	
OPS	0.33	42.79	58.90	1	3	5
SPL	0.33	46.33	62.72	1	3	5
SPLn	0.33	40.49	56.59	1	3	5
LOP	0.33	35.93	50.44	1	3	5
LnOP	0.33	36.72	52.15	1	3	5
LnLP	0.33	42.19	57.68	2	3	5
LOS	0.33	37.43	53.85	1	3	5
OLnS	0.33	37.03	52.76	1	3	5
LnLS	0.33	40.39	56.00	2	3	5
LLnO	0.33	40.15	56.29	2	3	5

[a]The Critical Limit is given as a percentage to two decimal places but is used as a pure ratio. For abbreviations see Table 1.

Table 2, is 0.6131. Since the observed $[MH]^+/\Sigma[DAG]^+$ ratio is greater than the Critical Limit, it is classified as Case 2, and this ratio indicates that this TAG gave an $[MH]^+$ base peak. The $[DAG]^+$ abundances then are calculated using the Case 2.3 equations given in the BUS. The Critical Limit is seen as the upper circular limit on the main axis in Figure 3.

Two notes must be considered regarding the Critical Limit for a Type II TAG: First, in the automated spreadsheet implementation given below, only the Critical Limit is calculated and used, because it is sufficient to classify Case 1 or 2. The Critical Value for a Type II TAG is not required in the automated implementation. Second, in the rare case where the $[MH]^+/\Sigma[DAG]^+$ ratio exactly equals the Critical Limit, either a Case 1 or a Case 2 solution may be used.

During the process of calculating the Critical Limit and classifying the base peak as Case 1 or Case 2, the identity of Case 3 or Case 4 is found. For Case 1.n, when Case 3 or 4 is known, the $\Sigma[DAG]^+$ can be calculated using the Critical Ratio $[AA]^+/[AB]^+$ or its inverse, $1/[AA]^+/[AB]^+$. For all Cases, the observed $([AA]^+/[AB]^+)_{Obs}$ ratio of the sample can be compared with the $[AA]^+/[AB]^+$ ratios of regiospecific standards through Equations 3 and 4 above. The linear interpolation of the $([AA]^+/[AB]^+)_{Obs}$ ratio, between the $[AA]^+/[AB]^+$ ratios of standards, $([AA]^+/[AB]^+)_{ABA}$ and $([AA]^+/[AB]^+)_{AAB}$, is depicted on the equatorial lines in Figure 3. The circles around the equatorial lines represent the $([AA]^+/[AB]^+)_{Obs}$ ratios of pure regioisomeric standards, such as those given in Table 1. Figure 3 shows $([AA]^+/[AB]^+)_{Obs}$ ratios between 0 and 1, which is the most common case. This is the Case 1.3 or Case 2.3 solution. The BUS works equally well for $([AA]^+/[AB]^+)_{Obs}$ ratios greater than 1, and those instances give a Case 1.4 or Case 2.4 solution. The BUS does not depend on the linear interpolation given by Equations 3 or 4. The use of the $([AA]^+/[AB]^+)_{Obs}$ ratio for calculation of the regioisomeric composition is separate from the BUS.

The equations in the BUS can be demonstrated using the data from the synthetic mixture of 35 TAG made from five FA

II) 'AAB/ABA' TAG Critical value = 0.5

Case 1.0 — $\sum[DAG]^+$, $[MH]^+$

Case 2.0 — $[MH]^+$, $\sum[DAG]^+$

Case 3 — $[AB]^+$, $[AA]^+$

Case 4 — $[AA]^+$, $[AB]^+$

$$\left(\frac{[MH]^+}{\sum[DAG]^+}\right) \overset{?}{<} 1$$

N ← → Y

$$\left(\frac{[MH]^+}{\sum[DAG]^+}\right) \overset{?}{\geq} Critical\ Limit \quad \overset{Y}{\longleftarrow} \quad \left(\frac{[MH]^+}{\sum[DAG]^+}\right) \overset{?}{\geq} Critical\ Value$$

N   N

Case 2.0
% [M+H]$^+$ = 100 % (base peak)

$$\text{if } \left(\frac{[AA]^+}{[AB]^+}\right) < 1.0 \text{ (usual):}$$

$$Limit = \cfrac{1}{1+\cfrac{[AA]^+}{[AB]^+}}$$

Case n.3

$$\text{if } \left(\frac{[AA]^+}{[AB]^+}\right) \geq 1.0 \text{ (unusual)}^\dagger:$$

$$Limit = \cfrac{1}{1+\cfrac{1}{\cfrac{[AA]^+}{[AB]^+}}}$$

Case n.4

†Implies strong [AA]$^+$ preference or large difference in FA unsat.

Case 2.0
% [M+H]$^+$ = 100 % (base peak)

$$\left(\frac{[AA]^+}{[AB]^+}\right) \overset{?}{<} 1.0 \text{ (usual)} \quad \overset{Y}{\longrightarrow} \quad \textbf{Case 2.3} \quad [AA]^+ < [AB]^+$$

N†

Same for Both Cases:

$$\%[AB]^+ = \cfrac{1}{\left(\cfrac{[MH]^+}{\sum[DAG]^+}\right)\left(1+\cfrac{[AA]^+}{[AB]^+}\right)} x100$$

Case 2.4†

$[AA]^+ \geq [AB]^+$

$$\%[AA]^+ = \cfrac{1}{\left(\cfrac{[MH]^+}{\sum[DAG]^+}\right)\left(1+\cfrac{1}{\cfrac{[AA]^+}{[AB]^+}}\right)} x100$$

Case 1.0
a [DAG]$^+$ = 100 % (base peak)

$$\left(\frac{[AA]^+}{[AB]^+}\right) \overset{?}{<} 1.0 \text{ (usual)} \quad \overset{Y}{\longrightarrow} \quad \textbf{Case 1.3}$$

% [AB]$^+$ = 100 % (base peak)

$$\%[AA]^+ = \left(\frac{[AA]^+}{[AB]^+}\right) x100$$

$$\% [M+H]^+ = \left(\frac{[MH]^+}{\sum[DAG]^+}\right)\left(1+\frac{[AA]^+}{[AB]^+}\right) x100$$

N†

Case 1.4†

% [AA]$^+$ = 100 % (base peak)

$$\%[AB]^+ = \cfrac{1}{\left(\cfrac{[AA]^+}{[AB]^+}\right)} x100$$

$$\% [M+H]^+ = \left(\frac{[MH]^+}{\sum[DAG]^+}\right)\left(1+\cfrac{1}{\cfrac{[AA]^+}{[AB]^+}}\right) x100$$

SCHEME 1, PART II. Equations to calculate the relative abundances of the [M + H]$^+$ and [DAG]$^+$ fragment ions for ABA/AAB TAG using Critical Ratios from APCI-MS data (Table 2). For abbreviation see Scheme 1, Part I.

randomly distributed among the three positions on the glycerol backbone, given in Table 2. For example, this synthetic mixture contains oleic, palmitic, linoleic, linolenic, and stearic acids, so the TAG made from these FA include POP, for which standards of pure regioisomers have been run on the same instrument, as given in Table 1. The Type II TAG POP/PPO from the synthetic mixture gave the ([AA]$^+$/[AB]$^+$)$_{Obs}$ ratio of 0.6528 in Table 2, as a pure ratio, and an [MH]$^+$/Σ[DAG]$^+$ ratio of

0.0055, as a pure ratio. These ratios are processed through the BUS, Scheme 1, Part II, as follows: the [MH]$^+$/Σ[DAG]$^+$ ratio is less than 1 and is also less than the Critical Value of 0.5. This allows classification of the solution for this TAG as being a Case 1 solution. There is no need to construct the Critical Limit, because the [MH]$^+$/Σ[DAG]$^+$ ratio is less than the Critical Value. Nevertheless, the Critical Limit can still be calculated as an example. For instance, the ([AA]$^+$/[AB]$^+$)$_{Obs}$ ratio

of 0.6528 for POP/PPO in Table 1 is less than 1, so it indicates a case n.3 solution. The Critical Limit can be calculated as:

$$\left(\frac{[MH]^+}{\Sigma[DAG]^+}\right)_{\substack{Critical \\ Limit}} = \frac{1}{1 + \dfrac{[AA]^+}{[AB]^+}} = \frac{1}{1 + 0.6528} = 0.6050$$

As expected, the $[MH]^+/\Sigma[DAG]^+$ ratio is less than the Critical Limit, so the solution for this TAG is categorized as a Case 1.3 solution. The Case 1.3 solution indicates that $[AB]^+$ is the base peak, equaling 100%, and the percent $[AA]^+$ is given as $[AA]^+ = (([AA]^+/[AB]^+)_{Obs} \times 100)$ ratio, or $0.6528 \times 100 = 65.28\%$. Finally, the $[MH]^+$ is calculated as $[MH]^+$ (%) $= ([MH]^+/\Sigma[DAG]^+) \times (1 + 1/([AA]^+/[AB]^+)_{Obs}) \times 100 = (0.0055)$ $(1 + 0.6528) \times 100 = 0.91\%$ abundance. This abundance is seen in the tabulated mass spectral data in Table 4. This small abundance is exactly as expected from a TAG with only one site of unsaturation. It can be seen from this example that the three abundances that make up the mass spectrum can be calculated from only the two Critical Ratios. Other example solutions are shown below.

As these examples demonstrate, the two Critical Ratios for a Type II TAG can be used to calculate the three abundances of the ions in the mass spectrum. Then the second Critical Ratio may also provide information regarding the percentage composition of regioisomers in the mixture. When the $([AA]^+/[AB]^+)_{Obs}$ ratio of 0.6528 for POP/PPO from the synthetic TAG mixture is inserted into Equation 3, with the ratios $([AA]^+/[AB]^+)_{ABA} = 0.29$ and $([AA]^+/[AB]^+)_{AAB} = 0.87$ for the pure regioisomeric standards from Table 1 [based on the report of Byrdwell and Neff (43)], the calculated % ABA is given as:

$$\%ABA = \frac{\left(\dfrac{[AA]^+}{[AB]^+}\right)_{AAB} - \left(\dfrac{[AA]^+}{[AB]^+}\right)_{Obs}}{\left(\dfrac{[AA]^+}{[AB]^+}\right)_{AAB} - \left(\dfrac{[AA]^+}{[AB]^+}\right)_{ABA}} x100 = \frac{0.87 - 0.6528}{0.87 - 0.29} x100 = 37.45\%$$
from
Table 1

This calculation indicates that the mixture appears to contain 37.45% POP. Since the FA in this mixture are statistically distributed among all possible positions on the glycerol backbone, the POP isomer would be expected to be present in an amount equal to one-third, or 33%, with PPO and OPP making up the other two-thirds. This synthetic mixture had previously been subjected to lipase hydrolysis, and it was determined that the FA were approximately statistically distributed (7), so it is not surprising that the $[AA]^+/[AB]^+)_{Obs}$ ratio for the POP in the synthetic mixture gives a percentage that is close to the expected value of 33%, even using tabulated values for regioisomeric standards. It must be noted that the tabulated values were obtained on the same instrument. Of course, when accurate quantification is sought, fresh standards should be analyzed. From the preceding discussion and examples below, one can see that, by using the Critical Ratios, the BUS provides the abundances that make up the mass spectrum, and one of the Critical Ratios may provide additional information regarding the composition of regioisomers.

The BUS for a Type III TAG. As already discussed, Type II TAG have a Critical Value and a Critical Limit for the $[MH]^+/\Sigma[DAG]^+$ ratio, which determine the identity of the base peak. Also, the number 1 serves as the Critical Value for the $[AA]^+/[AB]^+$ ratio to determine whether $[AA]^+$ or $[AB]^+$ is larger. Type III TAG have a Critical Value and a Critical Limit for the $[MH]^+/\Sigma[DAG]^+$ ratio, and a Critical Value and

TABLE 4
Spreadsheet Formulas for the Implementation of the Bottom-Up Solution[a]

The spreadsheet formulas, listed by TAG type, are as follows:

Type I:
$[MH]^+$: = IF(Q2=**1**,(E2),(100))
$[AA]^+$: = IF(Q2=**1**,(100),(100/(E2/100)))

Type II:
$[MH]^+$: = IF(Q7=**1**,(IF(R7=**3**,(E7*(1+(G7/100))),(E7*(1+(100/G7))))),(100))
$[AA]^+$: = IF(Q7=**1**,IF(R7=**3**,G7,100),(100/((E7/100)*(1+(1/(G7/100))))))
$[AB]^+$: = IF(Q7=**1**,IF(R7=**3**,100,G7),(100/((E7/100)*(1+(G7/100)))))

Type III:
$[MH]^+$: = IF(Q27=**1**,IF(R27=**3**,(IF(S27=**5**,(E27*(1+(G27/100))*(1+(I27/100))),(E27*(1+(G27/100))* (1+(100/I27))))),(E27*(1+(100/G27)))),100)
$[AC]^+$: = IF(Q27=**1**,IF(R27=**3**,(IF(S27=**5**,(G27*(1+(I27/100))),(G27*(1+(100/I27))))),(100)),(100/ ((E27/100)*(1+(100/G27)))))
$[AB]^+$: = IF(Q27=**1**,(IF(R27=**3**,(IF(S27=**5**,(100),(100/(I27/100)))),(1/((G27/100)*(1+(I27/100)))))), (100/((E27/100)*(1+(G27/100))*(1+(I27/100)))))
$[BC]^+$: = IF(Q27=**1**,(IF(R27=**3**,(IF(S27=**5**,((I27/100)*100),(100))),(1/((G27/100)*(1+(100/I27)))))), (100/((E27/100)*(1+(G27/100))*(1+(100/I27)))))

[a]Assume the columns in Table 2 were labeled A through J, and the rows were numbered from 1 to 37; then the Critical Ratios would be in columns E, G, and I, and the data would be in rows 2 to 36. Imagine the Case classification in Table 3 is in columns Q, R, and S, with the same rows as Table 2.

$$\left(\frac{[MH]^+}{\Sigma[DAG]^+}\right)_{Critical \atop Limit} = \cfrac{1}{\left(1+\cfrac{[AC]^+}{[AB]^++[BC]^+}\right)}\,xCL2 \quad or \quad \cfrac{1}{\left(1+\cfrac{1}{\cfrac{[AC]^+}{[AB]^++[BC]^+}}\right)}$$

Case 3   Case 4

$$\left(\frac{[AC]^+}{[AB]^++[BC]^+}\right)_{Critical \atop Limit\,2} = \cfrac{1}{1+\cfrac{[BC]^+}{[AB]^+}} \quad or \quad \cfrac{1}{1+\cfrac{1}{\cfrac{[BC]^+}{[AB]^+}}}$$

Case n.n.5   Case n.n.6

$$\cfrac{1}{\left(\cfrac{[MH]^+}{\Sigma[DAG]^+} \geq 1\right)}$$

Case 2
[M+H]$^+$ Base Peak

$$\Sigma\left([I]^+\right) = \Sigma([MH]^+ + \Sigma[DAG]^+) =$$

$$\left\{\left(1+\frac{[MH]^+}{\Sigma[DAG]^+}\right) x\,\Sigma[DAG]^+ \quad or \quad \left(1+\cfrac{1}{\cfrac{[MH]^+}{\Sigma[DAG]^+}}\right)\right\}$$

Case 1   Case 2
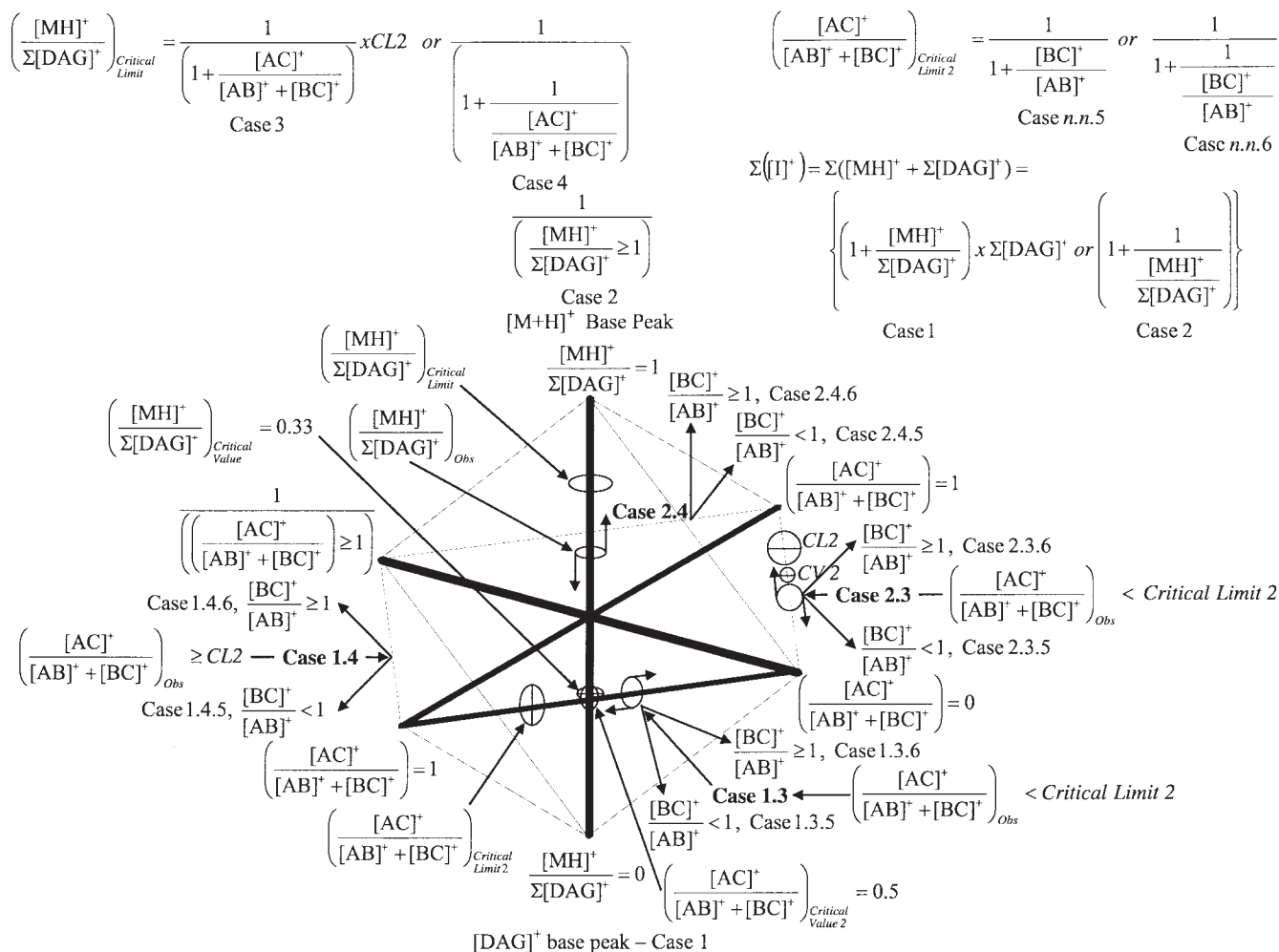
FIG. 4. The Shape of the Triacylglycerol Lipidome for a Type III TAG.

a Critical Limit for the $[AC]^+/([AB]^++[BC]^+)$ ratio, and the value 1 serves as the Critical Value for the $[BC]^+/[AB]^+$ ratio.

The first Critical Value for a Type III TAG is the Critical Value for the $[MH]^+/\Sigma[DAG]^+$ ratio, based on all ions being equal to 1. The Critical Value for the $[MH]^+/\Sigma[DAG]^+$ ratio of a Type III TAG is depicted in the right side of the fourth panel down in Figure 2. The Critical Value of the $[MH]^+/\Sigma[DAG]^+$ ratio for an ABC TAG is 1/3, or 0.33, as shown in Figure 2. A TAG with an $[MH]^+/\Sigma[DAG]^+$ ratio less than the Critical Value cannot have a protonated molecule base peak. The Critical Value for the $[MH]^+/\Sigma[DAG]^+$ ratio is depicted as the lower horizontal ring on the vertical axis in Figure 4. The Critical Values of TAG are inherent values based on the definition of the scale (= 100%) and do not depend on a particular Critical Ratio. An $[MH]^+/\Sigma[DAG]^+$ ratio greater than the Critical Value does not immediately indicate a protonated molecule base peak. The Critical Ratio must be further tested with another limit to determine whether the $[M + H]^+$ is the base peak. As with Type II TAG, the Critical Value serves as the lower limit for the possibility of having a protonated molecule base peak. The $[MH]^+/\Sigma[DAG]^+$ ratio may be above the Critical Value, yet still

not be the base peak, since the Critical Value is based on all $[DAG]^+$ being at their maximum values, which is not usually the case. A Critical Limit, on the other hand, is based on observed Critical Ratios from data. Critical Limits used for Type III TAG, including the limit of the $[MH]^+/\Sigma[DAG]^+$ ratio that defines whether the $[M + H]^+$ is the base peak, are discussed below.

(i) Critical Limit 1 for a Type III TAG. Critical Limit 1 is used to determine whether the $[M + H]^+$ or a $[DAG]^+$ fragment ion is the base peak. Just as the $[AA]^+/[AB]^+$ ratio for a Type II TAG was used to calculate the Critical Limit for a Type II TAG, the $[AC]^+/([AB]^+ + [BC]^+)$ ratio is used in an analogous way to calculate Critical Limit 1 for a Type III TAG. The $[AC]^+/([AB]^+ + [BC]^+)$ ratio is similar to the $[AA]^+/[AB]^+$ ratio in another way, which is that both have a statistically expected value of 0.5. The $[AC]^+$ fragment is one of three possible $[DAG]^+$ fragments, and is taken as a ratio to the other two, so the ratio $[AC]^+/([AB]^+ + [BC]^+)$ has a statistically expected value of 1/2, or 0.5. Also in an analogous way, the $[AC]^+/([AB]^+ + [BC]^+)$ ratio defines the Case 3 and Case 4 possibilities for a Type III TAG, as the $[AA]^+/[AB]^+$ ratio did for

A)

$$\frac{[MH]^+}{\sum[DAG]^+} > 1, \quad so [MH]^+ = 100\% \ and \ Case \ \mathbf{2.}n$$

$$Critical\ Limit = \frac{1}{1+\dfrac{8}{11}} = \frac{1}{\dfrac{19}{11}} = \frac{11}{19} = 0.579$$

$$\frac{[MH]^+}{\sum[DAG]^+} = \frac{100}{95} = \frac{20}{19}$$

$$\frac{[AA]^+}{[AB]^+} = \frac{40}{55} = \frac{8}{11}$$

$$(Not\ Used\ since\ \frac{[MH]^+}{\sum[DAG]^+} > 1)$$

$$\frac{[AA]^+}{[AB]^+} < 1, \ so\ Case\ 2.\mathbf{3}$$

$$Case\ 2.3$$

$$\%[AB]^+ = \frac{1}{\left(\dfrac{20}{19}\right)\left(1+\dfrac{8}{11}\right)} x100 = \frac{1}{\left(\dfrac{20}{19}\right)\left(\dfrac{19}{11}\right)} x100 = \frac{1}{\dfrac{20}{11}} x100 = \frac{11}{20} x100 = 11x5 = 55\%$$

$$\%[AA] = \frac{1}{\left(\dfrac{20}{19}\right)\left(1+\dfrac{1}{\dfrac{8}{11}}\right)} x100 = \frac{1}{\left(\dfrac{20}{19}\right)\left(1+\dfrac{11}{8}\right)} x100 = \frac{1}{\left(\dfrac{20}{19}\right)\left(\dfrac{19}{8}\right)} x100 = \frac{1}{\dfrac{20}{8}} x100 = \frac{8}{20} x100 = 8x5 = 40\%$$

B)

$$Critical\ Limit = \frac{1}{1+\left(\dfrac{1}{\dfrac{15}{14}}\right)} = \frac{1}{1+\dfrac{14}{15}} = \frac{1}{\dfrac{29}{15}} = \frac{15}{29} = .517$$

$$\frac{[MH]^+}{\sum[DAG]^+} = \frac{100}{145} = \frac{20}{29}$$

$$\frac{[AA]^+}{[AB]^+} = \frac{75}{70} = \frac{15}{14}$$

$$\frac{[MH]^+}{\sum[DAG]^+}\left(=\frac{20}{29}\right) \geq Critical\ Limit\left(=\frac{15}{29}\right),$$

$$so\ [M+H]^+ = 100\% \ and\ Case\ \mathbf{2.}n$$

$$Case\ 2.4 \qquad\qquad \frac{[AA]^+}{[AB]^+} \geq 1, so\ Case\ 2.\mathbf{4}$$

$$\%[AB]^+ = \frac{1}{\left(\dfrac{20}{29}\right)\left(1+\dfrac{15}{14}\right)} x100 = \frac{1}{\left(\dfrac{20}{29}\right)\left(\dfrac{29}{14}\right)} x100 = \frac{1}{\dfrac{20}{14}} x100 = \frac{14}{20} x100 = 14x5 = 70\%$$

$$\%[AA]^+ = \frac{1}{\left(\dfrac{20}{29}\right)\left(1+\dfrac{1}{\dfrac{15}{14}}\right)} x100 = \frac{1}{\left(\dfrac{20}{29}\right)\left(1+\dfrac{14}{15}\right)} x100 = \frac{1}{\left(\dfrac{20}{29}\right)\left(\dfrac{29}{15}\right)} x100 = \frac{1}{\dfrac{20}{15}} x100 = \frac{15}{20} x100 = 15x5 = 75\%$$

Continued

FIG. 5. Examples of the Bottom-Up Solution (BUS) to the Triacylglycerol Lipidome, using abundances to the nearest 5%.

the Type II TAG. Because of these similarities, the shape of the area bounded by the $[MH]^+/\Sigma[DAG]^+$ ratio and the $[AC]^+/([AB]^+ + [BC]^+)$ ratio, which are the first two Critical Ratios for a Type III TAG, is similar to the shape of the Type II TAG Lipidome pictured in Figure 3. In the diagram of the shape of the Lipidome for a Type III TAG, the $[AC]^+/([AB]^+ +$ $[BC]^+)$ ratio is on the equatorial axis instead of the $[AA]^+/$ $[AB]^+$ ratio, as shown in Figure 4.

The $[AC]^+/([AB]^+ + [BC]^+)$ ratio has a Critical Value of 0.5 that represents the minimum value that the ratio can have and still have an $[AC]^+$ abundance larger than or equal to the $[AB]^+$ and $[BC]^+$ abundances. If the $[AC]^+/([AB]^+ + [BC]^+)$ ratio has

C)

$$\frac{[MH]^+}{\sum[DAG]^+} = \frac{100}{200} = \frac{1}{2}$$

$$\frac{[AC]^+}{([AB]^+ + [BC]^+)} = \frac{55}{145} = \frac{11}{29}$$

$$\frac{[BC]^+}{[AB]^+} = \frac{60}{85} = \frac{12}{17}$$

e.g.- LnLP
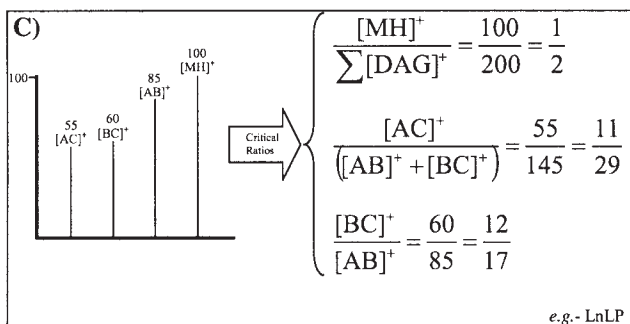
$\frac{[BC]^+}{[AB]^+} < 1$, so Case *n.n.***5** Critical Limit $2 = \dfrac{1}{1+\dfrac{12}{17}} = \dfrac{1}{\dfrac{29}{17}} = \dfrac{17}{29}$

$\dfrac{[AC]^+}{([AB]^+ + [BC]^+)} < C_{L2}$, so Case *n.***3**.*n*

Critical Limit $1 = \dfrac{1}{1+\dfrac{11}{29}} x C_{L2} = \dfrac{1}{\dfrac{40}{29}} x \dfrac{17}{29} = \dfrac{29}{40} x \dfrac{17}{29} = \dfrac{17}{40}$

$\dfrac{[MH]^+}{\sum[DAG]^+} \overset{?}{\geq} CL1: \dfrac{1}{2} \overset{?}{\geq} \dfrac{17}{40}:$ YES, so Case **2**.*n.n*

Therefore: Case 2.3.5

Case 2.3.5
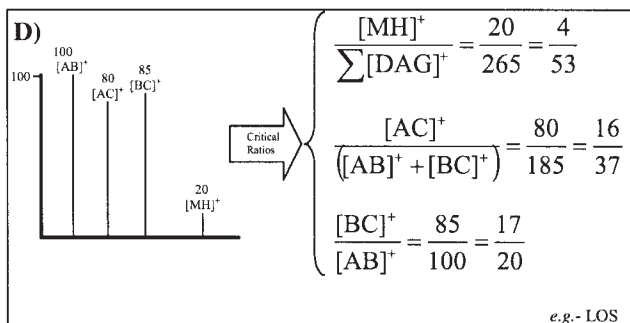
Case 2, so $[M+H]^+ = 100\%$ (base peak)

$$\%[AC]^+ = \frac{1}{\left(\frac{1}{2}\right)\left(1+\frac{1}{\frac{11}{29}}\right)} x100 = \frac{1}{\left(\frac{1}{2}\right)\left(1+\frac{29}{11}\right)} x100 = \frac{1}{\left(\frac{1}{2}\right)\left(\frac{40}{11}\right)} x100 = \frac{1}{\frac{20}{11}} x100 = \frac{11}{20} x100 = 55\%$$

$$\%[AB]+ = \frac{1}{\left(\frac{1}{2}\right)\left(1+\frac{11}{29}\right)\left(1+\frac{12}{17}\right)} x100 = \frac{1}{\left(\frac{1}{2}\right)\left(\frac{40}{29}\right)\left(\frac{29}{17}\right)} x100 = \frac{1}{\frac{40}{34}} x100 = \frac{17}{20} x100 = 17x5 = 85\%$$

$$\%[BC]^+ = \frac{1}{\left(\frac{1}{2}\right)\left(1+\frac{11}{29}\right)\left(1+\frac{1}{\frac{12}{17}}\right)} x100 = \frac{1}{\left(\frac{1}{2}\right)\left(\frac{40}{29}\right)\left(1+\frac{17}{12}\right)} x100 = \frac{1}{\left(\frac{1}{2}\right)\left(\frac{40}{29}\right)\left(\frac{29}{12}\right)} x100 = \frac{1}{\frac{40}{24}} x100 = \frac{3}{5} x100 = 60\%$$

D)

$$\frac{[MH]^+}{\sum[DAG]^+} = \frac{20}{265} = \frac{4}{53}$$

$$\frac{[AC]^+}{([AB]^+ + [BC]^+)} = \frac{80}{185} = \frac{16}{37}$$

$$\frac{[BC]^+}{[AB]^+} = \frac{85}{100} = \frac{17}{20}$$

e.g.- LOS

$\frac{[BC]^+}{[AB]^+} < 1$, so Case *n.n.***5** Critical Limit $2 = \dfrac{1}{1+\dfrac{17}{20}} = \dfrac{1}{\dfrac{37}{20}} = \dfrac{20}{37}$

$\dfrac{[AC]^+}{([AB]^+ + [BC]^+)} < C_{L2}$, so Case *n.***3**.*n*

Critical Limit $1 = \dfrac{1}{1+\dfrac{16}{37}} x C_{L2} = \dfrac{1}{\dfrac{53}{37}} x \dfrac{20}{37} = \dfrac{37}{53} x \dfrac{20}{37} = \dfrac{20}{53}$

$\dfrac{[MH]^+}{\sum[DAG]^+} \overset{?}{\geq} CL1: \dfrac{4}{53} \overset{?}{\geq} \dfrac{20}{53}:$ NO, so Case **1**.*n.n*

Therefore: Case 1.3.5

Case 1.3.5

Case 1.3.5, so $[AB]^+ = 100\%$ (base peak)

$$\%[BC]^+ = \frac{17}{20} x100 = 17x5 = 85\%$$

$$\%[AC]^+ = \left(\frac{16}{37}\right)\left(1+\frac{17}{20}\right) x100 = \left(\frac{16}{37}\right)\left(\frac{37}{20}\right) x100 = \frac{16}{20} x100 = 16x5 = 80\%$$

$$\%[MH]^+ = \left(\frac{4}{53}\right)\left(1+\frac{16}{37}\right)\left(1+\frac{17}{20}\right) x100 = \left(\frac{4}{53}\right)\left(\frac{53}{37}\right)\left(\frac{37}{20}\right) x100 = \frac{4}{20} x100 = 4x5 = 20\%$$

Continued

FIG. 5. (Continued)

E)

$$\frac{[MH]^+}{\sum[DAG]^+} = \frac{25}{250} = \frac{1}{10}$$

$$\frac{[AC]^+}{([AB]^+ + [BC]^+)} = \frac{70}{180} = \frac{7}{18}$$

$$\frac{[BC]^+}{[AB]^+} = \frac{100}{80} = \frac{5}{4}$$

$$\frac{[BC]^+}{[AB]^+} > 1, \text{ so Case } n.n.\mathbf{6}$$

$$\text{Critical Limit 2} = \frac{1}{1 + \frac{1}{\frac{5}{4}}} = \frac{1}{\frac{9}{5}} = \frac{5}{9}$$

$$\frac{[AC]^+}{([AB]^+ + [BC]^+)} < C_{L2}, \text{ so Case } n.\mathbf{3}.n$$

$$\text{Critical Limit 1} = \frac{1}{1 + \frac{7}{18}} x C_{L2} = \frac{1}{\frac{25}{18}} x \frac{5}{9} = \frac{18}{25} x \frac{5}{9} = \frac{2}{5}$$

$$\frac{[MH]^+}{\sum[DAG]^+} \overset{?}{\geq} CL1: \frac{1}{10} \overset{?}{\geq} \frac{2}{5}: \quad \text{NO, so Case } \mathbf{1}.n.n$$
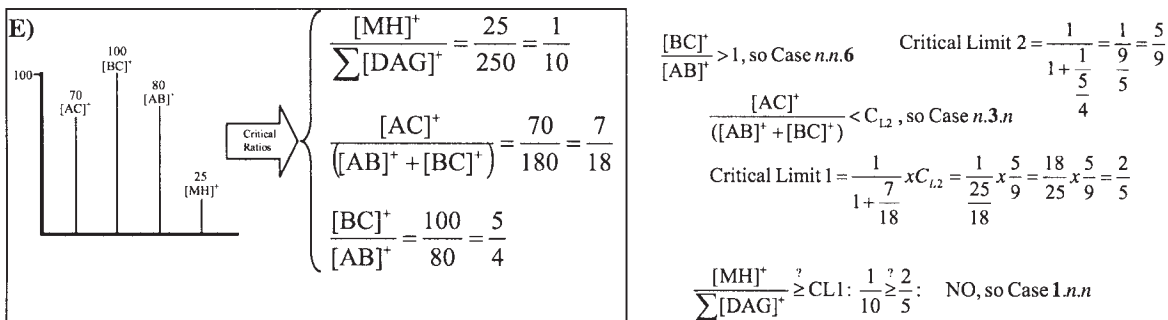
$$\text{Therefore: Case 1.3.6}$$
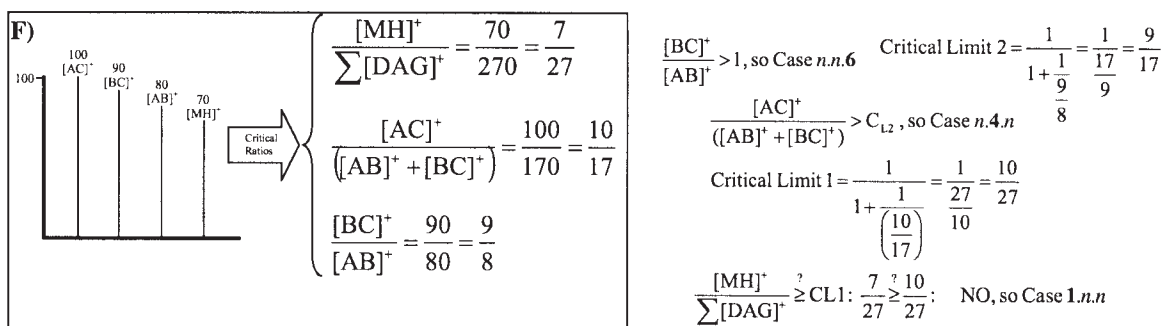
Case 1.3.6

Case 1.3.6, so $[BC]^+ = 100 \%$ (base peak)

$$\%[AB]^+ = \frac{1}{\left(\frac{5}{4}\right)} x100 = \frac{4}{5} x100 = 4 x 20 = 80\%$$

$$\%[AC]^+ = \left(\frac{7}{18}\right)\left(1 + \frac{1}{\frac{5}{4}}\right) x100 = \left(\frac{7}{18}\right)\left(\frac{9}{5}\right) x100 = \frac{7}{10} x100 = 70\%$$

$$\%[M+H]^+ = \left(\frac{1}{10}\right)\left(1 + \frac{7}{18}\right)\left(1 + \frac{1}{\frac{5}{4}}\right) x100 = \left(\frac{1}{10}\right)\left(\frac{25}{18}\right)\left(\frac{9}{5}\right) x100 = \frac{5}{20} x100 = 5 x 5 = 25\%$$

F)

$$\frac{[MH]^+}{\sum[DAG]^+} = \frac{70}{270} = \frac{7}{27}$$

$$\frac{[AC]^+}{([AB]^+ + [BC]^+)} = \frac{100}{170} = \frac{10}{17}$$

$$\frac{[BC]^+}{[AB]^+} = \frac{90}{80} = \frac{9}{8}$$

$$\frac{[BC]^+}{[AB]^+} > 1, \text{ so Case } n.n.\mathbf{6}$$

$$\text{Critical Limit 2} = \frac{1}{1 + \frac{1}{\frac{9}{8}}} = \frac{1}{\frac{17}{9}} = \frac{9}{17}$$

$$\frac{[AC]^+}{([AB]^+ + [BC]^+)} > C_{L2}, \text{ so Case } n.\mathbf{4}.n$$

$$\text{Critical Limit 1} = \frac{1}{1 + \frac{1}{\left(\frac{10}{17}\right)}} = \frac{1}{\frac{27}{10}} = \frac{10}{27}$$

$$\frac{[MH]^+}{\sum[DAG]^+} \overset{?}{\geq} CL1: \frac{7}{27} \overset{?}{\geq} \frac{10}{27}: \quad \text{NO, so Case } \mathbf{1}.n.n$$

$$\text{Therefore: Case 1.4.6}$$

Case 1.4.6

Case 1.**4**.n, so $[AC]^+ = 100 \%$ (base peak)

$$\%[M+H]^+ = \left(\frac{7}{27}\right)\left(1 + \frac{1}{\frac{10}{17}}\right) x100 = \left(\frac{7}{27}\right)\left(\frac{27}{10}\right) x100 = \frac{7}{10} x100 = 70\%$$

$$\%[AB]^+ = \frac{1}{\left(\frac{10}{17}\right)\left(1 + \frac{9}{8}\right)} x100 = \frac{1}{\left(\frac{10}{17}\right)\left(\frac{17}{8}\right)} x100 = \frac{1}{\frac{10}{8}} x100 = \frac{8}{10} x100 = 80\%$$

$$\%[BC]^+ = \frac{1}{\left(\frac{10}{17}\right)\left(1 + \frac{1}{\frac{9}{8}}\right)} x100 = \frac{1}{\left(\frac{10}{17}\right)\left(\frac{17}{9}\right)} x100 = \frac{1}{\frac{10}{9}} x100 = \frac{9}{10} x100 = 90\%$$

FIG. 5. (Continued)

a value less than 0.5, then $[AC]^+$ must be smaller than $[AB]^+$ or $[BC]^+$, and so is a Case $n.3.n$ solution. Coincidentally, this second Critical Value for a Type III TAG also equals the statistically expected value of this Critical Ratio. The Critical Value of this Critical Ratio is seen in Scheme 1, Part III, and it is shown as Critical Value 2 on the equatorial axis in Figure 4.

If the ratio $[AC]^+/([AB]^+ + [BC]^+)$ is greater than 1, then $[AC]^+$ is automatically known to be larger than $[AB]^+$ and $[BC]^+$, and Critical Limit 1 can be constructed based only on $[AC]^+/([AB]^+ + [BC]^+)$. Furthermore, if $[AC]^+/([AB]^+ + [BC]^+)$ is greater than 1, this indicates a Case $n.4.n$ solution. For a Case $n.4.n$ solution, the value of Critical Limit 1 is given as:

$$\text{Critical Limit } 1 = \cfrac{1}{1 + \cfrac{1}{\left(\cfrac{[AC]^+}{([AB]^+ + [BC]^+)}\right)}} \quad [7]$$

When the solution is classified as Case $n.4.n$ solution, $[AC]^+ = 100\% \ (= 1.00)$ at Critical Limit 1, because it is larger than $[AB]^+$ and $[BC]^+$, and so it is the peak against which the $[M + H]^+$ must be compared to determine the base peak. This is shown in the bottom panel of Figure 2.

When the $[AC]^+/([AB]^+ + [BC]^+)$ ratio is less than 1 but greater than 0.5, it must be compared with Critical Limit 2 to determine whether it is Case 3 or Case 4. The equation for Critical Limit 2 requires the use of the $[BC]^+/[AB]^+$ ratio, and so this ratio is first classified as either Case 5, in which the $[BC]^+/[AB]^+$ ratio is < 1, or Case 6, in which the $[BC]^+/[AB]^+$ ratio is ≥ 1. Knowing the Case for the third Critical Ratio for a Type III TAG allows Critical Limit 2 for the TAG to be calculated, which is:

$$\left(\frac{[AC]^+}{[AB]^+ + [BC]^+}\right)_{\substack{\text{Critical} \\ \text{Limit 2}}} = \cfrac{1}{1 + \cfrac{[BC]^+}{[AB]^+}} \ or \ \cfrac{1}{1 + \cfrac{1}{\cfrac{[BC]^+}{[AB]^+}}}$$

$$\text{Case 5} \qquad\qquad \text{Case 6}$$

Then, to fully calculate Critical Limit 1 for a Case $n.3.n$ Type III TAG, both Critical Ratio 2 and Critical Ratio 3 are used. The complete equation for Critical Limit 1 for a Case $n.3.n$ solution is given as follows:

For Case 5:

$$\left(\frac{[MH]^+}{\Sigma[DAG]^+}\right)_{\substack{\text{Critical} \\ \text{Limit 1}}} = \cfrac{1}{1 + \cfrac{[AC]^+}{[AB]^+ + [BC]^+}} \times \cfrac{1}{1 - \cfrac{[BC]^+}{[AB]^+}} = \cfrac{1}{\left(1 + \cfrac{[AC]^+}{[AB]^+ - [BC]^+}\right)\left(1 + \cfrac{[BC]^+}{[AB]^+}\right)} = \cfrac{1}{1 + \cfrac{[AC]^+}{[AB]^+ + [BC]^+}} \times CI.2$$

or, for Case 6:

$$\left(\frac{[MH]^+}{\Sigma[DAG]^+}\right)_{\substack{\text{Critical} \\ \text{Limit 1}}} = \cfrac{1}{1 - \cfrac{[AC]^+}{[AB]^+ + [BC]^+}} \times \cfrac{1}{1 - \cfrac{1}{\cfrac{[BC]^+}{[AB]^+}}} = \cfrac{1}{\left(1 - \cfrac{[AC]^+}{[AB]^+ + [BC]^+}\right)\left(1 + \cfrac{1}{\cfrac{[BC]^+}{[AB]^+}}\right)} = \cfrac{1}{1 + \cfrac{[AC]^+}{[AB]^+ - [BC]^+}} \times CI.2$$

(ii) Critical Limit 2 for a Type III TAG. As seen above, Critical Limit 2 is necessary to calculate Critical Limit 1 when the $[AC]^+/([AB]^+ + [BC]^+)$ ratio is Case 3. This is the statistically expected normal circumstance. As already mentioned, the statistically expected $[AC]^+/([AB]^+ + [BC]^+)$ ratio is 0.5. To determine whether the $[AC]^+$ abundance is less than $[AB]^+$ or $[BC]^+$, or whether it is greater than $[AB]^+$ and $[BC]^+$, the $[AC]^+/([AB]^+ + [BC]^+)$ ratio must be compared with Critical Limit 2. This determines whether $[AC]^+/([AB]^+ + [BC]^+)$ obeys a Case 3.0 or a Case 4.0 solution. Critical Limit 2, in turn, depends on whether the third Critical Ratio, $[BC]^+/[AB]^+$, is greater than or less than 1.

Critical Limit 2 is calculated as follows:

$$\text{if} \left(\frac{[BC]^+}{[AB]^+}\right) < 1.0, \text{ then } \textit{Critical Limit 2} = \cfrac{1}{1 + \cfrac{[BC]^+}{[AB]^+}} \ , \text{Else } \textit{Critical Limit 2} = \cfrac{1}{1 + \cfrac{1}{\left(\cfrac{[BC]^+}{[AB]^+}\right)}} \ [8]$$
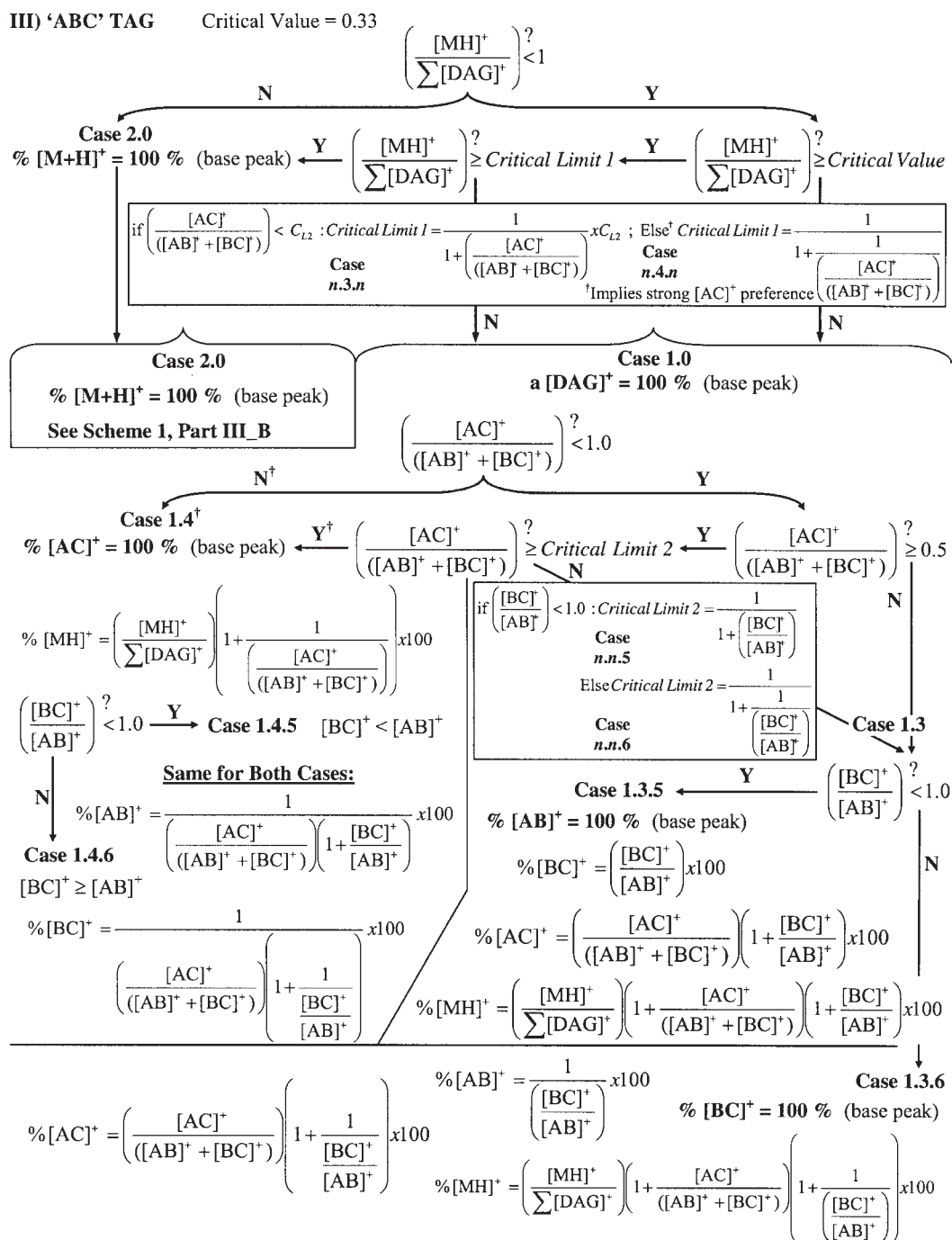
$$\text{Case } n.n.5 \qquad\qquad \text{Case } n.n.6$$

When this *Critical Limit 2* has been calculated, it is then used to calculate *Critical Limit 1*:

$$\text{if} \left(\frac{[AC]^+}{([AB]^+ + [BC]^+)}\right) < \textit{Critical Limit 2}, \text{ then } \textit{Critical Limit 1} = \cfrac{1}{1 + \left(\cfrac{[AC]^+}{([AB]^+ + [BC]^+)}\right)} x \textit{ Critical Limit 2};$$

$$\text{Else } \textit{Critical Limit 1} = \cfrac{1}{1 + \cfrac{[AC]^+}{([AB]^+ + [BC]^+)}} \qquad [9]$$

Critical Limit 1 is used to specify whether $[M + H]^+$ is the base peak, which determines either Case 1.0 or Case 2.0. Critical Limit 2 is used to specify whether $[AC]^+$ is larger than $[AB]^+$ and $[BC]^+$, which specifies either Case 3.0 or 4.0. The $[BC]^+/[AB]^+$ ratio alone (<1 or ≥ 1) specifies either Case 5 or 6. Thus, the complete Case classification can be given by comparison of the three Critical Ratios to Critical Limit 1, Critical Limit 2, and 1 (= Critical Value 3).

Once the Case has been classified, the complete set of equations necessary to calculate the abundance of every ion is given in Scheme 1, Part IIIA or IIIB, for the Case 1 or Case 2 solutions, respectively. Up to five specific values can be calculated from three Critical Ratios: (i) the abundance of the protonated molecule, (ii) the abundances of each of the three $[DAG]^+$ fragment ions, and (iii) the sum of all the ions. Three critical ratios are required to specify the four primary ions in an APCI-MS mass spectrum of an ABC-type TAG, plus the sum of all ions. Only two critical ratios are required to fully describe the three primary ions in the mass spectrum of an ABA/AAB-type TAG. Four specific values may be calculated for the mass spectrum of a Type II TAG: (i) the abundance of the protonated molecule, (ii) the abundances of each of the two $[DAG]^+$ fragment ions, $[AA]^+$ and $[AB]^+$, and (iii) the sum of all ions. Only one single Critical Ratio is necessary to describe an AAA, or Type I TAG. That one ratio specifies that one peak is the base peak and the other is a ratio to the first, and the sum of the ions is then given.
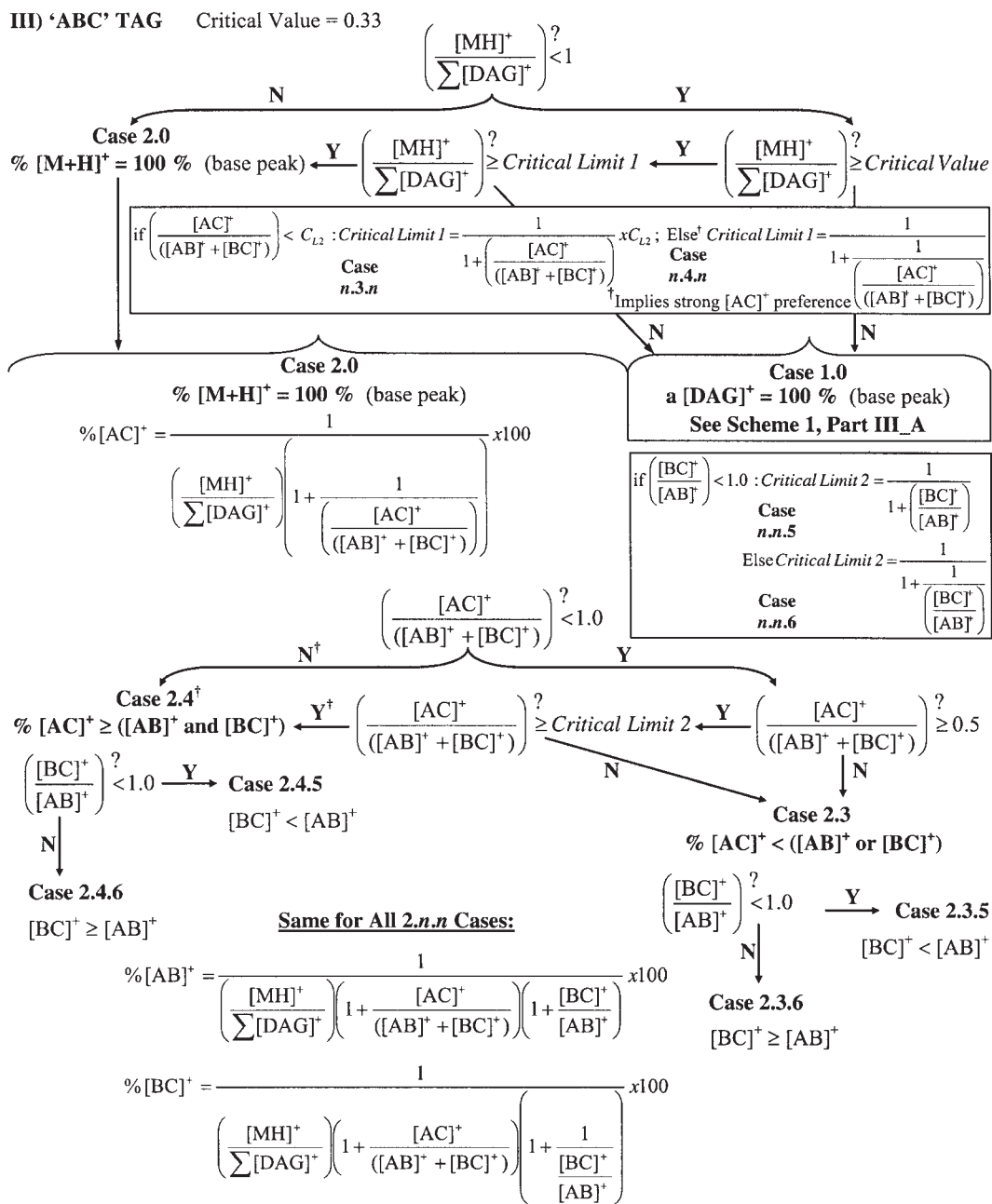
III) 'ABC' TAG   Critical Value = 0.33

$$\left(\frac{[MH]^+}{\sum[DAG]^+}\right)\overset{?}{<}1$$

N ——————————————————————— Y

Case 2.0
% $[M+H]^+$ = 100 % (base peak) $\overset{Y}{\longleftarrow}$ $\left(\frac{[MH]^+}{\sum[DAG]^+}\right)\overset{?}{\geq}$ Critical Limit 1 $\overset{Y}{\longleftarrow}$ $\left(\frac{[MH]^+}{\sum[DAG]^+}\right)\overset{?}{\geq}$ Critical Value

$$\text{if}\left(\frac{[AC]^+}{([AB]^++[BC]^+)}\right)<C_{L2}: Critical\ Limit\ 1 = \frac{1}{1+\left(\frac{[AC]^+}{([AB]^++[BC]^+)}\right)}xC_{L2}\ ;\ \text{Else}^\dagger Critical\ Limit\ 1 = \frac{1}{1+\frac{1}{\left(\frac{[AC]^+}{([AB]^++[BC]^+)}\right)}}$$

Case **n.3.n**   Case **n.4.n** †Implies strong $[AC]^+$ preference

N   N

Case 2.0   **Case 1.0**
% $[M+H]^+$ = 100 % (base peak)   a $[DAG]^+$ = 100 % (base peak)

See Scheme 1, Part III_B

$$\left(\frac{[AC]^+}{([AB]^++[BC]^+)}\right)\overset{?}{<}1.0$$

N† ——————————————————— Y

Case 1.4†
% $[AC]^+$ = 100 % (base peak) $\overset{Y^\dagger}{\longleftarrow}$ $\left(\frac{[AC]^+}{([AB]^++[BC]^+)}\right)\overset{?}{\geq}$ Critical Limit 2 $\overset{Y}{\longleftarrow}$ $\left(\frac{[AC]^+}{([AB]^++[BC]^+)}\right)\overset{?}{\geq}0.5$

N   N

$$\%[MH]^+ = \left(\frac{[MH]^+}{\sum[DAG]^+}\right)\left(1+\frac{1}{\left(\frac{[AC]^+}{([AB]^++[BC]^+)}\right)}\right)x100$$

$$\text{if}\left(\frac{[BC]^+}{[AB]^+}\right)<1.0: Critical\ Limit\ 2 = \frac{1}{1+\left(\frac{[BC]^+}{[AB]^+}\right)}$$

Case **n.n.5**

$$\text{Else}\ Critical\ Limit\ 2 = \frac{1}{1+\frac{1}{\left(\frac{[BC]^+}{[AB]^+}\right)}}$$

Case **n.n.6**

$$\left(\frac{[BC]^+}{[AB]^+}\right)\overset{?}{<}1.0\overset{Y}{\longrightarrow}\ \textbf{Case 1.4.5}\quad [BC]^+<[AB]^+$$

N

Case 1.4.6
$[BC]^+\geq[AB]^+$

Same for Both Cases:

$$\%[AB]^+ = \frac{1}{\left(\frac{[AC]^+}{([AB]^++[BC]^+)}\right)\left(1+\frac{[BC]^+}{[AB]^+}\right)}x100$$

Case 1.3.5 $\overset{Y}{\longleftarrow}$ $\left(\frac{[BC]^+}{[AB]^+}\right)\overset{?}{<}1.0$

% $[AB]^+$ = 100 % (base peak)

$$\%[BC]^+ = \left(\frac{[BC]^+}{[AB]^+}\right)x100$$

Case 1.3

N

$$\%[BC]^+ = \frac{1}{\left(\frac{[AC]^+}{([AB]^++[BC]^+)}\right)\left(1+\frac{1}{\frac{[BC]^+}{[AB]^+}}\right)}x100$$

$$\%[AC]^+ = \left(\frac{[AC]^+}{([AB]^++[BC]^+)}\right)\left(1+\frac{[BC]^+}{[AB]^+}\right)x100$$

$$\%[MH]^+ = \left(\frac{[MH]^+}{\sum[DAG]^+}\right)\left(1+\frac{[AC]^+}{([AB]^++[BC]^+)}\right)\left(1+\frac{[BC]^+}{[AB]^+}\right)x100$$

$$\%[AC]^+ = \left(\frac{[AC]^+}{([AB]^++[BC]^+)}\right)\left(1+\frac{1}{\frac{[BC]^+}{[AB]^+}}\right)x100$$

$$\%[AB]^+ = \frac{1}{\left(\frac{[BC]^+}{[AB]^+}\right)}x100$$

Case 1.3.6
% $[BC]^+$ = 100 % (base peak)

$$\%[MH]^+ = \left(\frac{[MH]^+}{\sum[DAG]^+}\right)\left(1+\frac{[AC]^+}{([AB]^++[BC]^+)}\right)\left(1+\frac{1}{\frac{[BC]^+}{[AB]^+}}\right)x100$$

SCHEME 1, PART IIIA. Equations to calculate the relative abundances of the $[M + H]^+$ and $[DAG]^+$ fragment ions for Type III TAG (= ABC), Case 1.*n.n*, using Critical Ratios from APCI-MS data (Table 2). For abbreviation see Scheme 1, Part I.

IMPLEMENTATION OF THE BUS

The Critical Ratios are the key elements of the BUS to the TAG Lipidome. During the process of investigating the relationships between the Critical Ratios and the structural information that they provide, it was observed that the Critical Ratios contained all of the information necessary to reconstruct the mass spectrum from which they came. Thus, the starting point for the BUS for TAG is the construction of the Critical Ratios for the TAG. The reasons for the identities of the Critical Ratios were given in the section entitled Construction of the Critical Ratios. The Critical Ratios may be constructed from abundances or areas in several ways. They may be constructed either from the abundances from a single mass spectrum or from an averaged mass spectrum obtained by averaging individual mass spectra over time from data obtained by infusion of an analyte solution

III) 'ABC' TAG   Critical Value = 0.33

$$\left(\frac{[MH]^+}{\sum[DAG]^+}\right)\overset{?}{<}1$$

N   Y

Case 2.0
% [M+H]$^+$ = 100 % (base peak) $\overset{Y}{\longleftarrow}$ $\left(\dfrac{[MH]^+}{\sum[DAG]^+}\right)\overset{?}{\geq} Critical\ Limit\ 1$ $\overset{Y}{\longleftarrow}$ $\left(\dfrac{[MH]^+}{\sum[DAG]^+}\right)\overset{?}{\geq} Critical\ Value$

$$if\left(\frac{[AC]^+}{([AB]^+ +[BC]^+)}\right)<C_{L2} : Critical\ Limit\ 1 = \frac{1}{1+\left(\frac{[AC]^+}{([AB]^+ +[BC]^+)}\right)}xC_{L2}\ ;\ Else^{\dagger}\ Critical\ Limit\ 1 = \frac{1}{1+\frac{1}{\left(\frac{[AC]^+}{([AB]^+ +[BC]^+)}\right)}}$$

Case n.3.n   **Case n.4.n**

$\dagger$Implies strong [AC]$^+$ preference

N   N

Case 2.0
% [M+H]$^+$ = 100 % (base peak)

$$\%[AC]^+ = \frac{1}{\left(\frac{[MH]^+}{\sum[DAG]^+}\right)\left(1+\frac{1}{\left(\frac{[AC]^+}{([AB]^+ +[BC]^+)}\right)}\right)}x100$$

Case 1.0
a [DAG]$^+$ = 100 % (base peak)
See Scheme 1, Part III_A

$$if\left(\frac{[BC]^+}{[AB]^+}\right)<1.0 : Critical\ Limit\ 2 = \frac{1}{1+\frac{[BC]^+}{[AB]^+}}$$

Case n.n.5

$$Else\ Critical\ Limit\ 2 = \frac{1}{1+\frac{1}{\frac{[BC]^+}{[AB]^+}}}$$

Case n.n.6

$$\left(\frac{[AC]^+}{([AB]^+ +[BC]^+)}\right)\overset{?}{<}1.0$$

N† Y

Case 2.4†
% [AC]$^+$ ≥ ([AB]$^+$ and [BC]$^+$) $\overset{Y^{\dagger}}{\longleftarrow}$ $\left(\dfrac{[AC]^+}{([AB]^+ +[BC]^+)}\right)\overset{?}{\geq} Critical\ Limit\ 2$ $\overset{Y}{\longleftarrow}$ $\left(\dfrac{[AC]^+}{([AB]^+ +[BC]^+)}\right)\overset{?}{\geq}0.5$

$\left(\dfrac{[BC]^+}{[AB]^+}\right)\overset{?}{<}1.0$ $\overset{Y}{\longrightarrow}$ **Case 2.4.5**
         [BC]$^+$ < [AB]$^+$

N   N

Case 2.4.6
[BC]$^+$ ≥ [AB]$^+$

Case 2.3
% [AC]$^+$ < ([AB]$^+$ or [BC]$^+$)

$\left(\dfrac{[BC]^+}{[AB]^+}\right)\overset{?}{<}1.0$ $\overset{Y}{\longrightarrow}$ **Case 2.3.5**
         [BC]$^+$ < [AB]$^+$

N

Case 2.3.6
[BC]$^+$ ≥ [AB]$^+$

Same for All 2.n.n Cases:

$$\%[AB]^+ = \frac{1}{\left(\frac{[MH]^+}{\sum[DAG]^+}\right)\left(1+\frac{[AC]^+}{([AB]^+ +[BC]^+)}\right)\left(1+\frac{[BC]^+}{[AB]^+}\right)}x100$$

$$\%[BC]^+ = \frac{1}{\left(\frac{[MH]^+}{\sum[DAG]^+}\right)\left(1+\frac{[AC]^+}{([AB]^+ +[BC]^+)}\right)\left(1+\frac{1}{\frac{[BC]^+}{[AB]^+}}\right)}x100$$

SCHEME 1, PART IIIB. Equations to calculate the relative abundances of [M + H]+ and [DAG]$^+$ fragment ions for Type III TAG (= ABC), Case 2.n.n, using Critical Ratios from APCI-MS data (Table 2). For abbreviation see Scheme 1, Part I.

at a constant rate, or from data by injection of analyte into an infused solvent flow. Further still, the mass spectrum used to construct the Critical Ratios may be an averaged-in-time mass spectrum across a chromatographic peak, or it may be constructed from the integrated-in-time normalized relative area abundances. For mass spectra across a chromatographic peak, the abundances are different in the middle, front, and back portions of the peak, as was mentioned by Mottram *et al.* (11) and in a recent review (45). For Type II TAG, it appears that the regioisomers may be partially separated across the breadth of the

peak. Construction of the Critical Ratios for the first, middle, and last portions of the chromatographic peaks may help to make more trends apparent. For polyunsaturated TAG, the [AA]$^+$/[AB]$^+$ ratio is higher than other TAG and is often greater than 1.

The averaged mass spectrum across a chromatographic peak shows all ions eluted at that particular time. Similarly, a plot of the areas under integrated peaks in ion chromatograms at a particular retention time, normalized to 1 (or 100%), appears the same as a mass spectrum averaged across that time window. The

averaged mass spectrum of each TAG of the 35-TAG mixture given in Table 5 is an average of the three sets of mass spectra given by the (abundance × time) integrated peak areas of each of three chromatographic runs, in which complete chromatographic resolution was achieved between almost all TAG molecular species. Peaks that appear to overlap in the total ion current chromatogram (TIC) are resolved in ion chromatograms of [DAG]⁺ fragments that are extracted out of the TIC, to form extracted ion chromatograms (EIC). Any overlapped peaks are apportioned as has been described previously (7,34). In the data set used herein, the only chromatographic peak that required apportionment was the P peak of OL and the O peak of SLn in the *m/z* 601.5 EIC, marked with an asterisk in Figure 6E. In whichever manner the percent relative abundances are obtained that represent the mass spectrum, the Critical Ratios can be calculated from the abundances or areas. One need not convert integrated peak areas to percent relative abundances, since the critical ratios can be calculated directly from the integrated areas as long as they are properly grouped by retention time for each TAG. However,

when averaging several runs, calculations should be based on normalized area percentages.

Error propagation in the Critical Ratios must be mentioned. In Table 2, the SD are not simply the SD of the three numerically calculated ratio values. Since the Critical Ratios are ratios of average abundances that each have a SD, error propagation is more correctly calculated as the square root of the sum of the squares of the percent relative SD of the abundances involved in the construction of the ratios. Table 2 shows the SD calculated in this way. When a ratio has been shown to have a linear relationship, such as the [AA]⁺/[AB]⁺ ratio for regioisomers, it may be appropriate to express the simpler SD in the ratio itself. In Table 2, the simple SD of the three numeric [AA]⁺/[AB]⁺ ratio values has been shown as SD2. In most cases, the peak that is the base peak in an averaged mass spectrum is the base peak in each of the averaged spectra, and so that abundance has a 0% SD from spectrum to spectrum. In the cases of highly unsaturated TAG, the error expressed as the square root of the sum of the squares of the SD of the abundances was larger than for TAG containing

TABLE 5
Percent Relative Ion Abundances Calculated from the Critical Ratios in Table 2, Using the Bottom-Up Solution in Scheme 1, Implemented by the Formulas in Table 4[a]

TAG	[MH]⁺	[AA]⁺ or [AC]⁺	[AB]⁺	[BC]⁺	ΣI%
PPP	0.00	100.00			100.00
SSS	0.00	100.00			100.00
OOO	3.24	100.00			103.24
LLL	100.00	83.28			183.28
LnLnLn	100.00	44.88			144.88
PSP/PPS	0.00	49.26	100.00		149.26
POP/PPO	0.91	65.28	100.00		166.19
PLP/PPL	0.74	84.11	100.00		184.85
PLnP/PPLn	21.77	69.94	100.00		191.71
SPS/SSP	0.00	40.91	100.00		140.91
SOS/SSO	0.79	75.14	100.00		175.93
SLS/SSL	0.77	82.89	100.00		183.66
SLnS/SSLn	15.44	60.98	100.00		176.42
OPO/OOP	2.57	36.12	100.00		138.69
OSO/OOS	1.57	39.82	100.00		141.39
OLO/OOL	17.91	50.10	100.00		168.01
OLnO/OOLn	52.31	41.62	100.00		193.93
LPL/LLP	52.20	88.84	100.00		241.04
LSL/LLS	76.54	76.07	100.00		252.61
LOL/LLO	77.60	74.62	100.00		252.22
LLnL/LLLn	100.00	33.74	64.93		198.67
LnPLn/LnLnP	100.00	42.19	56.49		198.69
LnSLn/LnLnS	100.00	79.50	83.60		263.11
LnOLn/LnLnO	100.00	44.99	53.69		198.68
LnLLn/LnLnL	100.00	30.51	47.61		178.12
OPS	1.10	63.91	100.00	69.79	234.80
SPL	0.99	56.42	100.00	59.43	216.85
SPLn	22.92	70.29	100.00	76.70	269.91
LOP	17.93	80.08	100.00	98.27	296.28
LnOP	74.01	80.54	100.00	91.76	346.31
LnLP	100.00	54.96	86.35	63.36	304.67
LOS	19.90	81.45	100.00	85.70	287.05
OLnS	53.87	80.49	100.00	89.53	323.89
LnLS	100.00	61.47	89.06	69.98	320.51
LLnO	100.00	50.63	70.93	55.08	276.65

[a]This is an exact reproduction of the average mass spectrum obtained as an average of three chromatographic runs. I, ion abundance; for other abbreviations see Table 1.

FA with fewer sites of unsaturation. TAG. Although the approach used to obtain an averaged mass spectrum affects the SD of the abundances, the BUS does not depend on the approach used to obtain the mass spectrum.

Figures 5A through 5F show examples of mass spectra and the construction of the Critical Ratios. For Type II TAG, the $[AA]^+/[AB]^+$ ratio can be used to assess the amounts of regioisomers; so instead of providing abundances, which would then need to be converted into the ratio that is compared to regioisomeric standards, one could provide the desired ratio directly, along with one or two other ratios, which constitute the set of Critical Ratios. These ratios can be tabulated in fewer values than the raw abundances. The ratios therefore are a more efficient means of storing information. They provide more information in fewer values.

Automated spreadsheet implementation of the BUS starts with the classification of the Critical Ratios into Cases. The classification can be accomplished using only the Critical Limits. The Critical Values do not need to be used in the automated implementation. If the columns in Table 2 were labeled A through J, and the rows were numbered from 1 to 37, then the Critical Ratios would be in columns E, G, and I, and the data would be in rows 2 to 36. Based on Table 2 numbered as mentioned, the following formulas allow the calculation of the Critical Limits:

Type II: J7: =
 IF(G7<100,(100/(1+(G7/100))),(100/(1+(100/G7))))

Critical Limit

Type III: J27: =
 IF(G27<M27,(100/(1+(G27/100))*(M27/100)),(100/(1+(100/G27))))

Critical Limit 1

M27: = IF(I27<100,(100/(1+(I27/100))),(100/(1+(100/I27))))

Critical Limit 2

G7–36: = Critical Ratio $[AA]^+/[AB]^+$ (Type II TAG)
 or $[AC]^+/([AA]^+ + [AB]^+)$ (Type III)

I27–36: = Critical Ratio $[BC]^+/[AB]^+$ (Type III TAG)

These formulas are the implementation of the equations for the Critical Limits that were given in the closed boxes in Scheme I, Parts II and III, and in Equations 7–9. These formulas may be pasted down the column for all TAG of each type, to automatically calculate the Critical Limits for all TAG. Notice that Critical Limit 1 for a Type III TAG depends on Critical Limit 2.

Notice that the formula for Critical Limit 2 for a Type III TAG is in the same form as the formula for the one Critical Limit of a Type II TAG. Once the Critical Limits have been calculated, then the Case classification can also be automated. The Critical Limits calculated from the Critical Ratios in Table 2 are given in Table 3, along with the Critical Values. Examples in the preceding text and in Figure 5 demonstrate calculation

of the Critical Limit.

In the spreadsheet implementation for Type I TAG, the $[MH]^+/\Sigma[DAG]^+$ ratio is simply compared with 1, so the classification is =IF(E2<100,**1**,**2**), where **1** and **2** are Case 1 and Case 2. For both Types II and III TAG, the $[MH]^+/\Sigma[DAG]^+$ ratio is compared with the first Critical Limit (formulas just shown) and is given by: =IF(E7<J7,**1**,**2**), where **1** and **2** are Case 1 and Case 2, with the Critical Limit in column J. Next, Case 3 and Case 4 are determined. For the Type II TAG, the $[AA]^+/[AB]^+$ ratio is simply compared with 1, so the classification formula is: =IF(G7<100,**3**,**4**), where **3** and **4** are Case 3 and Case 4. For a Type III TAG, the $[AC]^+/([AB]^++[BC]^+)$ ratio is compared with Critical Limit 2, so the classification formula is: =IF(G27<M27,**3**,**4**), where Critical Limit 2 is in column M. Finally, Case 5 and Case 6 are determined. The $[BC]^+/[AB]^+$ ratio is simply compared with 1 for this determination, so the classification formula in spreadsheet notation is =IF(G27<100,**5**,**6**).

From these formulas, the TAG are classified into their complete Case classifications. The case classifications for the 35-TAG mixture, for which Critical Ratios are given in Table 2, are shown in Table 3. Once they are classified, the solution equations are given in Scheme 1 of the BUS. Since they may not be obvious and might seem daunting at first, the formulas will be given here by which the entire BUS can be implemented. This actually requires only a few nested spreadsheet formulas. To exemplify this, imagine that the case classification in Table 3 is in columns Q, R, and S of the same spreadsheet as that envisioned for Table 2. Keeping the same row numbers (2 through 36), the following formulas use the Cases defined in Table 3 with the Critical Ratios given in Table 2 to calculate the abundances of all ions in the original mass spectra.

In the implementation in a spreadsheet, the comparison of the $[MH]^+/\Sigma[DAG]^+$ ratio to 1 and to its Critical Value can be skipped, since the Critical Limits are sufficient to determine which peak is the base peak. The comparison with 1 and with the Critical Value is done when the BUS is being used manually (not in a spreadsheet), to accomplish the case classification of the TAG with these simple values if possible, to save time and avoid calculation of the more complicated Critical Limit(s).

When the spreadsheet is used, the formulas given above can be typed in and then pasted down the column, so calculation of the Critical Limits requires minimal effort. Therefore, these formulas for the Critical Limits can be used without first testing the $[MH]^+/\Sigma[DAG]^+$ ratio with the Critical Value and 1.

Similarly, for a Type III TAG, Critical Limit 1 depends on Critical Limit 2. Since the spreadsheet calculates both of these values easily from the formulas for the Critical Limits given, Critical Limit 2 is easily determined without first testing the $[AC]^+/([AB]^+ + [BC]^+)$ ratio using its Critical Value of 0.5. The $[AC]^+/([AB]^+ + [BC]^+)$ ratio can simply be compared with Critical Limit 2 using the automated classification formulas just given, to arrive at the Case classification for Case 3 or Case 4.

Thus, the whole Critical Limit calculation process is accomplished with only the three formulas given, and these are used with the Critical Ratios to accomplish the complete Case
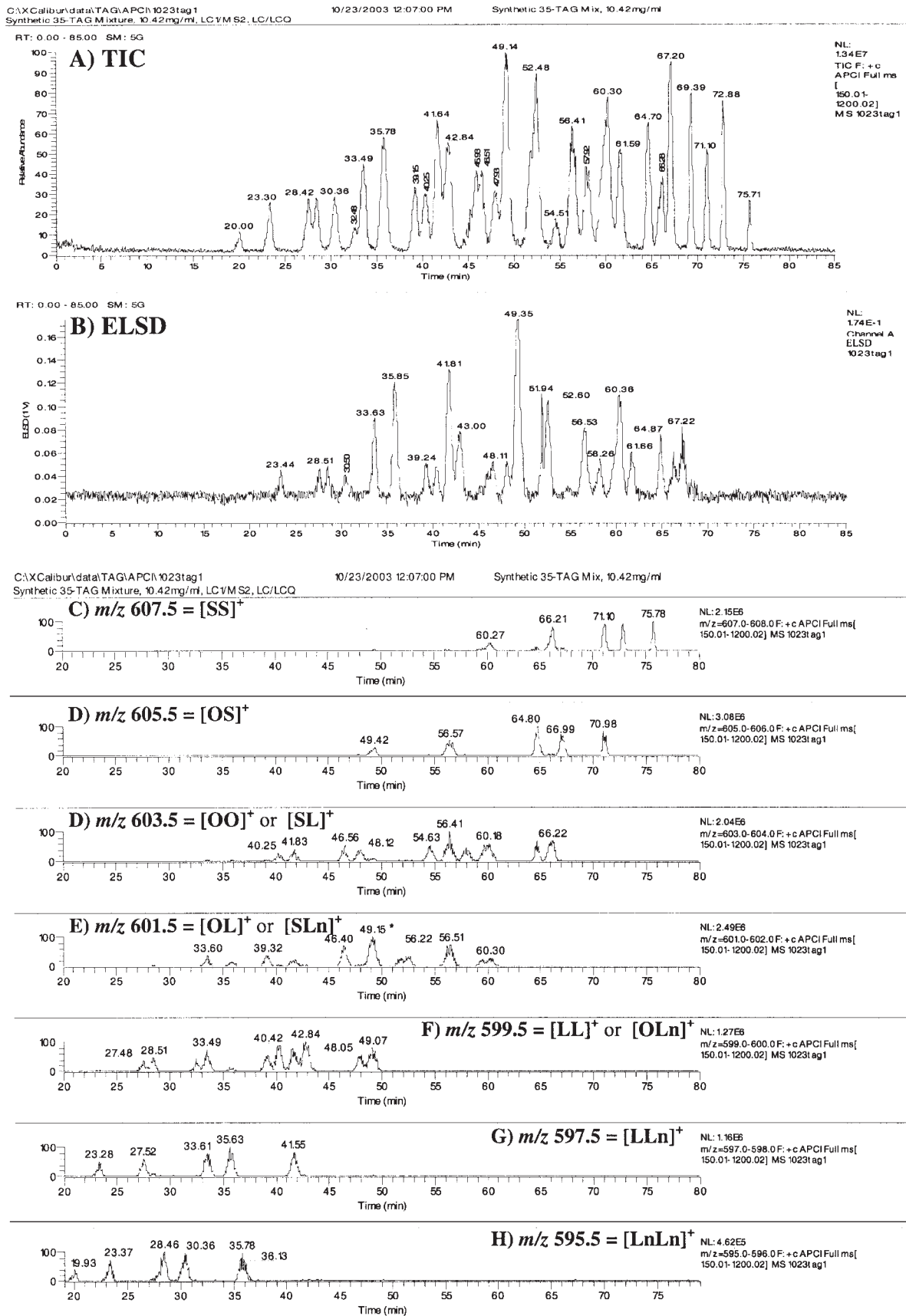
FIG. 6. Total ion current chromatogram (TIC), evaporative light-scattering detector (ELSD) chromatogram, and extracted ion chromatograms (EIC) of [DAG]⁺ fragment ion masses. S, stearic acid; Ln, linolenic acid; for other abbreviations see Figure 1.

classification of the TAG. Once the Case classification is accomplished, the BUS shows which equations to use to calculate the ion abundances for every TAG of every case. In looking at Scheme 1, it might appear difficult to implement the system of equations given in the BUS. However, the whole solution for every TAG can be implemented in only nine formulas that contain nested "if (*x*, then *y*, else *z*)" spreadsheet formulas, in which *x* is the case classification given in Table 3. There are nine types of [MH]$^+$ or [DAG]$^+$ fragment ions that can be produced from a Type I, II, or III TAG. The nine spreadsheet formulas necessary to calculate the abundance of every possible ion are provided in Table 4. These can be entered into the spreadsheet and then pasted down the column for each TAG type. Since there are only two possible cases for each Critical Ratio, the "if (*x*, then *y*, else *z*)" statement can be tested using Cases **1**, **3**, and **5** as *x*, and if any of the tests fails, then the inherent "else *z*" is the Case **2**, **4**, or **6** solution, respectively, by default. This is why, for a Type III TAG, only the values **1**, **3**, and **5** appear at the beginning of each "if (*x*, then *y*, else *z*)" statement. Notice in Table 4 that, for a Type III TAG, the "if (*x*, then *y*, else *z*)" statements are nested three levels deep, whereas for a Type II TAG, they are nested two levels deep. The spreadsheet formulas in Table 4 allow the abundances for every [MH]$^+$ ion and [DAG]$^+$ fragment from every TAG to be calculated based on the Critical Ratios tabulated in Table 2, using the Critical Limits and Case classification shown in Table 3. The abundances calculated from the spreadsheet formulas in Table 4 are given in Table 5.

Table 5 represents an average mass spectrum obtained from three chromatographic runs. The average mass spectrum was used to calculate the Critical Ratios. The values in Table 5 were calculated from the Critical Ratios in Table 2 processed through the equations in Table 4 and are exactly equal to the average mass spectrum to the number of significant figures given. In the spreadsheet, where many decimal places can be kept, the BUS reproduces the original mass spectrum to as many decimal places as desired. Figure 5 demonstrates that when theoretical Critical Ratios with infinite precision (perfect integer ratios) are used, the abundances are calculated with infinite precision. The abundances calculated and shown in Table 5, which are given by the BUS using the Critical Ratios in Table 2, are an exact reproduction of the average mass spectrum obtained from the average of three chromatographic runs, to two decimal places. The reproduced mass spectrum in Table 5 gives the Critical Ratios shown in Table 2. It should be noted that, since the abundances calculated from the BUS, shown in Table 5, required rounding to two decimal places, rounding error would occur each time the spectrum is reproduced from the Critical Ratios of a reproduced spectrum. In situations where the Critical Ratios are pure integer ratios, as shown in Figure 5, there is no error; and the Critical Ratios can be used to calculate the reproduced mass spectrum, and the Critical Ratios from the reproduced mass spectrum give the exact same Critical Ratios, with infinite precision. Just like the average mass spectra shown in Table 5, the abundances that

make up any individual APCI-MS mass spectrum can be exactly reproduced by the BUS. The Critical Ratios for any individual mass spectrum are processed through the BUS, and the abundances from which they came are reproduced to as many significant figures as were given for the Critical Ratios.

The structural trends that have been reported, as discussed in the foregoing sections, make up part of the Interpretation Matrix that is used to interpret information from the Critical Ratios. But the Interpretation Matrix is also used, if literature precedent has been reported, to make structural assignments that affect the Critical Ratios. The structural trends can be seen in the way the fragment ions are arranged in Table 5. It has already been discussed that the statistically expected [AA]$^+$/[AB]$^+$ ratio is 0.5. Thus, the [AA]$^+$ ion abundance is always expected to be smaller than the [AB]$^+$ abundance. It can be seen in Table 5 that the [AA]$^+$ ion abundance (identified as the [AA]$^+$ fragment by *m/z* value) is smaller than the [AB]$^+$ abundance for every TAG. With Type II TAG, there is no selection to be made regarding the identities of A and B, because whichever [DAG]$^+$ fragment has two of the same FA is the [AA]$^+$ fragment, and whichever [DAG]$^+$ fragment has two different FA is the [AB]$^+$. The 35-TAG mixture theoretically has equimolar amounts of regioisomers, since the FA are randomly distributed.

Based on linear interpolation of the ([AA]$^+$/[AB]$^+$)$_{Obs}$ ratio between the ([AA]$^+$/[AB]$^+$)$_{ABA}$ and ([AA]$^+$/[AB]$^+$)$_{AAB}$ ratios of pure standards, the [AA]$^+$/[AB]$^+$ ratio for the 35-TAG mixture should give an [AA]$^+$/[AB]$^+$ ratio that is ~1/3 of the way between the [AA]$^+$/[AB]$^+$ ratio of the ABA isomer and the [AA]$^+$/[AB]$^+$ ratio of the AAB/BAA isomer pair. The [AA]$^+$/[AB]$^+$ ratios of many TAG regioisomers have not yet been reported. Table 2 represents one point, obtained from a randomized mixture, on the line interpolated between the two regioisomeric standards. The [AA]$^+$/[AB]$^+$ ratios in Table 2 theoretically represent approximately the one-third (1/3) point on the line interpolated between the [AA]$^+$/[AB]$^+$ ratios of the ABA isomer and the AAB/BAA isomer pair. As already mentioned, the 35-TAG synthetic mixture for which Critical Ratios were given in Table 2 represents a mixture of regioisomers, and each of these is present as a racemic mixture of enantiomers.

The [AA]$^+$/[AB]$^+$ ratios in Table 2 show that the TAG that contained the diolein DAG combined with a saturated FA had some of the lowest [AA]$^+$/[AB]$^+$ ratios. Polyunsaturated TAG, containing linoleic and linolenic acids, gave the highest [AA]$^+$/[AB]$^+$ ratios, especially from the TAG containing one saturated FA. Perhaps construction of the [AA]$^+$/[AB]$^+$ ratios from a larger number of TAG mixtures and TAG standards will lead to a greater understanding of the effects of unsaturation in the FA, and of the regioisomeric placement of the FA, on the relative abundances of the [DAG]$^+$ fragment ions formed from Type II TAG.

Unlike Type II TAG, for Type III TAG the identities of the FA A, B, and C are not automatically known. However, the trends reported from APCI-MS data provide information to be able to classify the FA and deduce the structure of [AC]$^+$ and

therefore to know the identity of the B FA in the *sn*-2 position. As discussed in the preceding sections, the *sn*-1,3 [DAG]⁺ fragment has been reported to be energetically disfavored, and has been reported to exist in the least abundance (10,11) of the three [DAG]⁺ fragments that come from a Type III TAG. Based on this reported trend, the abundances of Type III TAG in Table 5 have been arranged such that the [AC]⁺ fragment is selected as the peak with the lowest abundance. Aligning the identity of [AC]⁺ as the ion with the smallest abundance implies that it is the [*sn*-1,3-AC]⁺ fragment. For instance, for OPS, the lowest [DAG]⁺ abundance was observed from the [OS]⁺ fragment (=[SO]⁺), so the [OS]⁺ fragment is labeled as the [AC]⁺ fragment. In this way, the previous structural trends that have been reported for TAG can be used for identification of at least one of the three possible regioisomers for a Type III TAG. Before constructing the Critical Ratios (such as in Table 2), the lowest [DAG]⁺ abundance should be properly identified as [AC]⁺, so that the [AC]⁺/([AB]⁺ + [BC]⁺) ratio will have its minimum value when the [AC]⁺ fragment is properly assigned. Of course, the equations of the BUS operate properly whether the ions have been assigned properly or not, but proper construction of the Critical Ratios allows additional structural information to be derived and trends observed. In Table 5, one can observe that all [AC]⁺ fragments have the lowest abundances of the three [DAG]⁺ fragments for each TAG. However, the trend reported for Type III TAG was based on a limited number of Type III TAG; therefore, this trend needs to be further verified with additional Type III TAG standards. Regardless of how the Critical Ratios are used to derive regiospecific structural information, the BUS works with all values of all Critical Ratios.

No definitive trend has been reported for [AB]⁺ vs. [BC]⁺ fragments. All else being equal, the [AB]⁺ vs. [BC]⁺ fragments are interchangeable. Thus, it is equally likely that a TAG could represent a Case 5 vs. a Case 6 solution. In the absence of a definitive trend, the data can be used to try to elucidate any subtle trends that may not be readily apparent. If one chooses to set the [BC]⁺ fragment equal to the smaller of the two possible abundances for [AB]⁺ or [BC]⁺, then perhaps the ratios will indicate some structural trends. For instance, in Table 5, the [BC]⁺ fragment is chosen so that the [BC]⁺ fragment is smaller than abundances for [AB]⁺. By doing this, one can observe that every Type III TAG in the mixture that has less than two saturated FA had the least saturated chain in the C, or *sn*-3, position. Seven of the ten Type III TAG in the 35-TAG mixture had one or no saturated FA. All seven of these TAG gave a lower abundance for the [BC]⁺ fragment than the [AB]⁺ fragment when the single saturate or monounsaturate (for LLnO) was in the *sn*-3 position. Of course, the *sn*-1 and *sn*-3 positions could be reversed, and all Type III TAG would have the [BC]⁺ fragment larger than the [AB]⁺ fragment. But whichever way they are labeled, it reveals a trend that the [DAG]⁺ fragment with more unsaturation is the larger fragment, in most cases, giving a [BC]⁺/[AB]⁺ ratio less than one, when the unsaturated TAG is labeled as the A, or *sn*-1, FA. Additional data from regioisomeric standards of Type III TAG will reveal which is the correct assignment. With the BUS, the mechanism, or the construct, is now in place to be able to

more easily identify and interpret structural trends, as they are reflected in the abundances of the [DAG]⁺ fragment ions in APCI-MS mass spectra, and the Critical Ratios made from the raw abundances. Regardless of whether the [BC]⁺ fragment is less than the [AC]⁺ fragment or vice versa, the BUS accurately calculates the abundances of each ion whether the [BC]⁺/[AB]⁺ ratio is larger than 1 or less than 1.

In a way analogous to proteomics, the sum of all possible species and structures of lipid molecules may referred to as the *lipidome*, and the study of the lipidome is referred to as *lipidomics* (46). The sum of all possible structures of TAG may be referred to as the TAG Lipidome. There is not a single TAG that cannot be represented by its Critical Ratios, and from these Critical Ratios, all abundances of ions may be reproduced. Thus, Scheme 1 represents the complete boundary to the solution of the TAG Lipidome, based on data from APCI-MS mass spectra. There is no TAG that cannot be represented within this construct. The structural trends that have just been mentioned, which were correlated to values or trends in the Critical Ratios, constitute the Interpretation Matrix that is part of the BUS. These correlations are not written here in a single table but have been discussed in detail. In the future, further information may be added to the Interpretation Matrix to allow a preference for [BC]⁺ vs. [AB]⁺ to be further described, or other information may be added to allow more information to be interpreted from the Critical Ratios. But, whereas this may provide incremental additional information, the essential construct of the BUS to the TAG Lipidome is complete in its entirety as given in Scheme 1, and the mass spectrum of any TAG may be reproduced from its equations. The BUS constitutes the first full solution to the TAG Lipidome.

FUTURE DIRECTIONS

Critical Ratios and their use in the BUS have been demonstrated using APCI-MS of TAG. This solution is also applicable to data obtained by ESI-MS. Since ESI-MS produces mostly the protonated molecule, with small abundances of [DAG]⁺ fragment ions, the [MH]⁺/Σ[DAG]⁺ ratio is, of course, higher for ESI-MS data, but as long as the Σ[DAG]⁺ is nonzero, the BUS may be applied to the same Critical Ratios calculated from ESI-MS data as from APCI-MS data. Alternatively, since ESI-MS mass spectra never give a zero abundance of protonated molecule (whereas APCI-MS spectra do), the completely bounded solution to the TAG lipidome by ESI-MS would best be constructed using the (Σ[DAG]⁺/[MH]⁺) ratio. This will give essentially the same construct as the TAG lipidome by APCI-MS, but with the (Σ[DAG]⁺/[MH]⁺) ratio having an inverse relationship to the [MH]⁺/Σ[DAG]⁺ ratio. Nevertheless, as long as the Σ[DAG]⁺ fragments is not zero, the same set of ions (an [MH]⁺ and up to three [DAG]⁺ fragment ions) can be used with the BUS for TAG analysis by ESI-MS as was used for analysis by APCI-MS. Furthermore, as several values obtained by ESI-MS in Table 1 show, the [AA]⁺/[AB]⁺ ratio obtained by ESI-MS may be useful for characterization of the regioisomers, just like the [AA]⁺/[AB]⁺ ratio obtained by APCI-MS.

Glycerophospholipids have some structural similarity to TAG, because both classes of molecules have a three-carbon glycerol backbone. This similarity is seen in the mass spectra of glycerophospholipids. Most glycerophospholipids produce a protonated molecule and one [DAG]⁺ fragment, which is the same type of DAG fragment that is produced by TAG. It should be obvious that these two ions could be represented by the ([MH]⁺/[DAG]⁺) ratio, and the abundances of the two ions could be found using Scheme 1, Part I, just like a Type I TAG. Furthermore, glycerophospholipids produce fragments ions by loss of one fatty acyl chain as either an acid or a ketene (44). Phospholipid fragments containing one FA, formed by loss of one fatty acyl chain as an acid or a ketene (44), are analogous to the [AA]⁺ or [AB]⁺ fragments from a Type II TAG, in that the fragments provide information to allow identification of regioisomers. It will be a very straightforward extension of the BUS to construct Critical Ratios from phospholipids and process them through a solution that will be very similar to this original BUS, but that will be customized to identify the ions observed from phospholipids.

This solution to the TAG lipidome was referred to as the BUS because it was accomplished through manual solutions to every possible case. Once the complete solution was accomplished, trends within the equations were observed, and the mathematical function behind those equations was developed. The new function that describes all possible combinations of two variables (abundances) interacting with each other is defined as the Unit Simulacrum. Once the patterns within the equations were recognized and the equations behind the equations were found, two more mathematically equivalent solutions to the TAG lipidome were produced, which are referred to as the term-wise simulacrum solution and the nested simulacrum solution. Since these other solutions were arrived at by using the equations behind the equations, it may be said that these solutions were developed using a "top-down" approach. These other solutions will be presented in another report. The masses of the fragments have not been discussed, since they are constant and are dictated by the identity of the TAG. For instance, it is automatically known that the TAG POL will produce a [PO]⁺ fragment having *m/z* 577.5, a [PL]⁺ fragment having *m/z* 575.5, an [OL]⁺ fragment having *m/z* 601.5, and a [POL + H]⁺ ion having *m/z* 857.8. These *m/z* values do not change and so do not need to be reiterated. It is the abundances of the protonated molecule and the [DAG]⁺ fragment ions that change and that are affected by unsaturation and by positional placement of the FA on the glycerol backbone. It is these structural features that the Critical Ratios elucidate. As demonstrated, these Critical Ratios can then be used to reconstruct the appearance of the APCI-MS mass spectrum of any TAG.

CONCLUSION

The BUS represents the first complete solution to the TAG lipidome. Critical Ratios have been defined that, used by themselves, provide direct information regarding the structural characteristics of TAG (e.g., amount of unsaturation and positional

isomer distribution). Furthermore, these Critical Ratios constitute a reduced data set from which the mass spectrum of any TAG can be reproduced in its entirety. This reduced data set has potential advantages for storage of library spectra. Normally, the abundances of all four ions in the mass spectrum of a TAG would be presented in tabular form to represent a mass spectrum. In using the BUS, only three pieces of data are required (the three Critical Ratios). This represents a saving of 25% (three values needed instead of four) for ABC TAG. For ABA/AAB TAG, only two critical ratios are necessary to provide all of the information necessary to reproduce the mass spectrum, compared with three abundance values that would be used to tabulate the spectrum. This constitutes a data storage reduction by 33% (two values needed instead of three) for ABA/AAB TAG. Since only one critical ratio is necessary to describe the mass spectral abundances of an AAA TAG completely, the BUS provides a 50% saving in data storage space required (one value needed instead of two). The benefit of reduced data storage requirements is in addition to the benefits of being able to use the Critical Ratios directly to determine the distribution of regioisomers and the degree of unsaturation.

In the past, articles often presented tabulated abundances of mass spectral ions (8,32,33,36,37), which could later be used to calculate the ratio of [AA]⁺/[AB]⁺ abundances to allow the positional isomer preference to be assessed (45). It has now been demonstrated that it is possible to list Critical Ratios that can be used directly to provide structural information (e.g., assessing the degree of unsaturation or assigning positional isomers) and that constitute a reduced data set that uses fewer values and therefore takes less space than conventional tabulated mass spectra. It has been demonstrated that the mass spectrum of any TAG can be reproduced from the Critical Ratios using the BUS, which uses Critical Values and Critical Limits, and an Interpretation Matrix, to define the Case of a TAG. Once the Case of the TAG is defined, the exact equations used to calculate the abundance of every ion in the mass spectrum are given by the BUS. Finally, all of the spreadsheet formulas that are necessary to implement the BUS have been provided. For the automated spreadsheet implementation, the following spreadsheet formulas are given: three formulas for Critical Limits, five formulas for the Case classification process, and nine formulas to calculate every possible [MH]⁺ or [DAG]⁺ fragment, which represent the primary ions in an APCI-MS mass spectrum, for a Type I, II, or III TAG.

REFERENCES

1. Kusaka, T., Ikeda, M., Nakano, H., and Numajiri, Y. (1988) Liquid Chromatography/Mass Spectrometry of Fatty Acids as Their Anilides, *J. Biochem. 104*, 495–497.
2. Kusaka, T., and Ikeda, M. (1992) Liquid Chromatography–Mass Spectrometry of Hydroperoxy Fatty Acids (in Japanese), *Proc. Jpn. Soc. Biomed. Mass Spectrom. 17*, 167–170.
3. Kusaka, T., and Ikeda, M. (1993) Liquid Chromatography–Mass Spectrometry of Fatty Acids Including Hydroxy and Hydroperoxy Acids as Their 3-Methyl-7-methoxy-1,4-benzoxazin-2-one Derivatives, *J. Chromatogr. 639*, 165–173.
4. Banni, S., Day, B.W., Evans, R.W., Corongiu, F.P., and Lom-

bardi, B. (1994) Liquid Chromatographic–Mass Spectrometric Analysis of Conjugated Diene Fatty Acids in a Partially Hydrogenated Fat, *J. Am. Oil Chem. Soc. 71*, 1321–1325.

5. Tyrefors, L.N., Moulder, R.X., and Markides, K.E. (1993) Interface for Open Tubular Column Supercritical Fluid Chromatography/Atmospheric Pressure Chemical Ionization Mass Spectrometry, *Anal. Chem. 65*, 2835–2840.
6. Byrdwell, W.C., and Emken, E.A. (1995) Analysis of Triglycerides Using Atmospheric Pressure Chemical Ionization Mass Spectrometry, *Lipids 30*, 173–175.
7. Byrdwell, W.C., Emken, E.A., Neff, W.E., and Adlof, R.O. (1996) Quantitative Analysis of Triglycerides Using Atmospheric Pressure Chemical Ionization–Mass Spectrometry, *Lipids 31*, 919–935.
8. Laakso, P., and Voutilainen, P. (1996) Analysis of Triacylglycerols by Silver-Ion High-Performance Liquid Chromatography–Atmospheric Pressure Chemical Ionization Mass Spectrometry, *Lipids 31*, 1311–1322.
9. Laakso, P., and Manninen, P. (1997) Identification of Milk Fat Triacylglycerols by Capillary Supercritical Fluid Chromatography–Atmospheric Pressure Chemical Ionization Mass Spectrometry, *Lipids 32*, 1285–1295.
10. Mottram, H.R., and Evershed, R.P. (1996) Structure Analysis of Triacylglycerol Positional Isomers Using Atmospheric Pressure Chemical Ionisation Mass Spectrometry, *Tetrahedron Lett. 37*, 8593–8596.
11. Mottram, H.R., Woodbury, S.E., and Evershed, R.P. (1997) Identification of Triacylglycerol Positional Isomers Present in Vegetable Oils by High Performance Liquid Chromatography/Atmospheric Pressure Chemical Ionization Mass Spectrometry, *Rapid Commun. Mass Spectrom. 11*, 1240–1252.
12. Byrdwell, W.C., and Borchman, D. (1997) Liquid Chromatography/Mass Spectrometric Characterization and Dihydrosphingomyelin of Human Lens Membranes, *Ophthal. Res. 29*, 191–206.
13. Karlsson, A.A., Michelsen, P., and Odham, G. (1998) Molecular Species of Sphingomyelin: Determination by High-Performance Liquid Chromatography/Mass Spectrometry with Electrospray and High-Performance Liquid Chromatography/Tandem Mass Spectrometry with Atmospheric Pressure Chemical Ionization, *J. Mass Spectrom. 33*, 1192–1198.
14. Qiu, D.F., Xiao, X.Y., Walton, T.J., Games, M.P.L., and Games, D.E. (1999) High-Performance Liquid Chromatography/Atmospheric Pressure Chemical Ionization Mass Spectrometry of Phospholipids in *Natronobacterium magadii*, *Eur. Mass Spectrom. 5*, 151–156.
15. Carrier, A., Parent, J., and Dupuis, S. (2000) Quantitation and Characterization of Phospholipids in Pharmaceutical Formulations by Liquid Chromatography–Mass Spectrometry, *J. Chromatogr. A 876*, 97–109.
16. Dobson, G., and Deighton, N. (2001) Analysis of Phospholipid Molecular Species by Liquid Chromatography–Atmospheric Pressure Chemical Ionisation Mass Spectrometry of Diacylglycerol Nicotinates, *Chem. Phys. Lipids 111*, 1–17.
17. Couch, L.H., Churchwell, M.I., Doerge, D.R., Tolleson, W.H., and Howard, P.C. (1997) Identification of Ceramides in Human Cells Using Liquid Chromatography with Detection by Atmospheric Pressure Chemical Ionization Mass Spectrometry, *Rapid Commun. Mass Spectrom. 11*, 504–512.
18. Van Breeman, R.B., Huang, C.R., Tan, Y., Sander, L.C., and Schilling, A.B. (1996) Liquid Chromatography/Mass Spectrometry of Carotenoids Using Atmospheric Pressure Chemical Ionization, *J. Mass Spectrom. 31*, 975–981.
19. Van Breeman, R.B., Xu, X., Viana, M.A., Chen, L., Stacewicz-Sapuntzakis, M., Duncan, C., Bowen, P.E., and Sharifi, R. (2002) Liquid Chromatography–Mass Spectrometry of *cis*- and all-*trans*-Lycopene in Human Serum and Prostate Tissue After Dietary Supplementation with Tomato Sauce, *J. Agric. Food Chem. 50*, 2214–2219.

20. Clarke, P.A., Barnes, K.A., Startin, J.R., Ibe, F.I., and Shepherd, M.J. (1996) High Performance Liquid Chromatography/Atmospheric Pressure Chemical Ionization–Mass Spectrometry for the Determination of Carotenoids, *Rapid Commun. Mass Spectrom. 10*, 1781–1785.
21. Hagiwara, T., Yasuno, T., Funayama, K., and Suzuki, S. (1997) Determination of Lycopene, α-Carotene and β-Carotene in Vegetable Juice by Liquid Chromatography/Atmospheric Pressure Chemical Ionization–Mass Spectrometry, *J. Food Hyg. Soc. Jpn. 38*, 211–218.
22. Hagiwara, T., Yasuno, T., Funayama, K., and Suzuki, S. (1998) Determination of Lycopene, α-Carotene and β-Carotene in Serum by Liquid Chromatography–Atmospheric Pressure Chemical Ionization Mass Spectrometry with Selected Ion Monitoring, *J. Chromatogr. B 708*, 67–73.
23. Kobayashi, Y., Saiki, K., and Watanabe, F. (1993) Characteristics of Mass Fragmentation of Steroids by Atmospheric Pressure Chemical Ionization Mass Spectrometry, *Biol. Pharmacolog. Bull. 16*, 1175–1178.
24. Ma, Y.C., and Kim, H.Y. (1997) Determination of Steroids by Liquid Chromatography/Mass Spectrometry, *J. Am. Soc. Mass Spectrom. 8*, 1010–1020.
25. Joos, P.E., and van Ryckeghem, M. (1999) Liquid Chromatography–Tandem Mass Spectrometry of Some Anabolic Steroids, *Anal. Chem. 71*, 4701–4710.
26. Byrdwell, W.C. (1998) APCI-MS for Lipid Analysis, *INFORM 9*, 986–997.
27. Byrdwell, W.C. (2001) Atmospheric Pressure Chemical Ionization Mass Spectrometry for Analysis of Lipids, *Lipids 36*, 327–346.
28. Laakso, P. (2002) Mass Spectrometry of Triacylglycerols, *Eur. J. Lipid Sci. Technol. 104*, 43–49.
29. Byrdwell, W.C. (2003) APCI-MS in Lipid Analysis, in *Advances in Lipid Methodology—Five* (Adlof, R.O., ed.), pp. 171–253, The Oily Press, Bridgwater, England.
30. Laakso, P. (1996) Analysis of Triacylglycerols—Approaching the Molecular Composition of Natural Mixtures, *Food Rev. Intt. 12*, 199–250.
31. Iwasaki, Y., and Yamane, T. (2000) Enzymatic Synthesis of Structured Lipids, *J. Mol. Catal. B: Enz. 10*, 129–140.
32. Neff, W.E., and Byrdwell, W.C. (1995) Soybean Oil Triacylglycerol Analysis by Reversed-Phase High-Performance Liquid Chromatography Coupled with Atmospheric Pressure Chemical Ionization Mass Spectrometry, *J. Am. Oil Chem. Soc. 72*, 1185–1191.
33. Neff, W.E., and Byrdwell, W.C. (1995) Triacylglycerol Analysis by High Performance Liquid Chromatography–Atmospheric Pressure Chemical Ionization Mass Spectrometry: *Crepis alpina* and *Vernonia galamensis* Seed Oils, *J. Liq. Chromatogr. Rel. Technol. 18*, 4165–4181.
34. Byrdwell, W.C., and Neff, W.E. (1997) Qualitative and Quantitative Analysis of Triacylglycerols Using Atmospheric Pressure Chemical Ionization Mass Spectrometry, in *New Techniques and Applications in Lipid Analysis* (McDonald, R.E., and Mossoba, M.M., eds.), pp. 45–80, AOCS Press, Champaign.
35. Byrdwell, W.C., Neff, W.E., and List, G.R. (2001) Triacylglycerol Analysis of Potential Margarine Base Stocks by High Performance Liquid Chromatography with Atmospheric Pressure Chemical Ionization Mass Spectrometry and Flame Ionization Detection, *J. Agric. Food Chem. 49*, 446–457.
36. Laakso, P. (1997) Characterization of α- and γ-Linolenic Acid Oils by Reversed-Phase High-Performance Liquid Chromatography–Atmospheric Pressure Chemical Ionization Mass Spectrometry, *J. Am. Oil Chem. Soc. 74*, 1291–1300.
37. Manninen, P., and Laakso, P. (1997) Capillary Supercritical Fluid Chromatography Atmospheric Pressure Chemical Ioniza-

tion Mass Spectrometry of Triacylglycerols in Berry Oils, *J. Am. Oil Chem. Soc. 74*, 1089–1098.

38. Mottram, H.R., Crossman, Z.M., and Evershed, R.P. (2001) Regiospecific Characterisation of the Triacylglycerols in Animal Fats Using High Performance Liquid Chromatography–Atmospheric Pressure Chemical Ionisation Mass Spectrometry, *Analyst 126*, 1018–1024.

39. Hsu , F.F., and Turk, J. (1999) Structural Characterization of Triacylglycerols as Lithiated Adducts by Electrospray Ionization Mass Spectrometry Using Low-Energy Collisionally Activated Dissociation on a Triple Stage Quadrupole Instrument, *J. Am. Soc. Mass Spectrom. 10*, 587–599.

40. Fauconnot, L., Hau, J., Aeschlimann, J.M., Fay, L.B., and Dionisi, F. (2004) Quantitative Analysis of Triacylglycerol Regioisomers in Fats and Oils Using Reversed-Phase High-Performance Liquid Chromatography and Atmospheric Pressure Chemical Ionization Mass Spectrometry, *Rapid Commun. Mass Spectrom. 18*, 218–224.

41. Byrdwell, W.C. (2003) APCI-MS in Lipid Analysis, in *Advances in Lipid Methodology–Five* (Adlof, R.E., ed.), p. 200, The Oily Press, Bridgwater, England.

42. Jakab, A., Jablonkai, I. and Forgacs, E. (2003) Quantification of the Ratio of Positional Isomer Dilinoleoyl-oleoyl Glycerols in Vegetable Oils, *Rapid Commun. Mass Spectrom. 17*, 2295–2302.

43. Byrdwell, W.C., and Neff, W.E. (2002) Dual Parallel Electrospray Ionization and Atmospheric Pressure Chemical Ionization Mass Spectrometry (MS), MS/MS and MS/MS/MS for the Analysis of Triacylglycerols and Triacylglycerol Oxidation Products, *Rapid Commun. Mass Spectrom. 16*, 300–319.

44. Hsu, F.F., and Turk, J. (2005) Electrospray Ionization with Low-Energy Collisionally Activated Dissociation Tandem Mass Spectrometry of Complex Lipids: Structural Characterization and Mechanisms of Fragmentation, in *Modern Methods for Lipid Analysis by Liquid Chromatography/Mass Spectrometry and Related Techniques (*Byrdwell, W.C., ed.), pp. 61–178, AOCS Press, Champaign.

45. Byrdwell, W.C. (2005) Qualitative and Quantitative Analysis of Triacylglycerols by Atmospheric Pressure Ionization (APCI and ESI) Mass Spectrometry Techniques, in *Modern Methods for Lipid Analysis by Liquid Chromatography/Mass Spectrometry and Related Techniques* (Byrdwell, W.C., ed.), pp. 298–412, AOCS Press, Champaign.

46. Han, X., and Gross, R.W., Toward Total Cellular Lipidome Analysis by ESI Mass Spectrometry from a Crude Lipid Extract, in *Modern Methods for Lipid Analysis by Liquid Chromatography/Mass Spectrometry and Related Techniques* (Byrdwell, W.C., ed.), pp. 488–509, AOCS Press, Champaign.